INVESTIGATION OF MINERAL FILLER EFFECTS ON THE AGING PROCESS OF ASPHALT MASTICS

By:
Raquel Moraes

A dissertation submitted in partial fulfillment of
the requirements for the degree of
Doctor of Philosophy

(Civil & Environmental Engineering)

at the
UNIVERSITY OF WISCONSIN – MADISON

2014

Date of final oral examination: 5/30/2014

The dissertation is approved by the following members of the Final Oral Committee:
Hussain U. Bahia, Professor, Civil and Environmental Engineering
Daniel Klingenberg, Professor, Chemical and Biological Engineering
William Likos, Associate Professor, Civil and Environmental Engineering
Gustavo Parra-Montesinos, Associate Professor, Civil and Environmental Engineering
James Tinjum, Associate Professor, Civil and Environmental Engineering

To all those who believe in God, to all those who have faith.

“Love and see what God's love is capable of.”

(Fr. Airton Freire)

ACKNOWLEDGEMENTS

I would like to express my sincere gratitude to my advisor, Professor Hussain U. Bahia, whose direction and lasting encouragement have been truly inspiring. Professor Bahia has both encouraged and challenged me throughout the course of my studies. I sincerely appreciate his technical and professional advice. My interactions with Dr. Bahia have opened career opportunities for which I will always be grateful.

A sincere thank you to my committee members, Professor Daniel Klingenberg, Professor William Likos, Professor Gustavo Parra-Montesinos and Professor James Tinjum for offering their time and input in completing this thesis. Their opinions and contributions are gratefully appreciated.

I would also like to extend my heartfelt gratitude to Dr. Raul Velasquez and Dr. Hassan Tabatabaee for the academic and professional advice.

Everyone from the Asphalt Research Group of the University of Wisconsin-Madison helped me to accomplish this goal. Some of them by answering my questions or teaching me different aspects of asphalt testing. Some others simply by making the work environment nice and friendly. Thank you.

Finally, I would like to thank all my loved ones. Even when they were not physically with me during this time, I know in my heart that they were always supporting me from afar.

ABSTRACT

Aging of asphalt binders is induced by chemical and/or physical changes during the production of the pavement and throughout its service life. The process is usually accompanied by stiffening and embrittlement of the binder phase, which adversely influences the asphalt pavement durability and rate of deterioration. As asphalt binder is present as a mix of asphalt and fine mineral filler particles in the pavement (asphalt mastic), the mechanisms of aging are expected to not only be influenced by the characteristics of asphalt binder but also by the properties of the mineral filler, as well as the molecular interaction between the two components. Since asphalts binders are used in conjunction with mineral aggregates in pavements and roofing, the interactions between binders and these minerals and the resulting changes in the molecular size distribution after oxidative aging is of concern. The purpose of this study is to develop a fundamental understanding of the mechanisms of interaction between binder and filler surface area with respect to aging characteristics of the mastic. The results are used to identify the filler characteristics responsible for the changes in mechanical and thermo-volumetric properties as a result of aging asphalt binders in the presence of mineral filler particles.

To this end an experimental testing matrix was design and executed to account for different chemical and physical conditions in the asphalt mastics. Mechanical properties, as measured by complex modulus (|G*|) and the viscoelastic master curve, show that due to the interaction between the two phases, the aged properties of the asphalt binder can differ from the bulk properties of the binder when in the presence of mineral filler.

Gel Permeation Chromatography (GPC) results supported the mentioned findings with regards to mechanical properties, as the presence of mineral filler appears to decelerate the rate of

production of larger molecular size oxidation products in the binder phase of mastics. The change in the asphalt molecular size distribution due to the interaction of mineral filler causing irreversible adsorption of the asphaltic polar fraction (i.e., asphaltenes) is hypothesized as the main cause of the softening of the mastics after the aging process. The implication of this finding is that the molecular size distribution of asphalts - a controlling factor in mechanical and thermo-volumetric behavior - can be engineered by the addition of appropriate mineral filler mineralogy and concentration.

Results showed that during oxidative aging of asphalt binders and mastics, both diffusion and adsorption mechanisms play a role in the rate of aging of the asphalt material. An analysis of the increase in diffusion path length in mastics was used to show that the increase in diffusion path alone cannot explain the magnitude of effect observed by addition of fillers to the binder.

It was also observed that aging decreased the slope of the binder master curve, thus indicating a decrease in temperature susceptibility. The most important observation with regards to the master curve of aged mastics was that the presence of the filler particles during aging resulted in a reversal of the master curve slope change observed during individual aging of the base binder. This finding is very significant, as it can potentially indicate that many of the mechanical properties attributed to aged binders from rheological testing will in fact be unimportant if the mastic phase is considered rather than individual consideration of the binder phase. A method to characterize the behavior of mastics with aging is through monitoring the complex modulus aging index (ratio of the complex modulus before and after aging). By selecting a proper type and amount of filler, the aging of the pavement and, consequently, the durability and performance (especially crack resistance), can be controlled.

List of Contents

List of Figures

List of Tables

List of Equations

I. Introduction

1.1 Background

The chemistry of asphalt determines its physical properties and, therefore, its performance. Thus, a variation in asphalt composition strongly affects its mechanical properties, chemical reactivity, and the number and type of products generated after oxidative aging (Iqbal et al., 2002; Becker et al., 2003).

The chemical composition of asphalt depends primarily on its crude oil source and processing. The asphaltic materials can be separated into four primary chemical classes based on differences in solubility and polarity: saturates, aromatics, resins, and asphaltenes (Corbett, 1969; Petersen, 1984). Asphalt is often envisioned as a colloidal dispersion of asphaltenes into an oily matrix constituted by saturates, aromatics, and resins (i.e., the maltene fraction).

Asphaltenes are stabilized by natural resins, which are surfactant-like agents. Asphaltenes and resins are responsible for the visco-elastic properties of the asphalt at ambient temperature (Read and Whiteoak, 2003).

The Gel Permeation Chromatography (GPC) technique can be used to determine the molecular size distribution (MSD) of asphalt binders. The changes in the molecular size distribution due to aging can significantly influence the asphalt binder consistency and, consequently, its mechanical and physical properties (Shen et al., 2006).

Aging of asphalt binders is induced by chemical and/or physical changes during the production of the pavement and throughout its service life. The process is usually accompanied by stiffening of the binders, which influence the deterioration of asphalt pavements. The most

important modes of pavement failure that are significantly affected by aging are traffic-loading-induced fatigue cracking, thermally-induced cracking, and moisture-induced raveling (Lu and Isacsson, 2000). In addition, excessive stiffening as a result of aging can also weaken the adhesion between the asphalt binder and aggregate, resulting in loss of materials at the surface layer and generate weakening of the asphalt mixture (Wu, 2009).

In chemical terms, aging leads first to a decrease in aromatic content and subsequently an increase in resin and asphaltene content (Wei et al., 1996). However, testing of aged asphalt alone does not appear to adequately predict mixture performance because of the apparent mitigating and/or catalytic effect that mineral filler may have on aging.

Asphalt pavements are composed of three constituents: aggregate (fine and coarse), asphalt binder, and air voids. Oxidative aging may produce substantial changes in the chemistry of the asphalt-aggregate interface, particularly with an asphalt-aggregate pair that is susceptible to aging. Therefore, the aging of asphalt-aggregate mixes is influenced by both asphalt and aggregate.

In a Hot Mix Asphalt (HMA) mixture, the majority of the asphalt-aggregate interface area is generated by the aggregate of fine gradation (referred to as ‘fines’), since such aggregates possess the highest surface area (Anderson et al., 1992). In HMA, such combination of filler (fine aggregate passing sieve no. 200) and asphalt binder is often referred to as “mastic”.

Several physical and chemical processes are thought to govern the effect of mineral fillers during the aging process of HMA: (1) Some mineral components on the surface of aggregates may catalyze bitumen oxidation (Petersen et al., 1974); (2) The adsorption of polar asphalt compounds (i.e., asphaltenes) onto aggregates is much larger than for other less polar or nonpolar compounds (Petersen et al., 1974; Clopotel, 2012). Such phenomenon, in turn, makes the asphalt less

oxidizable; (3) Asphalt absorbed within the pore space of the aggregate may have differing chemical and physical properties as compared to the bulk asphalt (Kennedy and Cominsky, 1990).

Therefore, for asphalt mastics, the mechanisms of aging are hypothesized to be influenced by the characteristics of asphalt binder and mineral filler, as well as the molecular interaction between the two components. Since asphalt binders are used in conjunction with mineral aggregates in pavements and roofing applications, the interactions between binders and these minerals and the resulting changes in molecular size distribution after oxidative aging is of concern.

The chemical and rheological changes associated with aging are well understood for neat binders, since numerous studies have been performed (Petersen and Harnsberger, 1998; Read and Whiteoak, 2003; Petersen, 2009). However, for asphalt mastics, many topics in this research area remain to be studied.

1.2 Problem Statement

In an HMA mixture, the majority of the asphalt-aggregate interface area is within the fine fraction (particles smaller than 0.075 mm) embedded in the asphalt binder due to the higher surface area when compared with the coarse aggregate.

Asphalt ages through oxidation, changing its chemical composition. These chemical changes affect the mechanical properties of the asphalt. As a result, chemical aging leads to a global stiffening and embrittlement of the material, which in turn increases the cracking susceptibility. Aging of pavements increases the elastic behavior and decreases the time-dependent viscoelastic behavior of the material, thus stress relaxes relatively slower when compared to fresh

pavements, critically affecting thermal cracking susceptibility. Furthermore, aged pavements accumulate damage more quickly. Therefore, through various mechanisms the durability and service life of asphalt pavements is greatly affected by aging.

The current state of knowledge is limited in terms of fundamental understanding of the mechanisms of interaction between asphalt binder and mineral aggregate filler with respect to aging characteristics of the mastic (blend of asphalt and mineral filler). The performance implications of filler properties in HMA pavements is unclear due to the various interaction effects of filler with asphalt binders, which will depend on the filler content, mineralogy, and its surface area, among other properties.

Fundamental understanding of the asphalt-filler interaction during the aging of the effective binder is needed to determine an appropriate method for characterization of aged pavement material properties and to improve current analysis methods used to select durable and aging-resistant material.

1.3 Research Hypothesis

The presence of mineral filler can affect the aging of asphalt binders due to changes in the chemical composition as indicated by changes in the molecular size distribution of the binder. The irreversible adsorption of the asphaltic polar fraction (i.e., asphaltenes) is hypothesized as the main mechanism that mitigates the mechanical and thermo-volumetric effect of aging on binders in the presence of filler particles.

1.4 Research Objectives

The objectives of this research are to:

1) Develop a fundamental understanding of the mechanisms of interaction between binder and mineral filler with respect to aging characteristics of the mastic through chemical, compositional, and mechanical evaluation.
2) Determine mineral filler characteristics that are responsible for the changes in mechanical and thermo-volumetric properties of asphalt binders as aging progresses.

1.5 Research Methodology and Scope

This thesis is structured into five main sections with the following contents:

Chapter I: Introduction - This chapter includes a background on aging of asphalt binders and mixtures. The background is followed by the problem statement, research hypothesis and research objectives.

Chapter II: Literature Review - This chapter discusses the current state of knowledge and historical scholarly work with regards to asphalt composition and structure, the aging process in asphalts, influence of mineral aggregates on aging, and finally the influence of aging on cracking behavior of asphalts.

Chapter III: Materials and Methods - This chapter presents a detailed description of the experimental design and materials used in this research. An experimental matrix, which included different binders, mineral fillers mineralogy and concentrations, to account for different chemical and physical conditions in the mastic interface is presented.

Chapter IV: Evaluation of the Fillers' Effect on the Oxidative Aging of Binders - This chapter presents gravimetrical analysis to verify the fillers influence on the asphaltenes production after oxidative aging. It also includes rheological analyses conducted to test changes in stiffness, glass-transition temperature, and contraction coefficient of the asphalt mastics that will dictate the cracking behavior. A statistical analysis was performed to verify effect of binder type and filler type on the aging index of complex modulus.

Chapter V: Verification of Fillers' Effects on Molecular Size Distribution of Asphalt Binders - This chapter presents analysis of changes in the molecular size distribution of binders and mastics after oxidative aging. The results are used to establish a relationship between chemical and compositional properties measured using the Gel Permeation Chromatograph (GPC) results and rheological data obtained with the Dynamic Shear Rheometer (DSR).

Chapter VI: Conclusions and Recommendations - Conclusions gathered from the most relevant testing results and recommendations based on these conclusions are offered in this section. Direction for future work is also provided based on the findings of this study.

II. Literature Review

This chapter discusses the current state of knowledge and historical scholarly work with regards to the fundamental principles of oxidative aging in asphalt mastics. These sections focus on: definition of asphalt composition, asphalt structure, aging process in asphalts, influence of mineral aggregates on aging, influence of aging on cracking behavior of asphalts, and oxidative aging evaluation of asphalt binders using Gel Permeation Chromatography (GPC).

2.1 Asphalt Composition

The chemical composition of asphalt depends primarily on its crude oil source and processing methodology (Read and Whiteoak, 2003). Is the chemistry of the asphalt that determines its physical properties and, therefore, its performance. Thus, a variation in its composition strongly affects its mechanical properties and chemical reactivity (Iqbal et al., 2006; Becker et al., 2003).

Asphalts are a complex mixture of high molecular weight hydrocarbon molecules, many containing nitrogen, oxygen, and sulfur heteroatoms and trace metals such as vanadium and nickel (Petersen and Harnsberger, 1998). These heteroatoms are responsible for the unique physical and chemical properties of asphalt; they can replace carbon atoms in an asphalt molecule and have the ability to form associations with other molecules by hydrogen bonding (Tarefder and Arisa, 2011).

Naturally occurring heteroatoms, nitrogen, sulfur, oxygen, and metals contribute to polarity within these molecules. Similarly, oxidation products formed upon aging are polar and further contribute to the polarity of the entire asphalt system. The polarity among asphalt molecules varies

widely and the physical properties of the binder are governed by the balance of polar and non-polar components (Robertson, 1991). Polar components tend to associate, while less polar and non-polar asphalt components can cause dissociation.

The SARA-separation test procedure ASTM D4124 - Standard Test Method for Separation of Asphalt into four fractions (2009) separates the crude oil into its four main chemical classes, based on differences in solubility and polarity. The four SARA-fractions are commonly designated as saturates (S), aromatics (A), resins (R), and asphaltenes (A) (Figure II-1).

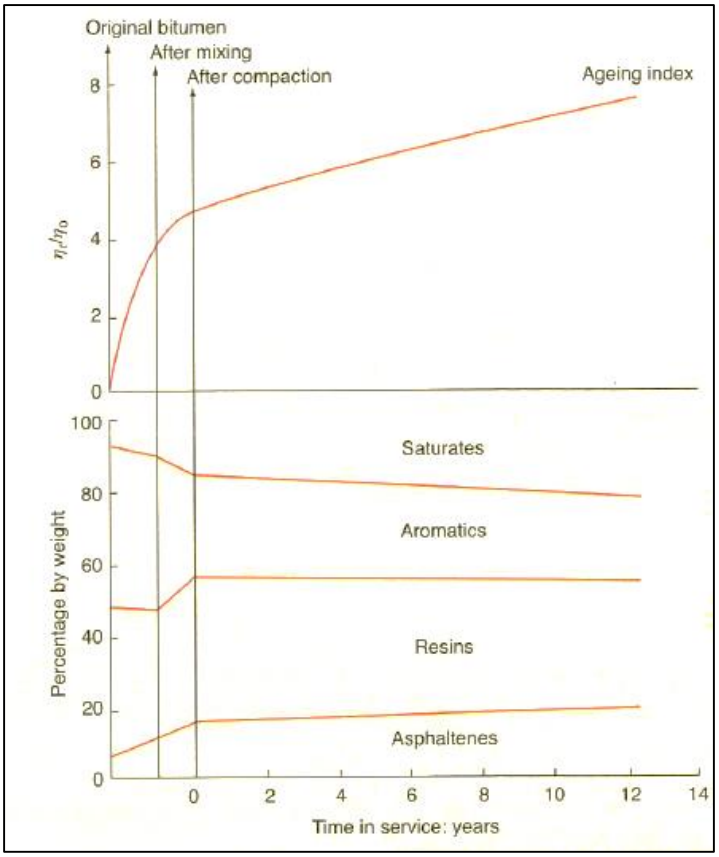

Figure II-1: Asphalt SARA analysis and the effect of service life on composition (Read and Whiteoak, 2003).

Saturates: Saturates (aliphatics) are non-polar hydrocarbons, without double bonds, but including straight-chain and branched alkanes, as well as cycloalkanes (naphtenes). Cycloalkanes contain one or more rings, which may have several alkyl side chains. The proportion of saturates in a crude oil normally decreases with increasing molecular weight fractions, thus saturates generally are the lightest fraction of the crude oil.

Aromatics: Are dark brown viscous liquids constituted of non-polar carbon chains with high dissolving ability. Aromatics generally increase asphalt viscosity and are a source of elasticity in asphalt. Aromatics are common to all petroleum, and by far the majority of the aromatics contain alkyl chains and cycloalkane rings, along with additional aromatic rings. Aromatics are often classified as mono-, di-, and tri-aromatics depending on the number of aromatic rings present in the molecule. Polar, higher molecular weight aromatics may fall in the resin or asphaltene fraction.

Resins: This fraction is comprised of polar molecules often containing heteroatoms such as nitrogen, oxygen or sulphur (Figure II-2). Resins have a higher hydrogen/carbon ratio than asphaltenes, 1.2-1.7 compared to 0.9-1.2 for the asphaltenes (Musser and Kilpatrick, 1998). Resins are structurally similar to asphaltenes, but lower in molecular weight (< 1000 g/mol). The resin fraction disperses (or peptizes) asphaltenes throughout maltene to provide a homogeneous liquid and imparts ductility to the asphalt (Tarefder and Arisa, 2011). Resins are dark brown, highly polar, adhesive compounds and are solid to semi-solid. Increasing resin content hardens asphalt and increases viscosity. The proportion of resins to asphaltenes in part governs the molecular structure of asphalt. Naphthenic acids are commonly regarded as a part of the resin fraction.

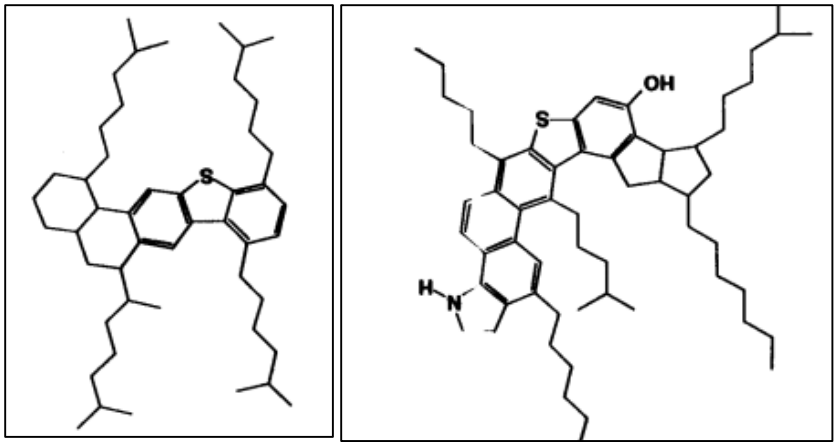

Figure II-2: Resin molecular structure (Murgich, 1996).

Asphaltenes: Are black or brown, highly polar, amorphous solid materials. Asphaltenes represent generally between 5 to 20 wt% of a binder (Lesueur, 2009). The asphaltenes fraction, like the resins, is defined as a solubility class, namely the fraction of the crude oil precipitating in light alkanes like pentane, hexane or heptane. This precipitate is soluble in aromatic solvents like toluene and benzene. The asphaltene fraction is responsible for viscosity and colloidal behavior of the asphalt (Tarefder and Arisa, 2011). The asphaltene fraction contains the largest percentage of heteroatoms (oxygen, sulfur, and nitrogen) and organometallic constituents (nickel, iron, and vanadium) in the crude oil. The structure of the asphaltenes is believed to consist of polycyclic aromatic clusters, substituted with varying alkyl side chains (Sheu and Mullins, 1995) (Figure II-3). The molecular weight of asphaltene molecules has been difficult to measure due to the asphaltenes tendency to self-aggregate, but molecular weights in the range of 500-2000 g/mol are believed to be reasonable assumption (Sheu, 2002).

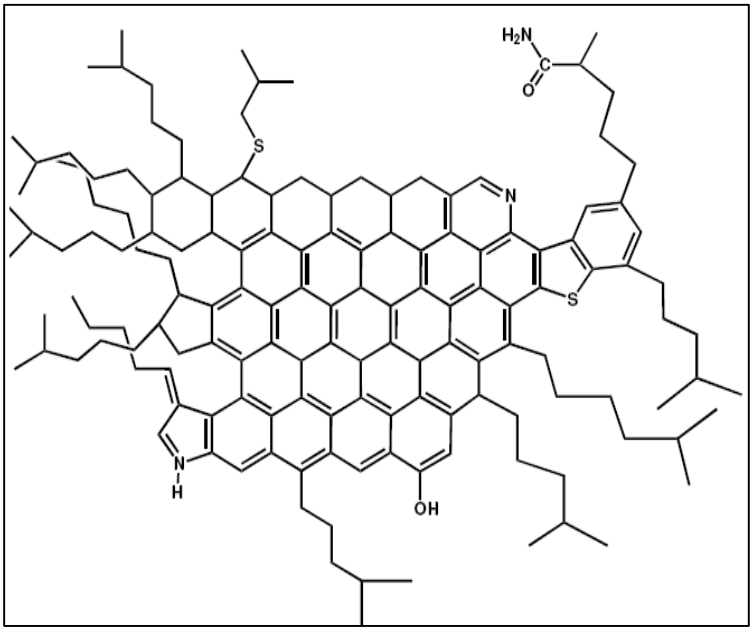

Figure II-3: Asphaltenes structure (Murgich et al., 1996).

In general, the mechanical or structural properties of asphalt binders are related to the intermolecular structuring among polar components. Asphalt binders should be considered as a continuum of molecules with a gradual transition in polarity, molecular weight, and functionality (Kriz et al., 2008). The ranking of the asphalt fractions regarding increase in molecular polarity is: saturates, naphthene aromatics, polar aromatics (resins), and asphaltenes (Corbett, 1969).

In an asphalt molecule, the polar matrix is responsible for the elastic component of the material, while the continuous non-polar phase gives the viscous component (Robertson, 1991). Oxidation causes aged asphalts to contain more polar molecules. Because polar molecules associate into a matrix which is dispersed in less polar and non-polar materials, polar oxidation products greatly alter the state of dispersion of asphalt components. This results in a change of the mobility and of the chemical reactivity of asphalt molecules susceptible to oxidation (Robertson, 1991; Petersen et al., 1996).

2.2 Asphalt Structure

Asphalt is often described as a colloidal dispersion of asphaltenes into an oily matrix constituted by saturates, aromatics, and resins. Figure II-4 illustrates the schematic of asphalt components.

It has been established that asphaltenes are stabilized in crude oils by natural resins which are surfactant-like agents. The action of resins on the asphaltene aggregation and precipitation processes is thought to be important. Due to their molecular constitution, asphaltenes and resins have a mutual intrinsic effect on the stability of molecular self-assembling, either in the form of asphaltene-resin association (which promotes re-dispersion) or asphaltene-asphaltene association (which promotes precipitation) (Ortega-Rodrıguez et al., 2003).

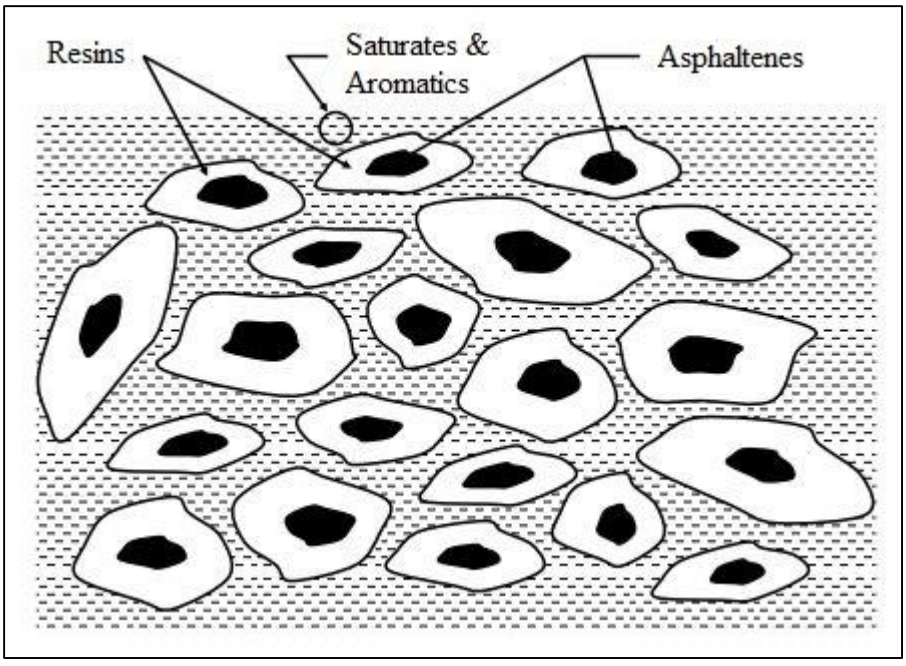

Figure II-4: Schematic of asphalt components.

Asphaltenes and resins are responsible for the visco-elastic properties of the asphalt at ambient temperatures (Read and Whiteoak, 2003). This is due to association of the polar molecules that leads to large structures, in some cases even to three-dimensional networks, i.e., 'GEL' type asphalt (Figure II-5a). The degree to which this association takes place depends on the temperature, the molecular weight distribution, the concentration of the polar aromatics and on the solvency power of saturates and aromatics in the maltenes phase. If the concentration and molecular weight of the asphaltenes is relatively low, the result will be a 'SOL' type asphalt (Figure II-5b). These colloidal states can largely reflect the rheological properties of asphalt.

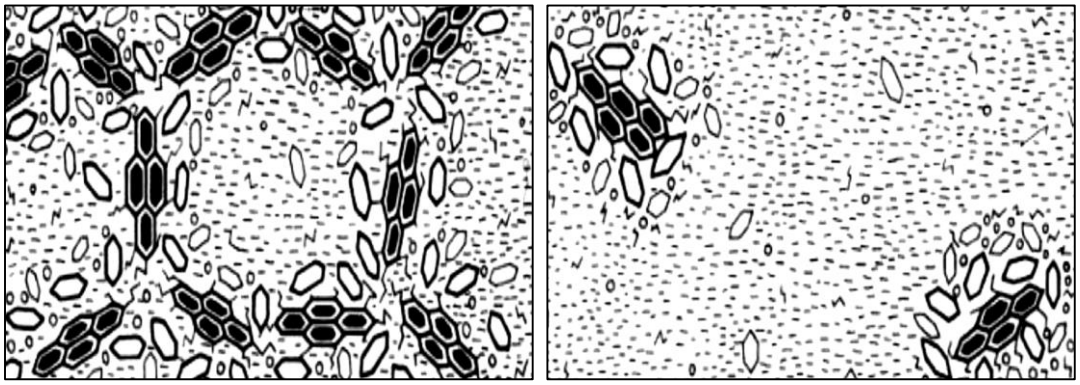

(a) (b)

Figure II-5: (a) GEL-type asphalt, and (b) SOL-type asphalt (Read and Whiteoak, 2003).

2.3 Aging Process in Asphalts

The factors affecting asphalt aging include characteristics of the asphalt binder and its content in the mix, nature of aggregates and particle size distribution, void content of the mix, production related factors, temperature and time (Lu and Isacsson, 2002). All these factors operate at the same time, making the process of asphalt aging very complex.

The aging process in asphalt pavements may be detrimental when excessive hardening or stiffening is observed, subjecting the pavement to cracking, either under traffic load or thermal stress. On the other hand, aging may be beneficial when a soft mixture hardens into an adequate pavement, avoiding rutting.

There are two types of aging in asphalt: (i) physical aging caused by temperature, and (ii) oxidative aging caused by air or oxygen. Physical aging is a reversible phenomenon that takes place as a consequence of cooling or quenching of amorphous materials from melt temperatures to below the glass-transition temperature (Bahia, 1991; Bahia and Anderson, 1993; Anderson and Marasteanu, 1999). Oxidative aging is irreversible hardening of asphalts. Figure II-6 illustrates these points schematically the effects of temperature, time, and oxidation on asphalt performance.

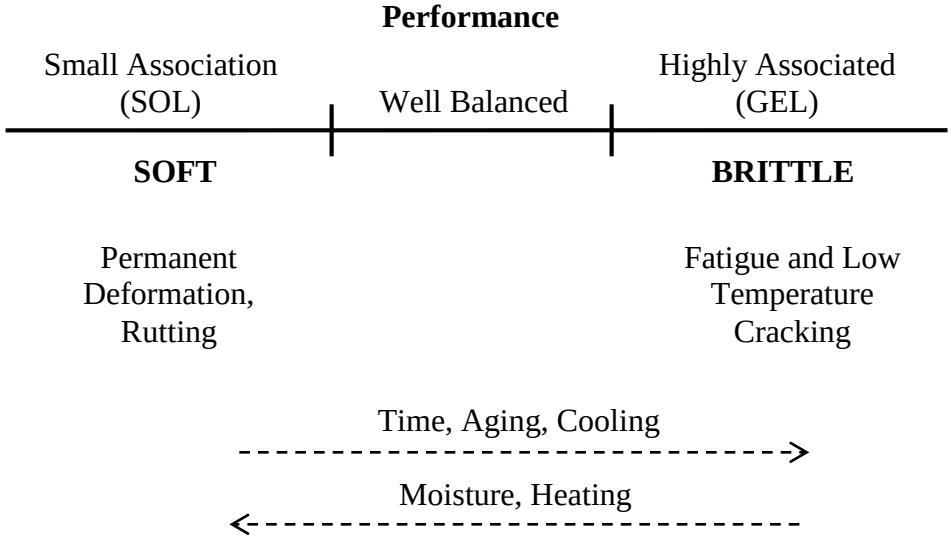

Figure II-6: Schematically effects of temperature, time, and oxidation on asphalt performance ("association" refers to the asphaltenes-resin association).

In general, as an asphalt binder ages, its viscosity increases and it becomes stiffer. The following factors have been reported to contribute to age hardening of the asphalt binder during mixing and/or in service:

(a) Oxidation: Oxidation is the reaction of oxygen with the binder. The rate depends on the composition of the asphalt and the temperature. According to Petersen (2009), the aging in asphalt binders occurs when the highly reactive hydrocarbons react with the oxygen in the atmosphere, following a free-radical mechanism that results in the formation of oxygenated compounds, such as ketones, carboxylic acid anhydrides and sulfoxides. Oxidation is the major factor responsible for the irreversible hardening of asphalts (Petersen, 2009).

(b) Volatilization: Volatilization is the evaporation of the light fractions from binders and is primarily a function of temperature, mainly occurring above the boiling temperature of the lighter fractions (approximately 150°C). It is usually not a significant factor contributing to long term aging in the pavement (Roberts et al., 1996).

(c) Polymerization: Polymerization is a combination of like molecules to form larger molecules, resulting in a progressive hardening. At low-temperatures the rate of association is considered slow due to the higher viscosity of the binder (Petersen and Harnsberger, 1998).

(d) Thixotropy: Thixotropy (Steric Hardening) is a progressive hardening due to the formation of a structure within the binder over a period of time, which can be destroyed to a degree by reheating and working the material (Bell et al., 1994).

(e) Syneresis: The separation of less viscous liquids from the more viscous asphalt binder molecular network. The liquid loss hardens the asphalt and is caused by shrinkage or

rearrangement of the asphalt binder structure due to either physical or chemical changes (Roberts et al., 1996).

(f) *Separation:* Separation is the removal of the oily constituents, resins, or asphaltenes from the bitumen caused by absorption by some types of porous aggregates (Roberts et al., 1996).

It is generally agreed that the aging process occurs in two distinct steps: (1) "short term aging" during construction (plant mixing, placement, and compaction) and (2) "long term aging" during the service life of the pavement. Significant aging takes place during short term aging where the binder is subject to high-temperature during production of the asphalt mixture. At this aging stage, both oxidation and volatilization processes take place (Roberts et al., 1996). The hardening of the binder during the service period of the pavement (long term aging) is mainly due to oxidation.

Figure II-7 demonstrates the significant difference in the rate of change for aging index between short term and long term aging. The aging index calculated is the ratio of viscosity of an aged binder to the viscosity of a virgin binder.

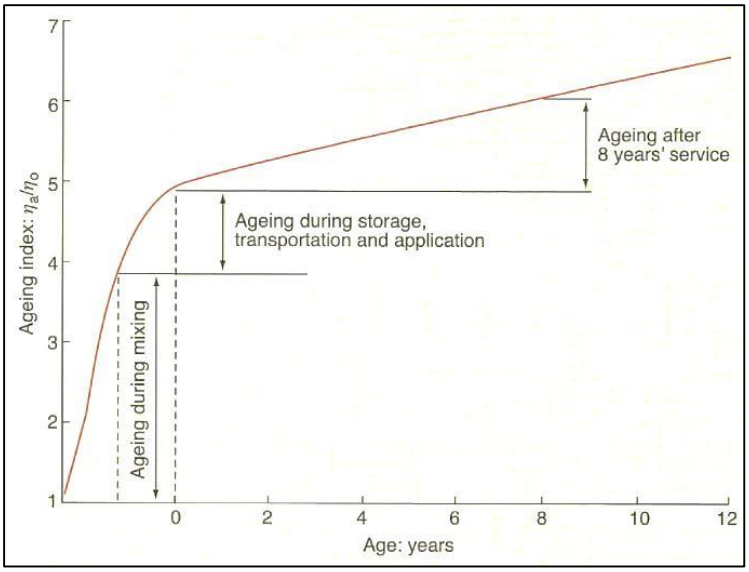

Figure II-7: Stages of in service aging (Read and Whiteoak, 2003).

2.3.1 Oxidative Aging of Asphalts

During the oxidative aging process of asphalt binders, the concentration of polar functional groups increases, resulting in an immobilization of molecules through intermolecular association (Petersen, 2009). Hence, the molecules or molecular agglomerates lose sufficient mobility to flow past one another under thermal or mechanical stress. This results in embrittlement of the asphalt, making it more susceptible to fracturing or cracking and resistant to healing (Tarefder and Arisa, 2011).

Asphaltenes and resins have heteroatoms that are strongly associated with polar functional groups. Therefore, these molecules have strong interaction and/or association forces and are highly reactive with highly electronegative oxygen (Tarefder and Arisa, 2011).

The changes in the asphalt fractions during oxidation have been observed as a conversion of components from the more non-polar fractions to the more polar fractions, as oxygen-containing functional groups are formed in the asphalt molecules (Petersen 2009).

According to the literature (Lu and Isacsson, 2000; Dehouche et al., 2012), thermo-oxidative aging increases the content of large asphalt molecules and decreases the content of small molecules, leading to an increase in the molecular weight of the asphalt binders. Because the various asphalt fractions have different reactivities toward oxidation, during oxidative aging a reduction of aromatics content is observed along with an increase in the content of resins and asphaltenes (Dehouche et al., 2012). Oxidation causes the oils (i.e., maltene fraction: naphthene aromatic and saturates) to convert to resins, and the resins to convert to asphaltenes (Rostler and White, 1962). The change in asphaltene-maltene ratio that occurs during oxidation affects the stiffness properties of the asphalt (O'Sullivan, 2011). Changes in the content of saturates are almost negligible due to their inert nature (Liu et al., 1998).

According to Tarefder and Arisa (2011) the association, agglomeration, and interaction of asphaltene and resin mainly depend upon the temperature and the amount of oxygen available. Petersen et al. (1974) showed that at high-temperatures 87% of the total oxidation occurred in the polar aromatic fractions (i.e., polar asphaltenes and resins) of the asphalt.

Asphaltenes are less likely to oxidize by air at ambient temperatures. However, at temperatures around 160 °C the molecular mobility of these molecules increases. Because of high molecular mobility, resin and asphaltene molecules become unassociated and susceptible to oxidation (Tarefder and Arisa, 2011).

The major types of functional group formed during asphalt oxidation have been identified as ketones and sulfoxides; smaller amounts of dicarboxylic anhydrides and carboxylic acids are formed during the later stages of oxidation (Plancher et al., 1976; Petersen and Harnsberger, 1998) (Figure II-8). Anhydrides, carboxylic acids and ketones are normally classified into carbonyl

functional group. The content of carbonyl compounds and sulfoxides increase during aging, and the degree of the changes is dependent on the asphalt binder source.

According to Petersen and Harnsberger (1998), asphalts with higher content of asphaltenes presented a slower increase of the carbonyl functionality, and higher changes in dynamic shear modulus; the reverse trend was observed for asphalts with lower content of asphaltenes (i.e., faster increase of the carbonyl functionality was associated with small change in the dynamic shear modulus).

Plancher et at. (1976) showed that the asphaltenes fraction is the dominant component controlling asphalt viscosity, and their effects on viscosity are different regarding the asphalt source. According to Petersen et al. (1996), the viscosity increase correlates directly with ketone formation, where each asphalt binder has its unique ketone-viscosity relationship. It has been proposed that the ketone functional group alone is not inherently responsible for the viscosity increase, but that its formation sufficiently changes the polarity, and thus the solubility, of the associated condensed aromatic ring components to cause them to agglomerate and become part of the asphaltene fraction, thus increasing viscosity (Petersen et al., 1996). This strongly implies that the ketones formed on aging are responsible for the formation of additional asphaltenes (Davis et al., 1966; Petersen et al., 1971; Petersen et al., 1993).

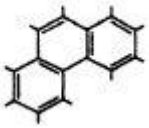

Polynuclear Aromatic (1)

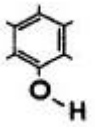

Phenolic (1)

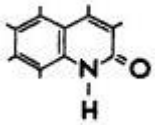

2-Quinolone Type (1)

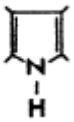

Pyrrolic (1)

Pyridinic (1)

- S -

Sulfide (1)

Sulfoxide (2)

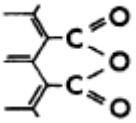

Anhydride (2)

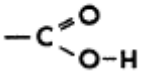

Carboxilic Acid (1, 2)

Ketone (2)

(1) Naturally occurring; (2) Formed on oxidative aging

Figure II-8: Chemical functionality in asphalt molecules normally present or formed on oxidative aging (Petersen, 1984).

2.3.2 Chemical Oxidation Mechanisms

A dual sequential asphalt oxidation mechanism was proposed by Petersen and Harnsberger (1998) (Figure II-9). They proposed that the rapid initial oxidation rate of asphalt results from reaction of oxygen with limited amounts of highly reactive hydrocarbons. Final oxidation products of this initial reaction are sulfoxides and, most likely, ring aromatization. During this initial reaction, a slower oxidation reaction of asphalt benzylic carbons is initiated; final products are ketones and sulfoxides. The ratio of ketones to sulfoxides formed and the rate of age hardening

were found to be dependent on temperature and oxygen pressure. Petersen and Harnsberger (1998) showed that the ratio of ketones to sulfoxides is also highly dependent on asphalt component compatibility (composition), with greater compatibility yielding more ketones relative to sulfoxides.

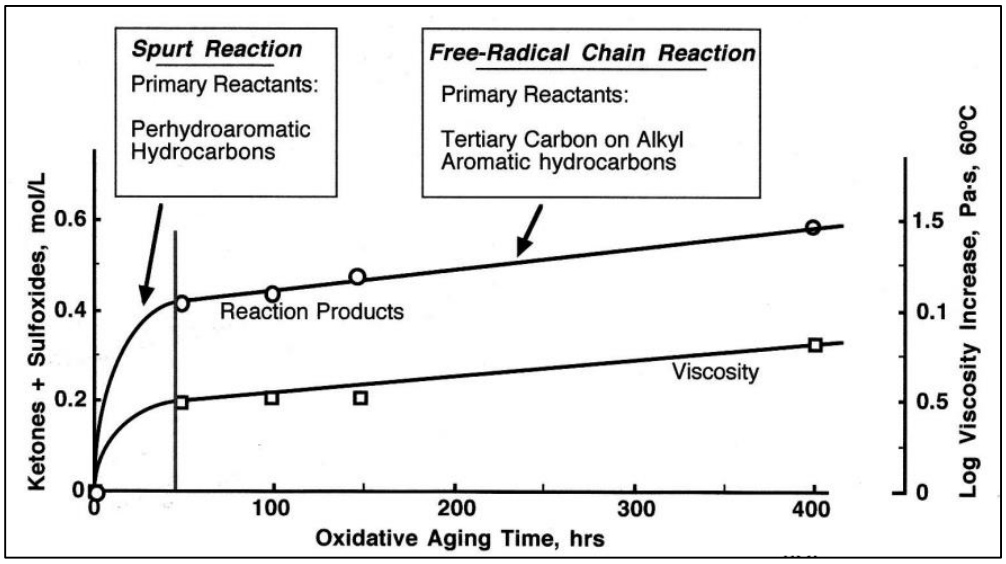

Figure II-9: Typical kinetics of the asphalt dual oxidation mechanism (Petersen, 2009).

2.4 Influence of Mineral Aggregates on Aging

Since asphalts binders are used in conjunction with mineral aggregates in pavements and roofing, the interactions between binders and these minerals is of concern. Barbour et al. (1974) showed that when the asphalt fractions were oxidized separately, the mineral aggregate surfaces were found to catalyze the oxidation of the lower polarity fractions.

Studies (Anderson et al., 1994; Read and Whiteoak, 2003) have shown that aggregates with low adsorption of highly polar fractions (e.g. Quartzite) exhibit the greatest catalytic effect in

asphalt oxidation, while aggregates with high adsorption (e.g. Limestone) exhibited the smallest catalytic effect. A study performed by Curtis et al. (1993) indicated that the presence of mineral material (i.e., filler, sand and aggregates) delays the increase of the viscosity of binders upon aging compared to bulk bitumen aging for equivalent aging times. This difference in viscosity is thought to have been caused by the aggregate particles adsorbing some of the oxidative functional groups that prevent formation of viscosity build-up (Curtis et al., 1993). Therefore, the adsorption process is responsible for changes in the mechanical properties (e.g., stiffness, viscosity) and thermo-volumetric properties (e.g., coefficients of thermal contraction and glass-transition temperature) of the asphalt mastics (Clopotel, 2012).

Plancher et al. (1976) showed that the beneficial effect of hydrated lime addition to the asphalt binder in reducing oxidative hardening is due to two effects: (i) lime reduces the formation of oxidation products by the removal of oxidation catalysts; and (ii) lime removes reactive polar molecules that would interact with oxidation products.

2.5 Influence of Aging on Cracking Behavior of Asphalts

The aging phenomenon has considerable effects on both asphalt binder and HMA properties, such as cohesive and adhesive bond strengths, stiffness, viscoelastic properties, fracture properties, healing, and recovery during rest periods (Knorr et al., 2002).

It is speculated that excessive molecular structuring leads to brittle material which tends to crack; on the other hand, lesser molecular structuring leads to materials which will deform under stress (Robertson, 1991). In asphalt binders, chemical aging leads to a global hardening of the material, therefore, increasing the cracking probability (Lesueur, 2009).

The chemical change that occurs in asphalt binders due to oxidative aging results in an increase of both viscous and elastic properties of the binder. Therefore, aged asphalt binder sustains high shear stress with deformation (high elastic stiffness), and it is unable to relax the stress through viscous flow (Jung, 2006). As a result, the pavement has a higher susceptibility to fatigue and thermal cracking.

2.5.1 Low-Temperature Cracking of Asphalts

Thermal cracking of hot-mix asphalt (HMA) pavements is one of the primary distress mechanisms in colder climates. It has generally been accepted that volume relaxation due to slow crystallization and/or asphaltene aggregation can cause asphalt cement to lose its ability to deform (Togunde and Hesp, 1997).

Low-temperature cracking is manifested as a set of parallel surface-initiated transverse cracks of various lengths and widths (Marasteanu et al., 2007). The cracks are predominantly perpendicular to the center line of the roadway. These cracks can allow water to infiltrate the pavement, therefore, reducing the structural capacity of the pavement. Furthermore, as the cracks grow in width, the ride quality of the pavement will be affected, leading to secondary cracking and structural distress (Anderson et al., 2001).

Low-temperature cracking of asphalts is associated with the volumetric contraction that occurs as the material experiences a decrease in temperature (Bahia, 1991; Bahia and Anderson, 1993). At low-temperature the non-polar materials of asphalt binders tend to organize into a very rigid material, and this rigid material will contract (shrink) (Robertson, 1991). The excessive brittleness due to the increase in stiffness and decrease in the ability to relax stress leads to the buildup of thermally induced stress and ultimately cracking of mixtures in pavements (Tabatabaee

et al., 2012a). Asphalt pavements are restrained from significant movement, thus thermally induced contraction can lead to significant stress buildup in the pavement.

As a further complication, asphalt concrete tends to become oxidized, leading to material embrittlement with time. The amount of aging, or the aging rate, has been found to vary significantly depending upon crude source, refining techniques, additives, climate, and characteristics of the mixture (i.e., asphalt content and air voids) (Buttlar et al., 2011).

Other factors that influence low-temperature cracking in HMA are coefficients of thermal expansion/contraction, glass-transition temperature, stiffness, relaxation modulus, cooling rate, shape of master curve at low-temperatures and tensile strength (Jung and Vison, 1994). Asphalt aging can influence low-temperature cracking of HMA due to two factors: (i) the increase in stiffness of the asphalt binder with age and the resulting hardening causes the pavement to become more susceptible to thermal cracking; and (ii) the probability of exposure to a low critical temperature increases with time.

2.5.2 Asphalt Stiffness

In asphalt binders the two most important considerations for low-temperature cracking are the stiffness or consistency (i.e., viscosity or penetration) at low-temperature, and the material temperature susceptibility (i.e., the range in consistency with temperature) (Jung and Vison, 1994). For example, lower viscosity (or higher penetration) of an asphalt binder will produce a lower rate of increase in stiffness with decreasing temperature; therefore, reducing the potential of low-temperature cracking. Low-temperature thermal cracks have been controlled historically by limiting the asphalt binder stiffness. Assuming similar asphalt binder tensile strengths and

coefficients of thermal expansion/contraction, binders with a higher stiffness will crack at a higher temperature than softer binders (Kim, 2005).

Binder oxidation has a significant impact on age-related pavement failure, since through oxidation the binder becomes stiffer and more brittle reducing the performance of the pavement (Petersen et al., 1993; Domke et al., 2000; Jung, 2006).

Aging changes the time-temperature dependence of asphalt binder, which is known to be viscoelastic (Swiertz, 2010). Rheological curves demonstrate an increased effect of aging on physical properties with increased time and increased temperature (Bahia et al., 2009). As asphalts age, they harden; this results in a progressive increase in the stiffness modulus of the asphalt, together with a reduction in its stress relaxation capability (Read and Whiteoak, 2003).

It can be seen in Figure II-10 that the aging of asphalt binder will cause an increase in the material complex modulus (|G*|), and a decrease in the loss tangent (δ). The complex modulus is correspondent to asphalt stiffness, and m-value to loss tangent. As a result of aging the asphalt layer will become less deformable, creating more stresses per unit strain. This increase in binder stiffness is not detrimental to rutting or other plastic deformation resistance, but is seen as detrimental for fatigue and thermal cracking at intermediate and low-temperatures, respectively (Swiertz, 2010). Thermal cracking is further enhanced with the drop in loss tangent, which is proportional to the capacity of asphalt to relax stresses (m-value). The increase in complex modulus allows for more stresses to build up within the pavement during heating and cooling cycles, while the decrease in loss tangent does not allow these stresses to dissipate, creating thermal cracks. However, the drop in loss tangent allows for a decrease in the ratio of energy stored to energy dissipated, hence the pavement becomes more elastic (Swiertz, 2010). This increase in elasticity is beneficial for fatigue and rutting resistance (Bahia and Anderson, 1995).

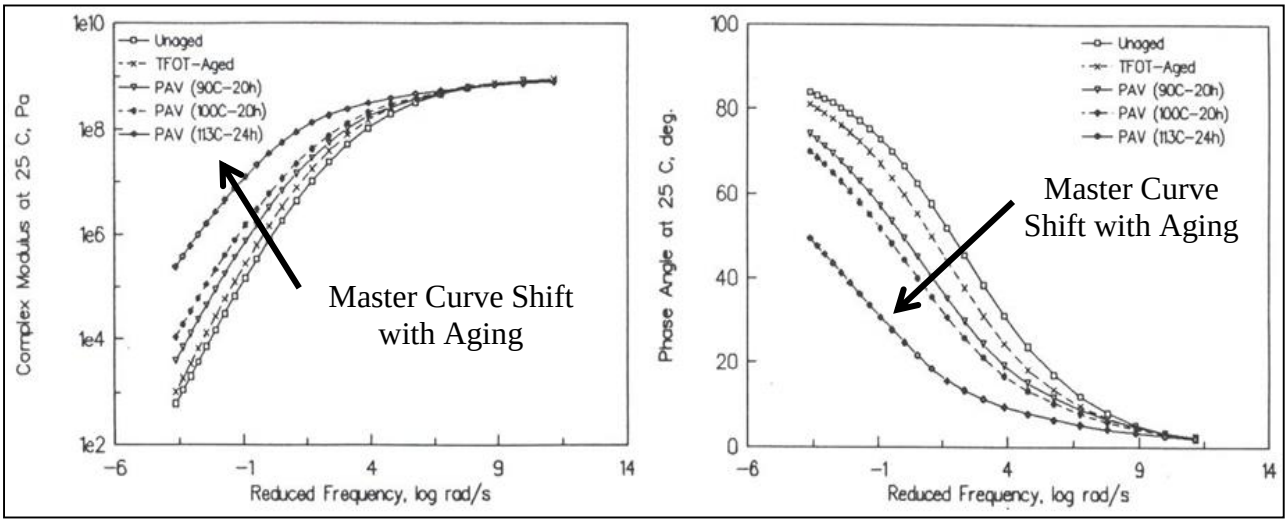

Figure II-10: Rheological master curve shifts due to oxidative aging conditions (Bahia & Anderson, 1995).

2.5.3 Glass-Transition Temperature

The glass-transition temperature (T_g) is a fundamental property of amorphous materials, including asphalt binders. Below the glass-transition temperature there is insufficient thermal energy in a material to allow large-amplitude molecular motion (Turner and Branthaver, 1997). Therefore, the T_g is a temperature below which a material shows glassy (elastic) behavior and above which shows viscous (rubbery) behavior. It is defined as the temperature at which there is a change in the slope of the specific volume-temperature curve. The glass-transition temperature is a point temperature at which the rate of change of specific volume with respect to temperature undergoes a discontinuity (Tarefder and Arisa, 2011). The concept of T_g is schematically shown in Figure II-11.

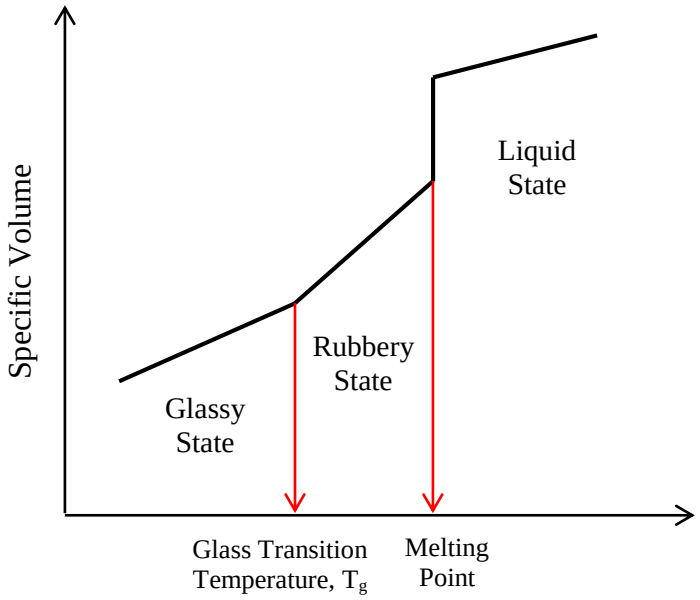

Figure II-11: Schematic of the glass-transition temperature.

The transition to a glassy state is accompanied by a change in the mechanical, optical and thermodynamic properties of the material (Kriz et al., 2008). The glass-transition temperature is important to understand the hardening behavior, which generally appears below T_g.

The T_g has been considered as a characterization parameter that helps to determine the process and aging level of asphalts (Dong et al., 2005). The glass-transition temperature depends on the asphalt source and the degree of aging, since complex arrangements of molecules are formed (Turner and Branthaver, 1997). There are speculations in the asphalt community that the glass-transition temperature of asphalt is responsible for low-temperature cracking (Marasteanu et al., 2007; Tabatabaee et al., 2012a; Tabatabaee et al., 2012b). Asphalt can have a wide range of values of the glass-transition temperature depending upon its composition (e.g., between -3.1 °C and -27.5 °C) (Tarefder and Arisa, 2011).

Mineral fillers are not amorphous, thus they do not have a glass-transition temperatures. Therefore, when testing the low-temperature performance of asphalt mastics the changes in the glass-transition could be attributed to the modification of the asphalt matrix. This phenomenon is independent of the mechanical reinforcement effect of the filler (Droste and Dibenedetto, 1969).

Considering asphalt mastics it can be assumed that if there is interaction between the mineral filler and the asphalt matrix, the molecular properties of the asphalt matrix will be affected. The nature of the molecular change will, therefore, depend specifically on the type of interaction involved. It follows that an asphalt mastics, in which a significant fraction of the binder is in contact with a mineral filler surface and which has interaction between filler and binder, should exhibit the degree of interaction (regardless of mechanism) by changes in the thermodynamic and viscoelastic properties of the asphalt matrix.

Glass-transition temperature has been related to the average molecular weight of asphalts, and it also complements the viscoelastic properties of these materials at low-temperature (Jiménez-Mateos et al., 1996). Conducting glass-transition measurements on asphalts with different amount of asphaltenes, Wada (1960) showed that the glass-transition temperature becomes higher with an increase of the asphaltenes content (Figure II-12).

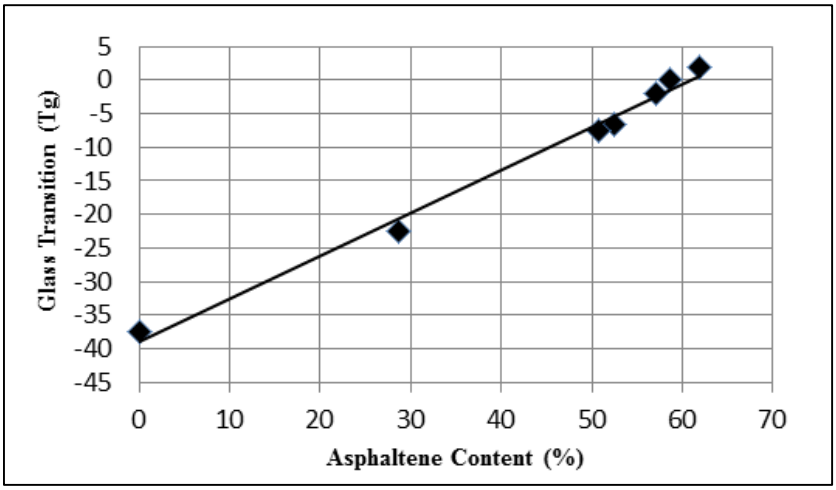

Figure II-12: Increase in glass-transition temperature with an increase of the asphaltenes content (Recreated from Wada, 1960).

2.5.4 Coefficients of Thermal Expansion/Contraction

Engineering materials generally expand when subjected to an increase in temperature, and they contract when subjected to a decrease in temperature, under restriction-free conditions. The thermal deformation (i.e. expansion-contraction) of a material is calculated using a thermal coefficient, denoted by α. In general mechanics, α is termed the coefficient of thermal expansion. In pavement engineering, since the concern is the stress built up at low-temperatures, α is often called the coefficient of thermal contraction. The thermal coefficient describes the relationship between the change in temperature and the change in thermally induced strain.

The coefficient of thermal expansion/contraction (CTE) is a property which describes the potential for thermal deformation of the asphalt material. In HMA, thermal cracking will occur when the asphalt binder becomes too stiff to withstand the thermally induced stress, and it is related to the coefficient of thermal expansion and the relaxation characteristics of the mixtures (Read and Whiteoak, 2003).

Literature states the importance of the non-linearity of the CTE of both asphalt binders and mixtures in the overall thermal cracking performance of the pavement (Bahia, 1991; Bahia and Anderson, 1993; Nam and Bahia, 2009).

Thermal deformation of many elastic materials is nearly a linear function of temperature in the temperature range of interest. For asphalt binders, however, a linear approximation of the thermal deformation is no longer appropriate because the glass-transition exists usually within the temperature range of interest (Nam and Bahia, 2009).

Oxidative aging affects asphalt binder properties. Therefore, the glass-transition temperature values and the coefficients can significantly influence the calculations of both thermal stress and thermal strain in thermal analysis.

2.6 Oxidative Aging Evaluation of Asphalt Binders Using Gel Permeation Chromatography

Gel Permeation Chromatography is used to determine the molecular size distribution (MSD) of asphalt binders (aged, unaged, modified and unmodified), providing a distinct and reproducible molecular-size distribution curve (chromatogram) of the asphalt sample in solution (Altgelt, 1965; Gehrke and Ruyle, 1968; Jacobson et al., 1968; Snyder, 1969; Bynum and Traxler, 1970; Haley, 1971; Jennings et al., 1980; Kim and Burati, 1993; Churchill et al., 1995).

In this method, the asphalt binder is dissolved in a solvent and is injected into the GPC system. The injected sample travels through a series of columns which separates the sample based on molecular size. The larger molecular size particles exit the columns first and are detected by the system's detectors. The smaller molecular size particles travel into the pores of the columns

and, therefore, have longer retention times. As a result, a molecular size distribution (which can be thought of as analogous to a type of sieve analysis of the sample) is obtained (Figure II-13).

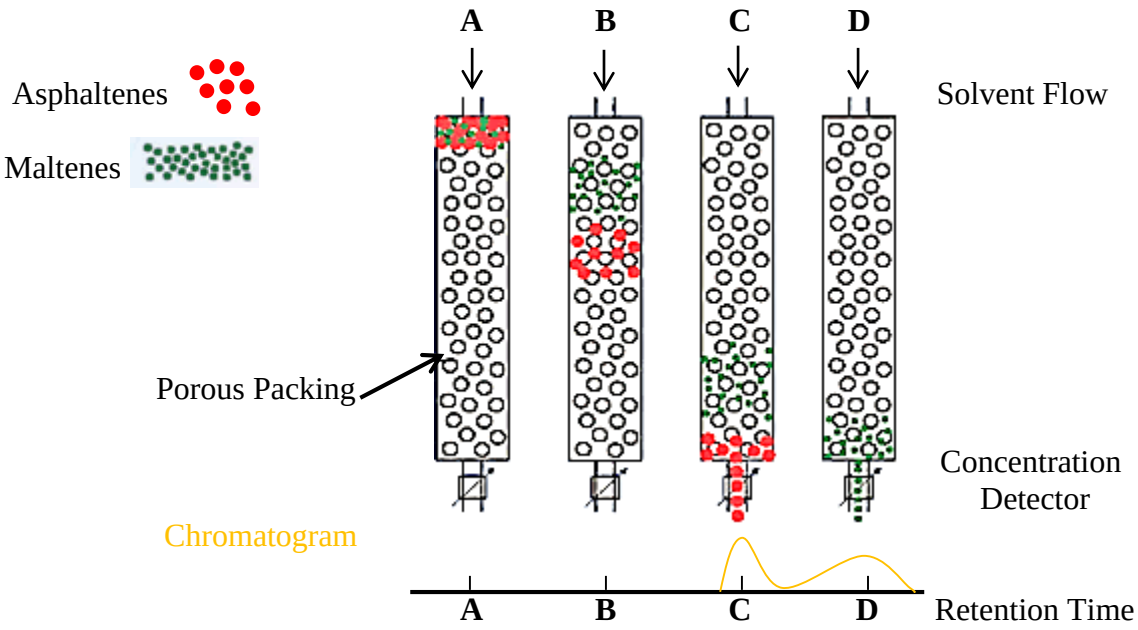

Figure II-13: Example of Gel Permeation Chromatography.

One of the great advantages of Gel Permeation Chromatography is its ability to separate by molecular size rather than by solubility or adsorptivity. The GPC is a simple separation technique available that responds to molecular weight alone and not to chemical structure. This feature makes GPC especially suited for fractionating complex mixtures, like asphalt binders. For complex materials, ordinary fractionation methods fail because they are usually based on solubility, which in turn differentiates by both molecular weight and chemical structure. Regular chromatographic methods are based on either solubility or on adsorptivity, which also depends on both molecular properties (Altgelt, 1965).

Table II-1 presents an overview of the literature involving the application of Gel Permeation Chromatography (GPC) to asphalt binders.

Table II-1: Examples of application of GPC to asphalt binders.

Gel Permeation Chromatography Application	Literature
Determine asphalt molecular weight distributions.	Snyder, 1969; Ying et al., 2013.
Use of GPC to characterize asphalt properties and the relationship of GPC parameters to pavement performance.	Jennings et al., 1980; Jennings et al., 1993; Yapp et al., 1991.
Evaluate the effects of oxidative aging on asphalt binders and mixtures using the gel permeation chromatography procedure.	Kim and Burati, 1993; Churchill et al., 1995; Siddiqui and Ali, 1999; Lu and Isacsson, 2002; Doh et al., 2008; Lee et al., 2009.
Estimate absolute viscosity of aged binder in Reclaimed Asphalt Pavement (RAP) by using gel permeation chromatograph technique.	Kim et al., 2006.
Characterize blends of laboratory-aged crumb rubber modified binders (CRM) and rejuvenating agents by using GPC.	Shen et al., 2007.
Demonstrate that GPC can be used as a simple screening test to identify when asphalt binder has been modified with a polymer.	McCann et al., 2011.
Evaluate Reclaimed Asphalt Pavement (RAP) blending efficiency by using gel permeation chromatograph technique.	Bowers, 2013.
Investigate the oxidative aging levels of polymer-modified asphalt produced with Warm Mix Asphalt (WMA) technologies.	Kim et al., 2013.
Correlated an increase in large molecular sizes to the complex modulus (|G*|) of asphalt binder.	Zhao et al., 2013.

The Gel Permeation Chromatography test is adopted from the polymer industry and includes the classification of the chemical composition of the asphalt binder into three groups based on molecular size by analyzing the GPC chromatographic profiles (chromatograms) of the binders (Al-Abdul Wahhab et al., 1999; Xiao et al., 2009). These groups are the large molecular size (LMS), medium molecular size (MMS), and small molecular size (SMS).

Jennings et al. (1980) divided the GPC chromatogram into 13 equal elution time areas, and classified the molecules eluted during the first third of the elution period as large molecular size (LMS), those eluted during the second third as medium molecular size (MMS), and those eluted in the last third as having small molecular size (SMS). Figure II-14 shows a typical chromatogram for an asphalt binder sample, showing the three parts of the elution time.

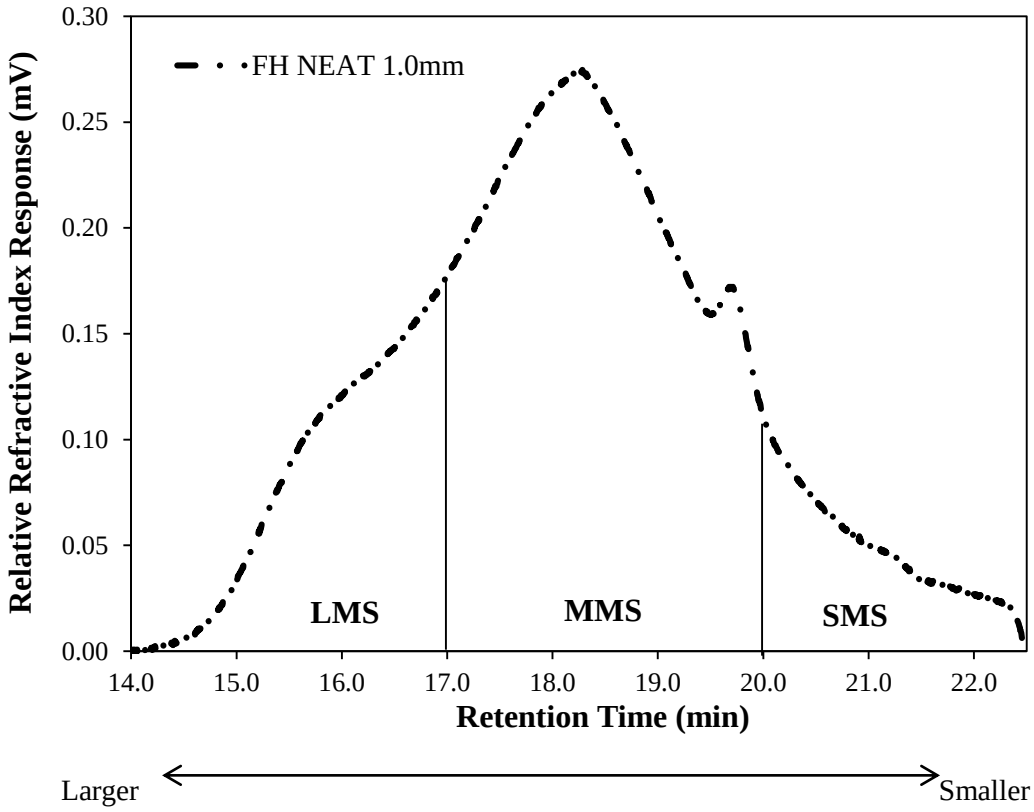

LMS = large molecular size; MMS = medium molecular size; SMS = small molecular size

Figure II-14: Typical GPC chromatogram of an asphalt binder showing three elution times fractions.

The molecular size distribution can have a significant effect on the physical properties of the asphalt binders such as viscosity, penetration, temperature susceptibility, and viscosity ratio

(Garrick, 1994; Al-Abdul Wahhab et al., 1999). Additionally, the classification based on molecular size was found to be effective in analyzing the aging process that affects asphalt binders (Jennings et al., 1980; Churchill et al. 1995; Kim et al., 2006; Bowers, 2013).

The chromatograms provide some insight about what fractions of the asphalt binder were affected after oxidative aging. Upon aging, the LMS fraction tends to increase (Glover et al. 1988). The increment of LMS due to aging was known to create increasing viscosity (Jennings et al., 1980; Churchill et al. 1995) and loss of consistency (Noureldin and Wood, 1989). The LMS has been related to low-temperature cracking of pavements (Jennings et al., 1980; Plummer and Zimmerman 1984). Other studies (Zenewitz and Tran, 1987; Glover et al. 1988; Enustum et al., 1990) have also found that the lower the LMS and higher the SMS contents, the higher is the asphalt "tenderness".

The GPC chromatogram defines the molecular size distribution (MSD) of asphalt binders. The changes in the molecular size distribution due to aging can significantly influence the asphalt binder consistency and consequently its physical properties (Shen et al. 2006). Since asphalts binders are used in conjunction with mineral aggregates in pavements and roofing, the interactions between binders and these minerals and the resulting changes in molecular size distribution after oxidative aging is of concern and is thus an important focus of the present study.

III. Materials and Methods

3.1 Materials

3.1.1 Fillers

Four types of mineral fillers with varying properties (Table III-1) were selected: hard limestone (LH_1), hard granite (GH_1), soft dolomite (DS_2), and hydrated lime (HL). The selected fillers have also different mineralogy as revealed by their chemical compositions. Mineral fillers with different chemistry show differences in adsorption of polar components from the asphalt binder, since each aggregate of a given bulk mineralogical type has a unique surface chemistry.

Table III-1: Fillers characteristics and chemical composition after (NCHRP 9-45).

Filler Characteristics								
Filler	**Rigden Voids (%)**	**Fine Modulus**	**Methylene Blue Volume**	**Specific Gravity**	**Loss on Ignition**	**Solubility (%)**	**Surface Area (m^2/g)**	**Average Pore Dimension (Å)**
LH_1	32.2	5.63	0.62	2.65	0.1	1	1.07	148.6
GH_1	42.6	4.06	2.35	2.66	0.36	2.3	2.17	224.5
DS_2	29.4	4.73	1.82	2.7	0.35	0.7	1.98	186.7
HL	------	------	------	------	------	------	21.05	306.5

Filler Chemical Composition						
Filler	**CaO**	**SiO_2**	**Al_2O_3**	**FeO**	**MgO**	**K_2O**
LH_1	43.1	5.0	1.9	0.1	5.4	0.3
GH_1	3.5	62.2	15.0	3.6	1.8	3.3
DS_2	27.0	20.2	4.5	0.5	15.7	1.9

The selected fillers also present very different Braunauer-Emmett-Teller (BET) surface areas, as shown in Table III-1. Braunauer-Emmett-Teller (BET) theory explains the physical adsorption of gas molecules on a solid surface and serves as the basis for an important

analysis technique for the measurement of the specific surface area of a material (Braunauer et al., 1938).

High surface area implies that a single filler particle can potentially adsorb more asphaltenes as there is a higher interface surface between the two materials. Clopotel (2012) showed that the only filler factor that controls adsorption in asphalt mastics is the surface area.

A fifth filler type comprised of zirconia and silica with 0.5 mm diameter was also included in the study for comparison to the mineral fillers. This filler was denominated “inert”, assuming that its composition will not interact with the asphalt binder. The major motivation for the selection of zirconia-silica fillers is the fact that combination of zirconia and silica is a thermally stabile material (Sajjad et al., 2012).

All fillers used for production of mastics in this study were passed through the #200 sieve (0.075 mm), with the exception of the comparative experiment between the “inert” filler and granite mastics. For these tests, in order to establish a comparison between both inert and mineral filler without the confounding effect of different size distributions, granite aggregate with particle size passing the No. 30 sieve (0.6 mm) and retained by the No. 50 (0.3 mm) sieve was used for comparison to the “inert” filler, to have a similar average diameter.

3.1.2 Asphalt Binders

Two asphalt binders commonly used in the Mid-West region of the United States were selected in this study: Flint Hills (FH) PG 64-22 and Valero (VAL) PG 64-16. A low (10% by volume) and a higher (40% by volume) concentration of mineral filler were selected to produce the asphalt mastics. The asphalt mastics (i.e. asphalt binder + mineral filler, Figure III-1) were produced by mixing at 150 ˚C for 30 minutes.

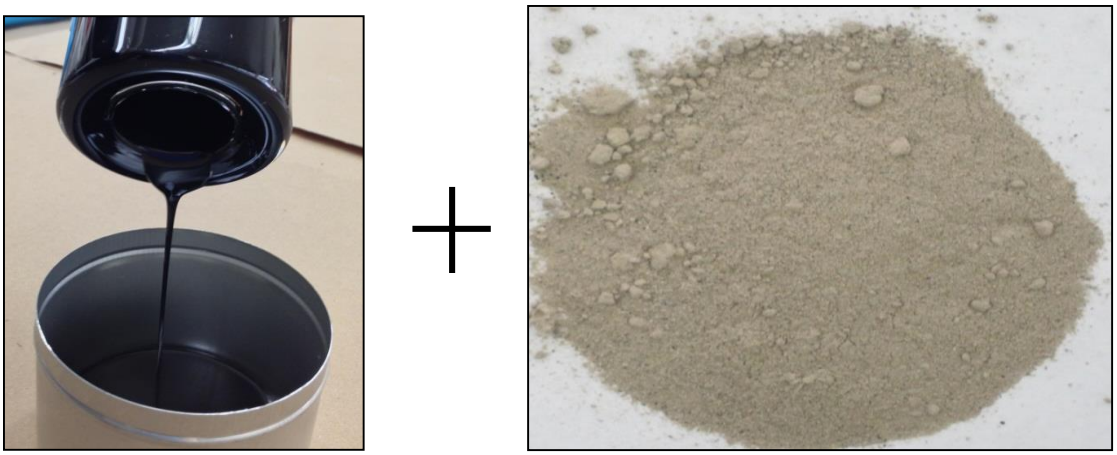

(a) Asphalt binder (b) Particles smaller than 0.075 mm

Figure III-1: Asphalt mastic.

3.2 Methods

3.2.1 Pressure Aging Vessel Test Procedure

The Pressure Aging Vessel (PAV) (Figure III-2) is an aging procedure proposed by the Strategic Highway Research Project (SHRP) to simulate long-term field oxidative aging of asphalt binders. In this procedure, samples are aged in a heated vessel pressurized to 2.10 MPa (305 psi or 20.7 atmospheres) in order to simulate in-service aging over a 7 to 10 year period. The vessel temperature is 100°C. Samples are then stored for use in mechanical tests. For the PAV aging, samples were prepared by pouring 50 g of hot asphalt into the metal pan. For the asphalt mastics, the sample weight was determined dividing 50 g by the percent by mass of binder. Table III-2 shows the PAV tests conducted for this study.

Figure III-2: (a) Pressure Aging Vessel (PAV); (b) PAV pan; and (c) PAV pan holder.

Table III-2: PAV tests.

Sample	PAV Conditioning Time (h)
FH 64-22 Neat	0, 3, 6, 24, and 30
FH 64-22 + LH_1 10%	0, 6, and 24
FH 64-22 + LH_1 40%	0, 6, and 24
FH 64-22 + GH_1 10%	0, 6, and 24
FH 64-22 + GH_1 40%	0, 6, and 24
FH 64-22 + GH_1 R_{50} 40%	0 and 24
FH 64-22 + Inert Filler 40%	0 and 24
FH 64-22 + DS_2 10%	0 and 24
FH 64-22 + DS_2 40%	0 and 24
FH 64-22 + HL 4%	0 and 24
FH 64-22 + HL 10%	0 and 24
VAL 64-16 Neat	0 and 24
VAL 64-16 + LH_1 10%	0 and 24
VAL 64-16 + LH_1 40%	0 and 24
VAL 64-16 + GH_1 10%	0 and 24
VAL 64-16 + GH_1 40%	0 and 24
VAL 64-16 + DS_2 10%	0 and 24
VAL 64-16 + DS_2 40%	0 and 24
VAL 64-16 + HL 4%	0 and 24
VAL 64-16 + HL 10%	0 and 24

3.2.2 Asphaltenes Extraction Test Procedure

Neat Binder: Asphaltenes content was determined according to ASTM D 6560 - Standard Test Method for Determination of Asphaltenes (Heptane Insolubles) in Crude Petroleum and

Petroleum Products (2012), in which 5 grams of asphalt binder was mixed with 150 mL of n-heptane. The mixture was boiled under reflux for 120 minutes. The precipitated asphaltenes were removed from the solution by vacuum filtration using a Whatman 934-AH glass microfiber filter. After filtration, n-heptane was evaporated and the asphaltenes were obtained.

Asphalt Mastics: The asphaltene content of asphalt mastic was determined using the same procedure applied for the neat binder (Figure III-3a). However, further steps were added in order to separate the asphaltenes from the mineral filler. As it can be seen in Figure III-1a, after the evaporation of n-heptane, both asphaltenes and filler were collected in the microfiber filter. Therefore, toluene was added in order to dissolve the asphaltenes and to allow precipitation of the mineral filler. To achieve this, the solution was successively filtered under vacuum conditions in order to separate the insoluble fraction (i.e., the mineral filler) (Figure III-3b).

(a) (b)

Figure III-3: (a) Asphaltenes + filler precipitated; (b) Mineral filler separated from asphaltenes.

To re-precipitate the asphaltenes, the toluene + asphaltene solution was then separated using the rotary evaporator (Figure III-4). After this process, the amount of precipitated asphaltene was determined by mass.

Figure III-4: Rotary evaporator.

3.2.3 Glass-Transition Test Procedure

A dilatometric system was used to measure the glass-transition temperature of the asphalt binder and mastics (Figure III-5). Currently no formal standard for this device is available and therefore the test was performed following a modified version of the procedure developed by Bahia and Anderson (1993). Calculation of the glass-transition temperature (T_g) is based on a non-linear model proposed originally by Bahia (1991) and later successfully used by Nam and Bahia (2009) and Tabatabaee et al. (2012a). The relationship is shown in Equation III-1,

$$\varepsilon = \frac{\Delta V}{V_0} = C + \alpha_g\left(T - T_g\right) + ln\left\{\left[1 + e^{\frac{T-T_g}{R}}\right]^{R\left(\alpha_l - \alpha_g\right)}\right\} \quad \text{(III-1)}$$

where,

$\frac{\Delta V}{V_0}$ = relative change of volume;

C = intercept with no physical meaning;

α_l and α_g = liquid and glassy coefficients, respectively, of thermal contraction and expansion;

T_g = glass-transition temperature; and

R = parameter representing curvature between the two linear asymptotes

The formulation fits two linear portions to the curves above and below the nonlinear glass-transition region, the slopes of which are defined as the liquid (α_l) and glassy (α_g) coefficients of thermal contraction and expansion (Tabatabaee et al., 2012). The glass-transition temperature (T_g) is defined as the temperature at the intersection of the two linear sections. The parameter R represents the strength of the transition, which is a measure of the difference of slopes before and after the transition as well as the length and curvature of the transition region. Equation III-1 was used to calculate volumetric change at any given temperature in the present study.

The concept behind the procedure is based on precise measurements of volume change with time of an asphalt binder specimen when the temperature decreases at a constant rate (Tabatabaee et al., 2012). For the T_g test, the sample is prepared by pouring 10 g of hot asphalt into a circular silicone rubber mold with a diameter of 40 mm and a height of 8.0 mm. For the asphalt mastics, the sample weight was determined as described in Equations III-2 and III-3,

$$M_m = S_m \times V_m \quad \text{(III-2)}$$

$$S_m = S_b (1- \phi) + \phi S_f \quad \text{(III-3)}$$

where,

M_m = Mastic Weight (g)

V_m = 10 g

S_m = Mastic Specific Gravity

S_b = Asphalt Specific Gravity

ϕ = Volume Fraction

S_f = Filler Specific Gravity

In this system, the dilatometric cell is connected to a vertical capillary tube (i.e., ϕ = 1 mm) which has an open top end. The volume changes in the sample are calculated by estimating the change in the height of the ethyl alcohol column inside the capillary tube (Velasquez et al., 2011). The asphalt and mastic samples were cooled from 30 to -50 °C at a rate of 1 °C/min and the change in the height was measured at 5 second intervals. Table III-3 shows the binder tests conducted for this study.

Dilatometric cell

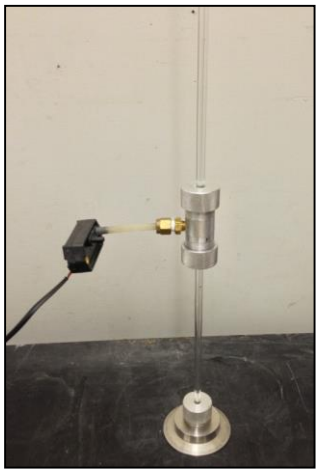

Capillary tube

Cooling system (Velasquez et al., 2011)

Figure III-5: Dilatometric system was used to measure the glass-transition temperature of the asphalt binder and mastics.

Table III-3: T_g tests.

Sample	PAV Conditioning Time (h)	Temperature Range (°C)	Cooling Rate
FH 64-22 Neat	0, 3, 6, 24, and 30	30 to -50	1 °C/min
FH 64-22 + LH_1 10%	0, 6, and 24	30 to -50	1 °C/min
FH 64-22 + LH_1 40%	0, 6, and 24	30 to -50	1 °C/min
FH 64-22 + GH_1 10%	0, 6, and 24	30 to -50	1 °C/min
FH 64-22 + GH_1 40%	0, 6, and 24	30 to -50	1 °C/min

3.2.4 Dynamic Shear Rheometer Test Procedure

The dynamic shear rheometer (DSR) (Figure III-4b) was proposed by the Strategic Highway Research Project (SHRP) and is used to characterize the viscous and elastic behavior of asphalt binders at medium to high-temperatures. The basic DSR test uses a thin asphalt binder sample (Figure III-6a) compressed between two circular plates. In this system, the lower plate is fixed while the upper geometry oscillates back and forth across the asphalt sample to create a shearing action. DSR tests were conducted on unaged and PAV aged asphalt binder and mastics samples.

(a) (b)

Figure III-6: (a) DSR sample, and (b) DSR equipment.

The DSR measures a specimen's complex shear modulus (|G*|) and phase angle (δ). The complex shear modulus (|G*|) can be considered the sample's total resistance to deformation when repeatedly sheared, while the phase angle (δ), is the lag between the applied shear stress and the resulting shear strain (Pavement Interactive, 2011). Larger the phase angles (δ) represent viscous the materials. Phase angle (δ) limiting values are: $\delta = 0°$, purely elastic material; and $\delta = 90°$, purely viscous material.

Frequency Sweep: In this study, a 1% strain amplitude was applied using a frequency sweep over the range of 0.1 through 30 Hz. For all tests, 8 mm diameter parallel plate geometry with a fixed 2 mm sample height was used. Frequency sweeps were conducted over a range of five temperatures (i.e., 10 °C, 20 °C, 25 °C, 30 °C, and 40 °C), and the data was used to produce a master curve using the time-temperature superposition principle and a fit to the Williams-Landel-Ferry (WLF) equation (Fesko and Tschoegl, 1971; Ferry, 1980; Klompen, 1996; Bahia et al., 2001). The selected reference temperature for the master-curves was 25 °C. It is expected that the shear modulus master curves can show the effect of stiffening due to oxidative aging. Table III-4 shows the DSR tests conducted for this study.

Table III-4: DSR tests.

Sample	PAV Conditioning Time (h)	Temperature (°C)	Reported Parameters
FH 64-22 Neat	0 and 24	10, 20, 25, 30, and 40	|G*|, δ
FH 64-22 + LH_1 10%			
FH 64-22 + LH_1 40%			
FH 64-22 + GH_1 10%			
FH 64-22 + GH_1 40%			
FH 64-22 + DS_2 10%			
FH 64-22 + DS_2 40%			
FH 64-22 + HL 4%			
FH 64-22 + HL 10%			
FH 64-22 + GH_1 R_{50} 40%			
FH 64-22 + Inert Filler 40%			
VAL 64-16 Neat			
VAL 64-16 + LH_1 10%			
VAL 64-16 + LH_1 40%			
VAL 64-16 + GH_1 10%			
VAL 64-16 + GH_1 40%			
VAL 64-16 + DS_2 10%			
VAL 64-16 + DS_2 40%			
VAL 64-16 + HL 4%			
VAL 64-16 + HL 10%			

3.2.5 Bending Beam Rheometer

The Bending Beam Rheometer (BBR) was used in accordance with the AASHTO T 313 - Determining the Flexural Creep Stiffness of Asphalt Binder Using the Bending Beam Rheometer (2005) standard for measuring the change in flexural-creep stiffness (i.e., S(t)) and the m-value (i.e., m(t)) of both asphalt binder and mastics beams.

The BBR test simulates asphalt binder stiffness after two hours of loading at the minimum hot mix asphalt (HMA) pavement design temperature. Creep stiffness (S(t)) is related to thermal stresses in an HMA pavement due to shrinking while the m-value is related to the ability of an HMA pavement to relieve these stresses. Thus, the Strategic Highway Research Program (SHRP)

binder specifications require a maximum limit on creep stiffness and a minimum limit on m-value, where binder must have some minimum ability to relieve thermal stresses without cracking.

The m-value is the slope of the curve of the creep stiffness (S(t)) and loading time, plotted on a log-log scale (Figure III-7). By using basic beam theory (Equation III-4), the BBR calculates beam stiffness (S(t)) and the rate of change of that stiffness (m-value) as the load was applied. The BBR basically subjects a simple asphalt beam to a small (100 g) load over 240 seconds. The Strategic Highway Research Program (SHRP) specification sets criterion limits for the values of the creep stiffness and m-value at 60 seconds of BBR creep loading, designated S(60) and m(60), respectively.

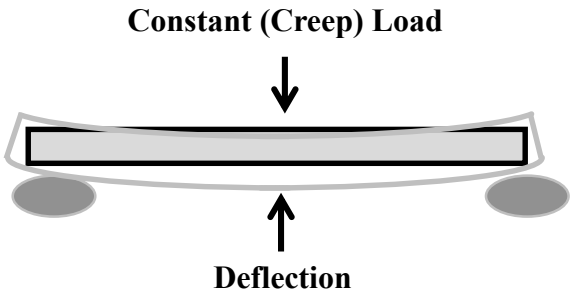

(a)

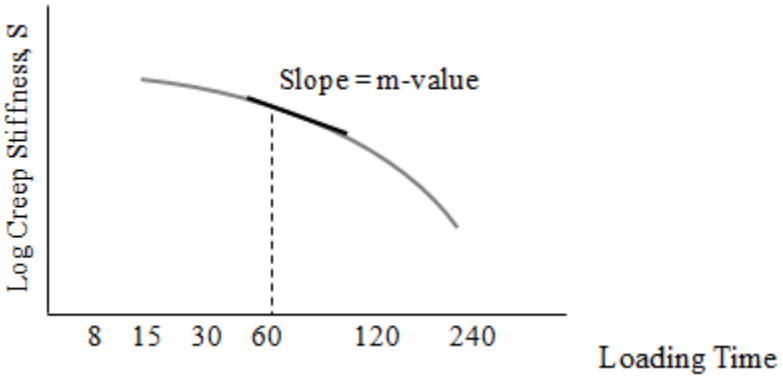

(b)

Figure III-7: BBR (a) load and (b) response.

$$S(t) = \frac{PL^3}{4bh^3\delta(t)} \quad \text{(III-4)}$$

where:

S(t) = creep stiffness at time, t = 60 seconds

P = applied constant load obtained using a 100 g load. Note that 100 g multiplied by the force of gravity (9.8 m/s^2) = 0.98 N, or 980 mN

L = distance between beam supports, 102 mm

b = beam width, 12.5 mm

h = beam thickness, 6.25 mm

δ(t) = deflection at time, t = 60 seconds

In this study, the PG grade and plus one grade was selected for testing. For example, the Flint Hills PG 64-22 binder was tested at -6 °C and -12 °C for low-temperature analysis. The standard load of 980 mN was used for both asphalt binders and mastics. Table III-5 displays the BBR tests conducted for this study.

Table III-5: BBR tests.

Sample	Temperature (°C)	PAV Conditioning Time (h)	Reported Parameters
FH 64-22 Neat	-6, -12 and -18	0 and 24	S(t), m-value
FH 64-22 + LH_1 40%			
FH 64-22 + GH_1 40%			
FH 64-22 + DS_2 40%			
VAL 64-16 Neat			
VAL 64-16 + LH_1 40%			
VAL 64-16 + GH_1 40%			
VAL 64-16 + DS_2 40%			

Preparation of specimens for testing in the BBR for low-temperature characterization follows standard procedure. To accommodate the stiffer, more viscous mastics samples, BBR mold clamps were used to secure the ends of the beam while being molded and trimmed. Beams were cast and trimmed according to standard procedure. Figure III-8 below shows the de-molded base binder and mastics beams used for the BBR low temperature analysis procedure.

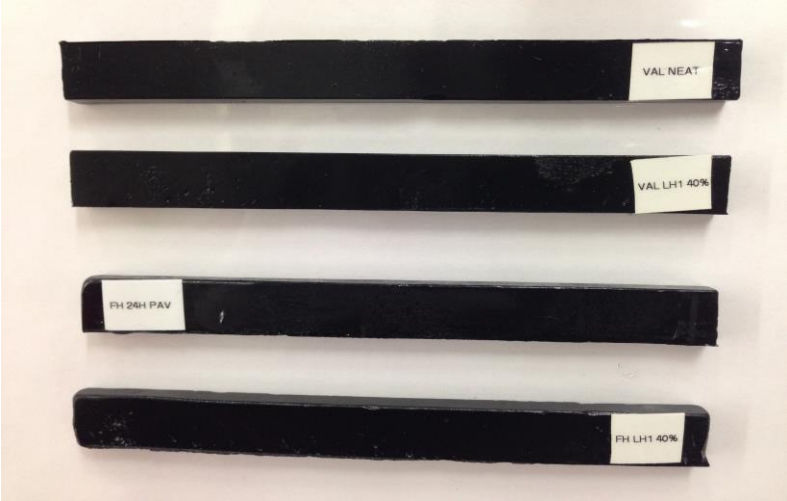

Figure III-8: BBR specimens for low-temperature analysis.

Please note that the mastics samples are have the same dimensions as that of the neat binder samples and were perfectly uniform in appearance. The mastics samples presented in Figure III-5 were made with 40% by volume of filler.

3.2.6 Gel Permeation Chromatograph

Gel Permeation Chromatograph (GPC) was used to measure the molecular size distribution of both binder and mastics. The detector used for the GPC analysis was the differential refractometer, which is a concentration sensitive detector that measures the difference in refractive

index (dRI) between the eluent in the reference side, and the sample + eluent in the sample side. The GPC columns used were PolyPore 5 um mixed, 300 x 7.5 mm. The flow rate was 1 mL / min and the testing temperature was 40 °C.

Each GPC test has the duration of approximately 30 minutes. The GPC samples were prepared in accordance to the following procedure:

(1) Approximately 30 mg of sample was dissolved in 1 mL of tetrahydrofuran (THF);

(2) The solution was then filtered through a 0.20 μm phobic PTFE syringe filter;

(3) After the filtration, the solution was placed at ambient temperature for 8 hours, until the complete solvent evaporation;

(4) The remaining asphalt film was weighted and THF solvent was added to achieve the concentration of 5 mg / 2 mL;

(5) In the final step, each sample dissolved into THF was filtered through a 0.45 μm syringe filter prior to the injection.

Please note that this procedure was followed for preparation of both binder and mastic samples to assure that the asphalt film used to perform the GPC analysis would be equivalent. Figure III-9 depicts the selected GPC testing procedure.

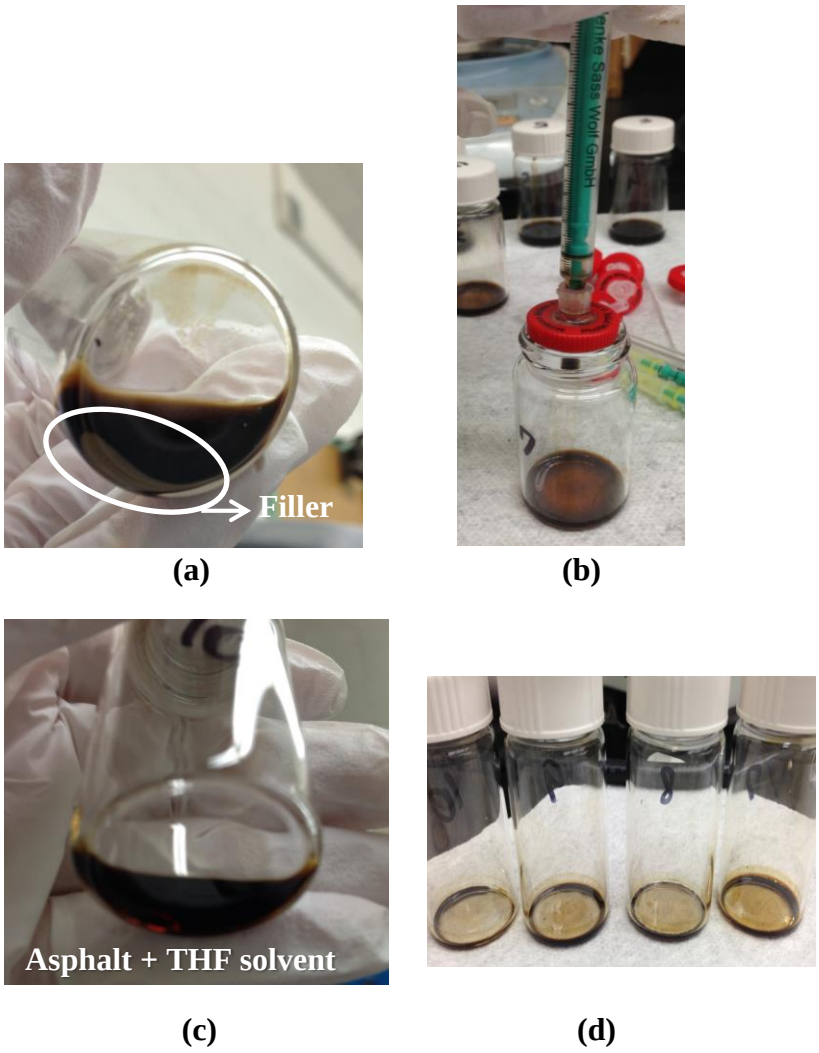

Figure III-9: GPC sample preparation: (a) solution of mastic sample and THF solvent; (b) solution was filtered through a 0.20 µm phobic filter; (c) filtered solution leaved for evaporation of the solvent; and (d) remaining asphalt film.

In the Gel Permeation Chromatograph (GPC) procedure the separation is based strictly on the size of the sample in solution, not chemistry (Yau and Malone, 1967). The mode of separation is not based on molecular weight, but on the size of the material being analyzed in solution. Once the sample has been suitably dissolved, it is introduced via an injection mechanism onto a set of columns which act as a molecular filtration system. The columns are packed with a gel which

contain surface pores. These pores vary in size and act as molecular filters. Thus, the larger size molecules will not fit into the smaller pores. Conversely, the smaller molecules will fit into most of the pores, and be retained longer. A typical GPC chromatogram is shown in Figure III-10.

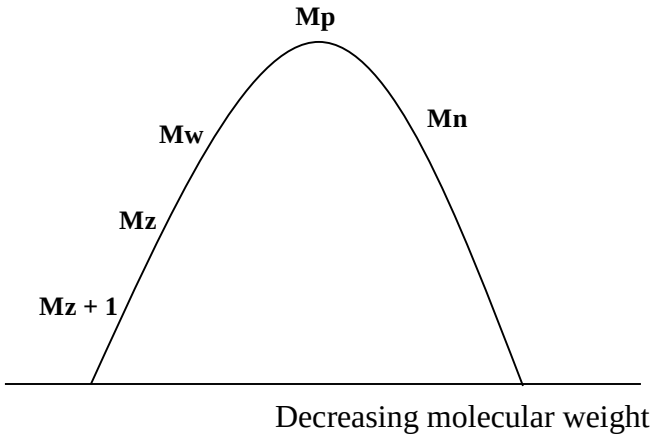

Figure III-10: Typical GPC chromatogram curve with Mw (weight-average molecular weight), Mn (number-average molecular weight), Mz (z-average molecular weight), Mz+1 ((z+1)-average molecular weight), and Mp (peak molecular weight).

The commonly calculated average is actually called the number-average molecular weight, abbreviated to Mn. As it can be seen in Figure III-7, the Mn value marks the value at which there are equal numbers of molecules on each side, at higher and lower molecular weight. The value of Mn influences the thermodynamic properties of the molecule (Dawkins, 1979). Mw is defined as the value at which there are equal masses of molecules on each side, at higher and lower molecular weight. Mw is large-molecule sensitive and influences the bulk properties and toughness of the material. Mw affects many of the physical properties of material, and is the most often quoted molecular weight average (Dawkins, 1979). As well as Mn and Mw, there are other molecular weight averages that take increasing account of the higher molecular weight components of the

sample, such as z-average molecular weight (Mz) and Mz+1. Mz is sensitive to even larger molecules and influences viscoelasticity and melt flow behavior. The ratio of Mw to Mn is used to calculate the polydispersity index (PDI) of a polymer, which provides an indication of the material's range of molecular mass. The broader the molecular weight distribution, the larger the PDI. The molecular weights are of the order Mz > Mw > Mn. The GPC most common parameters are given in Equation III-5 through Equation III-8.

$$Mn = \frac{\sum N_i M_i}{\sum N_i} \quad \text{(III-5)}$$

$$Mw = \frac{\sum N_i {M_i}^2}{\sum N_i M_i} \quad \text{(III-6)}$$

$$Mz = \frac{\sum N_i {M_i}^3}{\sum N_i {M_i}^2} \quad \text{(III-7)}$$

$$M_{z+1} = \frac{\sum N_i {M_i}^4}{\sum N_i {M_i}^3} \quad \text{(III-8)}$$

where:

Mn = number-average molecular weight (daltons)

Mw = weight-average molecular weight (daltons)

Mz = z-average molecular weight (daltons)

Mz+1 = (z+1)-average molecular weight (daltons)

Mp = peak molecular weight (daltons)

Mi = molecular weight (daltons)

Ni = number of molecules of molecular weight Mi

In this study, the GPC spectrum was divided into 13 equal elution time areas as showed in Figure III-11 (Jennings et al. 1980):

- Molecules eluted during first third of the elution period = large molecular size (LMS) → *1 to 5*
- Molecules eluted during second third = medium molecular size (MMS) → *6 to 9*
- Molecules eluted in the last third = small molecular size (SMS) → *10 to 13*

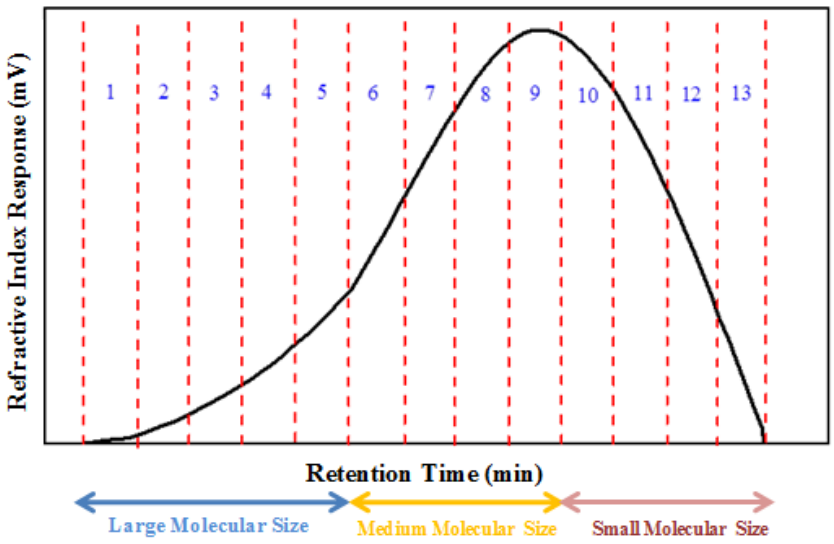

Figure III-11: GPC spectrum divided into 13 equal elution time areas.

In asphalt binders, aging results in a shift towards the higher molecular weight (Hagos, 2008). Oxidative aging causes formation of more polar molecules at the expense of the lower weight molecules. Many studies indicated that the large molecular size of asphalt binder (LMS) presents good correlations with asphalt mixture properties (Jennings et al., 1980; Kim and Burati, 1993; Al-Abdul Wahhab et al., 1999). Incremental increase of LMS due to aging can be correlated

to asphalt physical properties (Bynum and Traxler, 1970; Jennings et al., 1980; Kim and Burati, 1993).

Table III-6 displays the GPC tests conducted for this study.

Table III-6: GPC tests.

Sample	PAV Conditioning Time (h)	Reported Parameters
FH 64-22 Neat	0, 24 and 48	Mn, Mw, Mz, LMS, MMS, SMS
FH 64-22 + LH_1 40%		
FH 64-22 + GH_1 40%		
FH 64-22 + DS_2 40%	0 and 24	
FH 64-22 + HL 4%		
FH 64-22 + HL 10%		
VAL 64-16 Neat	0, 24 and 48	
VAL 64-16 + LH_1 40%		
VAL 64-16 + GH_1 40%		
VAL 64-16 + DS_2 40%	0 and 24	
FH 64-22 + HL 4%		
FH 64-22 + HL 10%		

IV. Evaluation of the Effect of Fillers on Oxidative Aging of Binders

This chapter discusses the results of gravimetrical analysis to verify the influence of fillers on the production of asphaltenes due to oxidative aging. It also includes rheological analyses conducted to test changes in stiffness, in addition to glass-transition temperature, and contraction coefficient measurements of the asphalt mastics. A statistical analysis was performed to verify the effect of binder type and filler type on the aging index based on complex modulus.

4.1 Analysis of Asphaltenes Extraction Results

As it can be seen in Table IV-1, the procedure for asphaltene extraction of the neat binder before and after different aging conditioning is in accordance with the literature (Rostler and White, 1962; O'Sullivan, 2011; Dehouche et al., 2012), showing that the asphaltenes content increased after aging.

Table IV-1: Asphaltenes extraction results for neat binder after different aging conditioning.

Sample	Asphaltenes Content
FH 64-22 Unaged	16 %
FH 64-22 3h PAV	16 %
FH 64-22 6h PAV	18 %
FH 64-22 24h PAV	23 %
FH 64-22 30h PAV	25 %

Table IV-2 presents the asphaltenes content extracted from the asphalt mastics before and after PAV aging. As it can be seen in Table IV-2, the effect of mineral filler on the aging process shows that the mastics with 10% of mineral filler by volume resulted in lower asphaltenes content

after oxidative aging in comparison to the aged neat binder. This result can be an indicator that the aggregate inhibited the asphaltenes development during aging. However, for mastics with 40% of mineral filler the asphaltenes content was higher than that of the neat binder, before and after aging. One reason for this result can be explained by the extraction process where due to the higher volume of filler, a larger number of filler particles may have inadvertently remained in the separated asphaltenes, despite all attempts to limit such occurrences, thus falsely contributing to the measured increase of asphaltenes mass.

Table IV-2: Asphaltenes extraction results for mastics.

Sample	**Asphaltenes Content**		**Percentage Change**
	Unaged	**24 h PAV Aged**	
FH 64-22	16 %	23 %	-44
FH + LH_1 (10%)	16 %	20 %	-25
FH + LH_1 (40%)	22 %	24 %	-9
FH + GH_1 (10%)	18 %	20 %	-11

It is important to mention that the higher amount of asphaltenes extracted from the aged and unaged mastic when compared to the neat binder is most likely due to the extraction process. Even though the solution of toluene and asphaltenes were filtered four times in order to separate the solid portion (i.e., filler), a small portion of the filler might not be completely extracted. Similarly, incomplete recovery of the asphaltene fraction from the asphaltene-toluene solution could also lead to erroneously high numbers. A distinct odor of toluene existed even after rotary evaporation, indicating there may have been residual toluene in the flask.

Comparing asphaltenes measures may not be necessary or helpful because it is only explaining part of the aging mechanism while not capturing any variation in other asphalt fractions.

4.2. Analysis of DSR Testing Results

Two base binders were used for the mastic aging analysis using the Dynamic Shear Rheometer in this study. The FH 64-22 base binder had an asphaltenes content of 23% after 24 hours of PAV aging. Another base binder, (VAL 64-16) with lower asphaltenes content (i.e. 20% after 24 hours of PAV aging) was included in this study for comparison and confirmation of the trend on rheological data achieved using the FH base binder. The analysis results using both base binders are presented in the following sections.

4.2.1 Mastics Using Flint Hills 64-22 Base Binder

4.2.1.1 DSR Master Curves

DSR data was used to construct master curves for each of the aging times. As it can be seen in Figure IV-1 (a), oxidative aging distorted the shape of the neat binder master curve by decreasing the slope and thus decreasing the time-dependency of the material response in this frequency range. This effect for binders as a result of aging is not unexpected and is in line with previous reported research (Anderson and Bonaquist, 2012). On the other hand, the addition of mineral filler to the binder during aging shifted the curve toward higher frequencies and thus a more elastic response, which is to be expected due to the addition of elastic filler particles (Figures IV-1(b) through (d)). The most important observation is that aging of the mastic with 40% filler, regardless of filler mineralogy, also resulted in a rotation of the master curve in the reverse direction of that caused by aging of the binder alone. The result of which is aged mastic master curves that are only shifted in comparison to the neat, without the distortion and rotation observed for aging of binder alone. This finding is very significant, as it can potentially indicate that many

of the changes in mechanical properties attributed to aging binder from rheological testing may be of lower significance to the overall mixture performance, if the possible counter-effect of fillers in the mastic phase is considered.

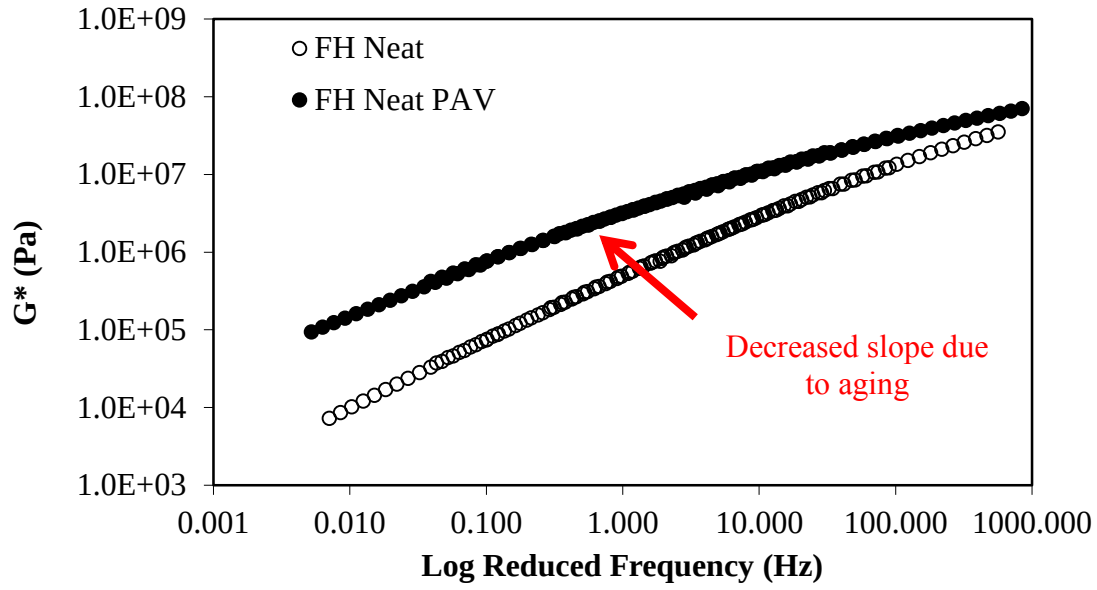

(a)

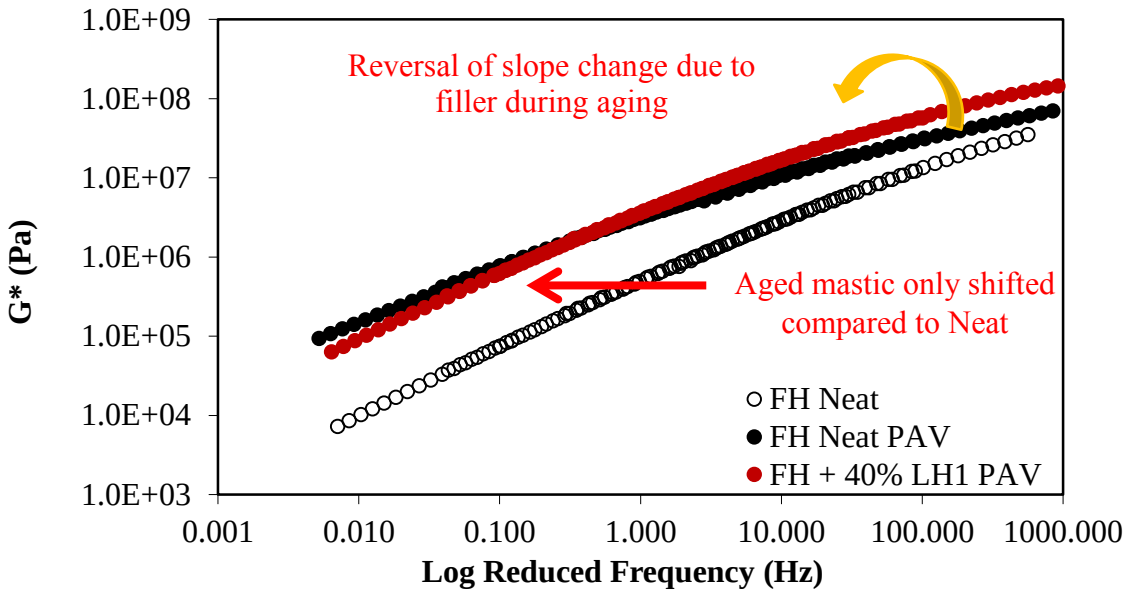

(b)

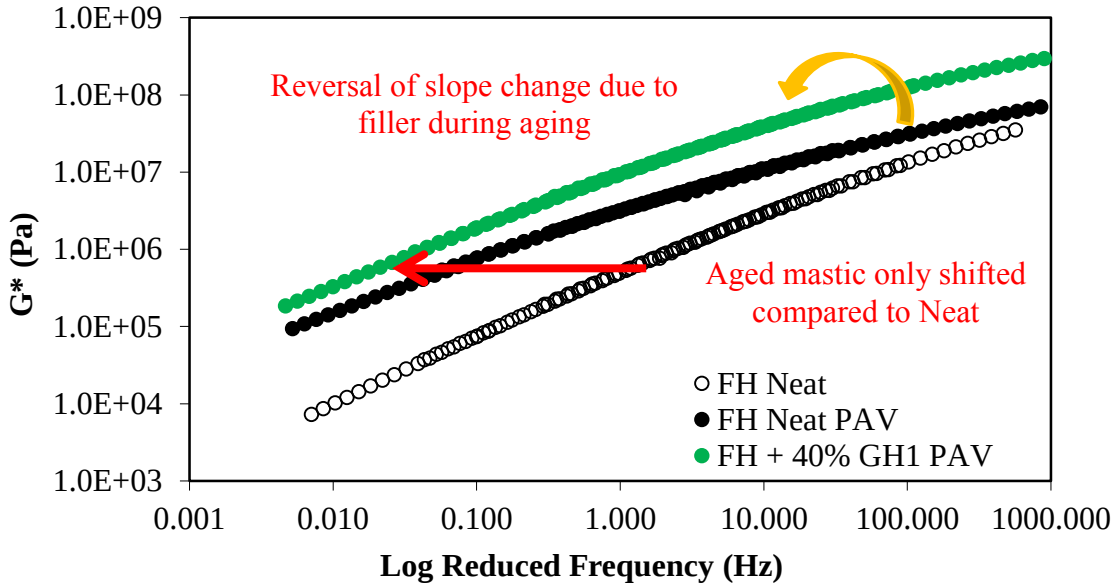

(c)

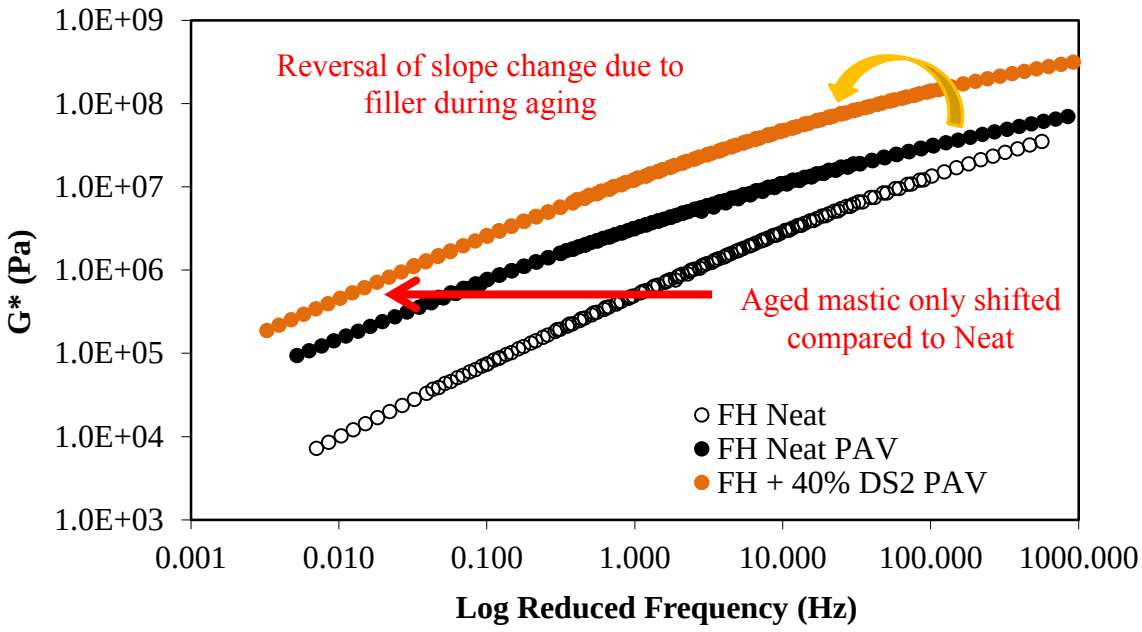

(d)

Figure IV-1: (a) Oxidative aging of FH binder, oxidative aging of FH binder and mastics with (b) 40% LH_1, (C) 40% GH_1 and (d) 40% DS_2.

As it can be seen in Figure IV-2, the mastics with 10% of mineral filler showed similar behavior to the neat aged base binder, regardless the filler mineralogy. This results show that the rheological changes occasioned by the addition of 10% of fillers is not significant.

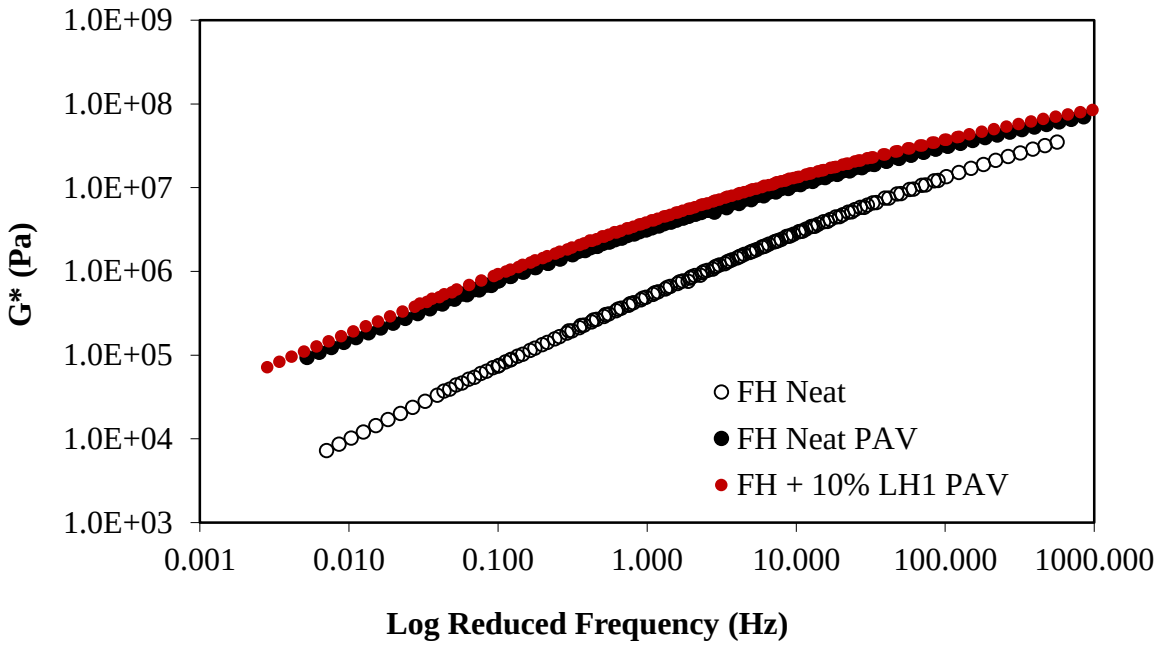

(a)

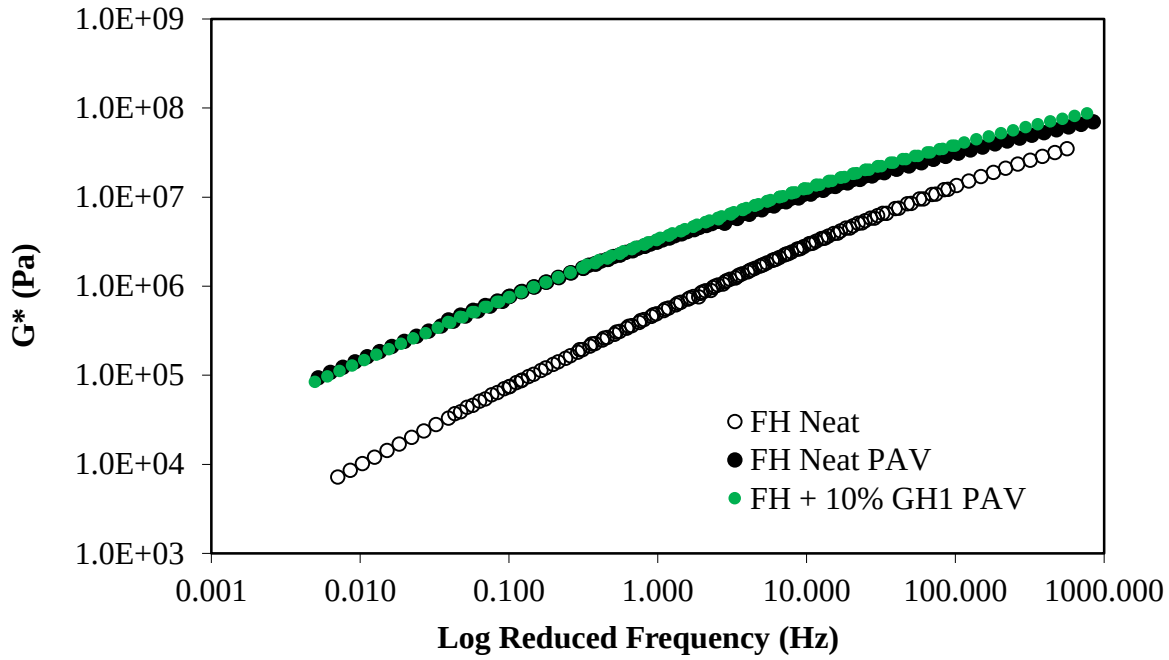

(b)

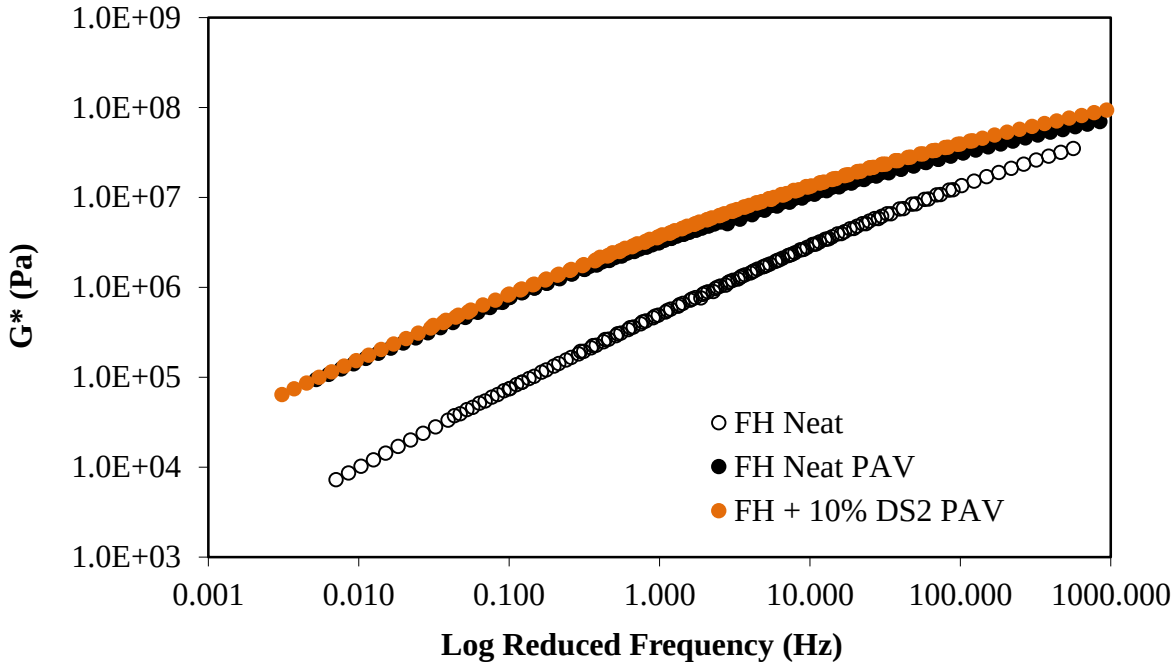

(c)

Figure IV-2: (a) Oxidative aging of FH binder and mineral filler for 10% LH_1, (b) 10% GH_1, and (c) 10% DS_2.

4.2.1.2 DSR Aging Index

In order to investigate the relation between oxidative aging and mineral filler concentration, an aging index was calculated using |G*| at 10°C and 30 Hz (representing lower temperatures or higher traffic speed) and at 40°C and 0.1 Hz (representing higher temperatures or lower traffic speed). The aging indexes were calculated according to Equation IV-1.

$$\textbf{Aging Index } (|\mathbf{G}*|) = \frac{(|\mathbf{G}^*|)_{\textbf{After 24h PAV}}}{(|\mathbf{G}^*|)_{\textbf{Unaged}}} \qquad \text{(IV-1)}$$

According to Bahia and Anderson (1995) the mechanism of pressure oxidation of asphalt in the PAV involves a diffusion mechanism; therefore, film thickness is expected to be an important factor during aging in PAV. In order to investigate the film thickness effect, different binder thicknesses were selected and aged for 24 hours. As it can be seen in Figure IV-3, the aging index decreases by increasing the binder film thickness, which will result in an increase in the diffusion path length, thus a general decrease in the amount of aging. For example, it is observed that increasing the binder film thickness by approximately 50% (from 3.39 to 5.09 mm) resulted in more than 40% decrease in the aging ratio.

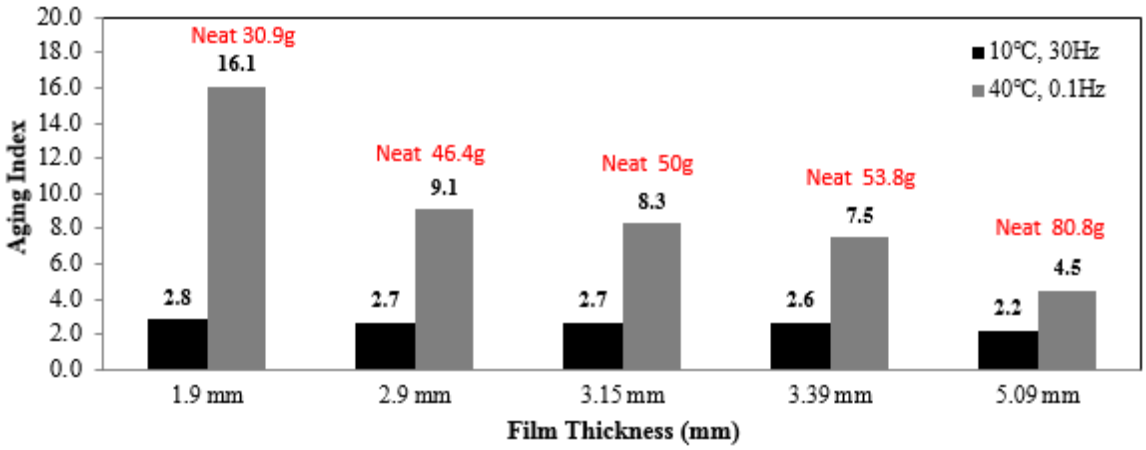

Figure IV-3: Effect of binder film thickness during 24 hours of PAV aging.

Figure IV-4 shows that a power law describes the trend of aging index change with film thickness. It should be noted that by pouring the standard 50 g of binder in the PAV pan a film thickness of 3.15 mm is achieved.

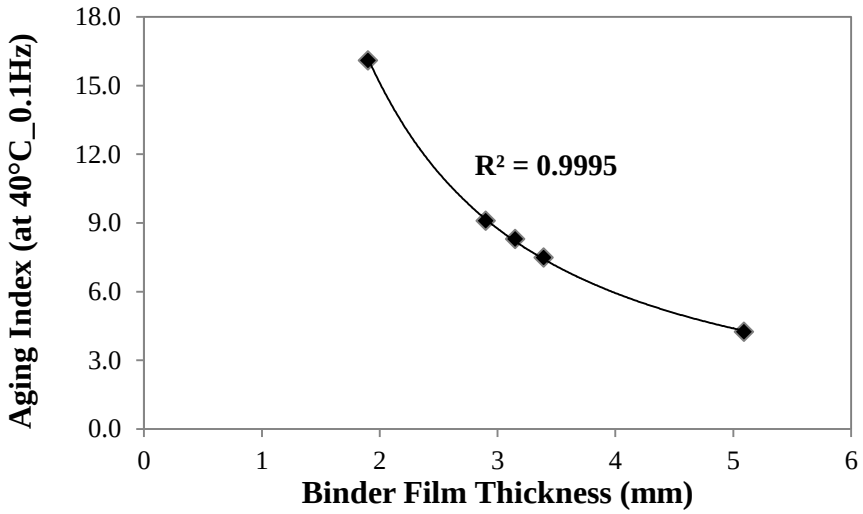

Figure IV-4: Power law relationship between PAV film thickness and aging index.

Figure IV-5 shows the aging index of the neat binder after being aged in the PAV with a film thickness of 1.9 mm. This thickness is equivalent to the thickness of the binder content of 3.15 mm film of 40% filler mastic in the PAV.

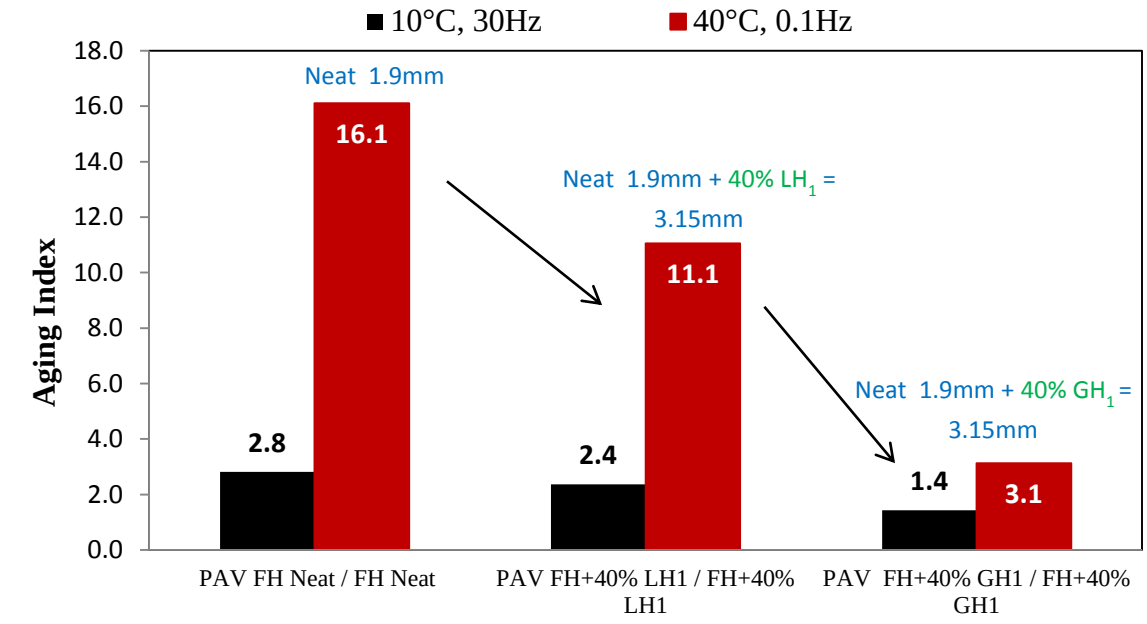

(a)

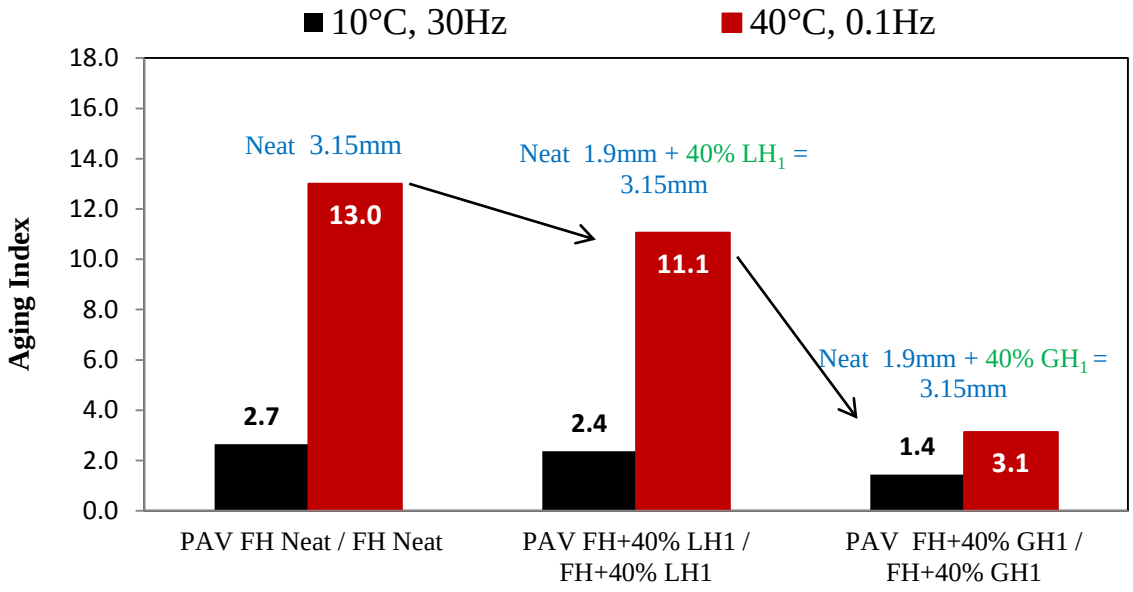

(b)

Figure IV-5: Aging index of mastic with (a) 1.19 mm neat film thickness (30.9g of asphalt was present in each pan), and (b) 3.15 mm neat film thickness (50g of asphalt was present in the neat pan).

A comparison between aging index of both binder and mastics with the same film thickness is performed and depicted in Figure IV-6, where the binder has a film of 5.09 mm, which corresponds to 50 gr of mastic with 40% by volume of filler. Results of this comparison show that the presence of mineral filler decelerates the age hardening of asphalt mastics, when compared to the base binder. The adsorption of the asphaltic polar fraction (i.e. asphaltenes) is the main cause of the softening of the mastics after the aging process. When comparing granite and limestone fillers, the granite has a higher specific surface area than the limestone (as shown in Table III-1). Therefore, it is expected that the aging index for all granite mastics would have lower values than that of the limestone mastics, as it is supported by the presented data.

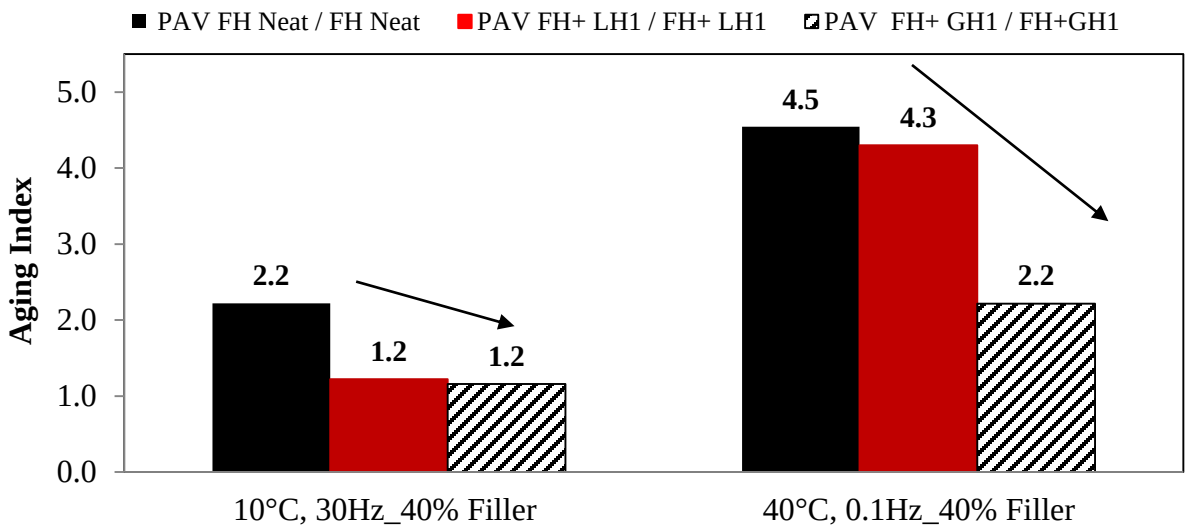

Figure IV-6: Aging indexes of neat binder, limestone and granite mastics with neat binder.

4.2.1.3 Reinforcing Effect of Filler Particles

It is important to mention that, according to the presented results the mineral filler reduces the aging index of the mastics. One concern regarding the use of the DSR (or other mechanical

testing methods) to obtain an aging index for asphalt mastics is the unaccounted effect of particle to particle contact that significantly affect stiffness and strength of a composite material such as mastics. When calculating such indices the reinforcement effect of mineral particles needs to be taken into account. Consider the two classical asymptotic composite materials models (i.e., Voight and Reuss) with typical values for volume fractions and stiffness for mastics in Figure IV-7. It can be seen from the calculations that the significant reduction of aging index in mastics (i.e., inhibiting aging) presented using DSR results can be partially explained by the reinforcement effect of the particles. Note that the expected behavior of asphalts mastics will be represented in between these two ideal situations.

In the present study this effect was eliminated as a confounding factor by using a ratio of changes, thus approximately eliminating the constant particle interaction effect in the mastics through a normalization process.

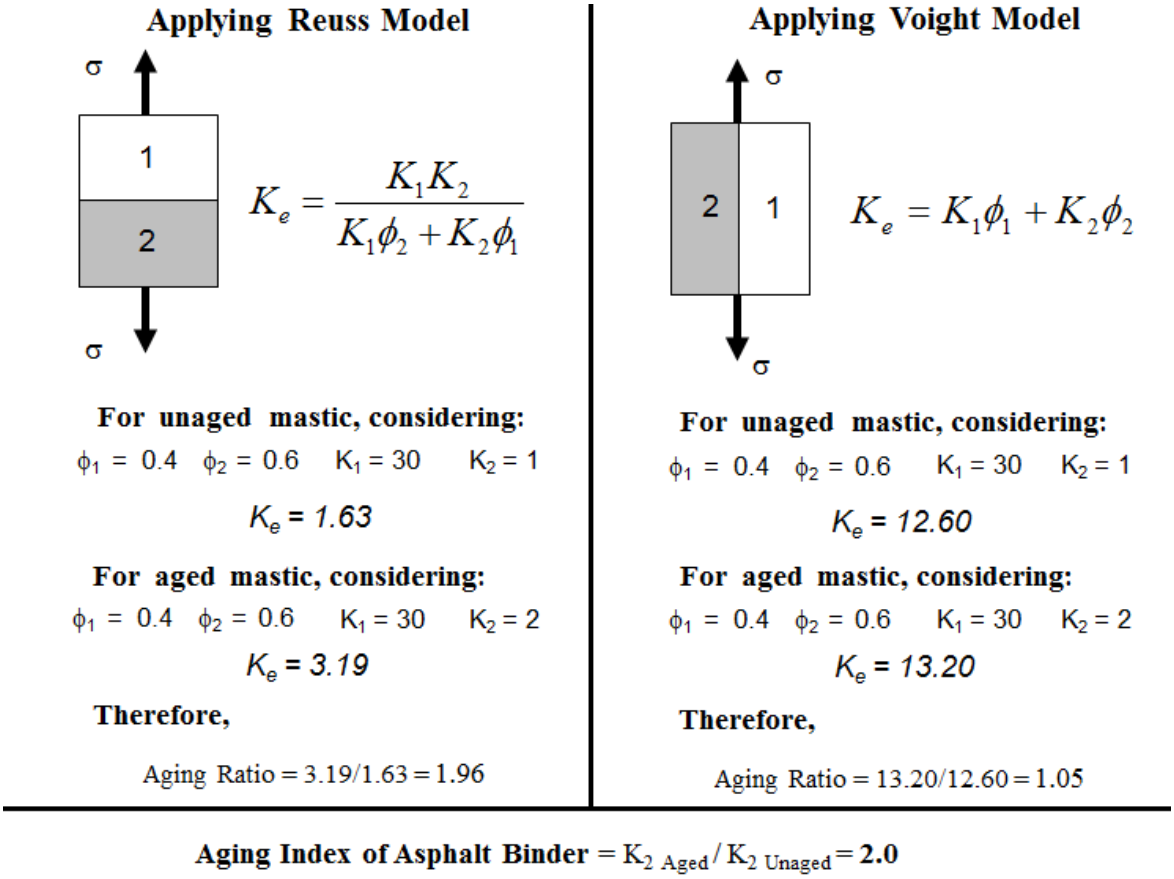

Figure IV-7: Example of aging index of mastics for two asymptotic behaviors.

4.2.1.4 Comparison with Hydrate Lime as Filler

Due to the high surface area of the HL (hydrated lime) it was not possible to blend 40% by volume with the binder (Figure IV-8). Two methods were tried: manually, and using a mechanical blender while increasing the temperature to approximately 180 °C.

Thus, in order to investigate if the filler's surface area is the most important filler's characteristic to decelerate age hardening of binders, a comparison based on equal total surface area was performed (as measured using the BET specific area). BET surface area of GH_1 is 1/10 of HL, thus a volume fraction of 4% HL will have equal total filler surface area to 40% GH_1.

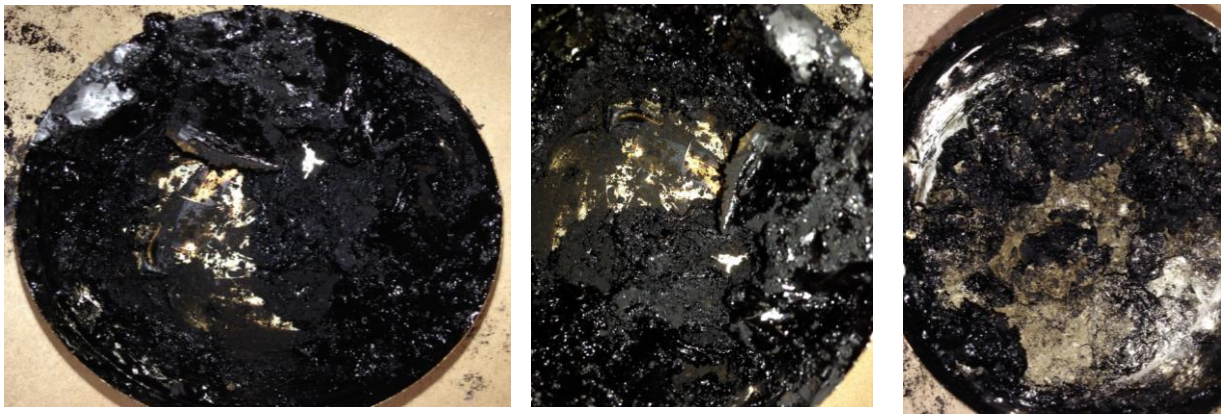

Figure IV-8: Blending of asphalt binder with 40% by volume of hydrated lime.

As it can be seen in Figure IV-9, the DSR aging index results showed that not only filler surface area is important to decelerate age hardening of binders. Observed effect on aging was not equal in the fillers, even though surface area was equal.

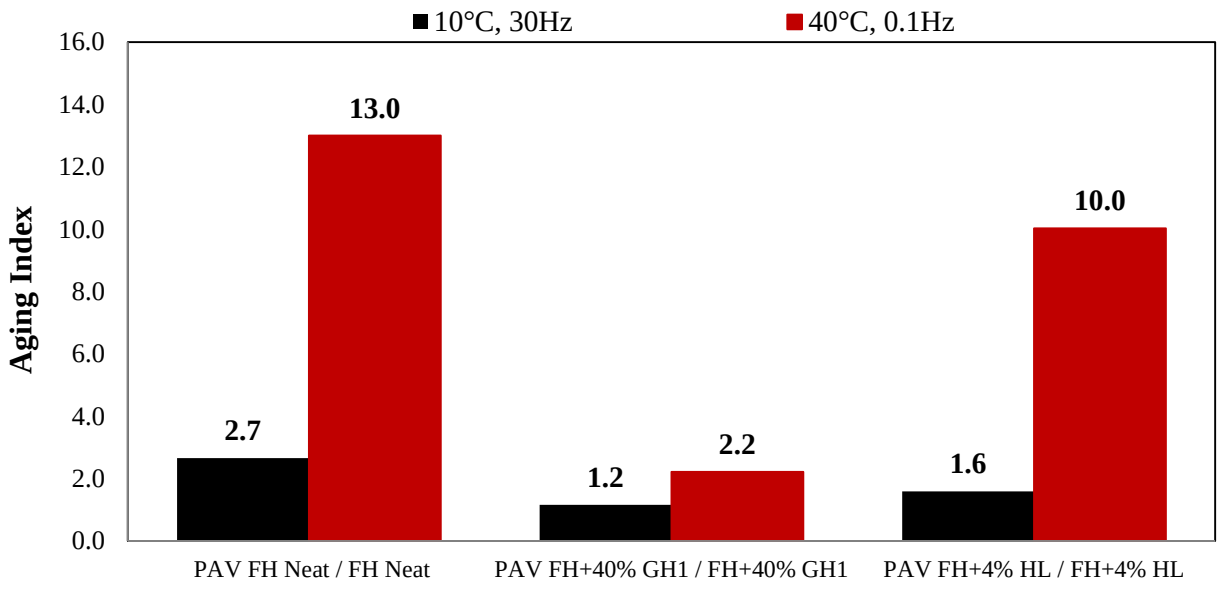

Figure IV-9: Aging indexes of FH neat binder, granite and hydrated lime mastics. Comparison based on equal total surface area (relative to BET specific area).

DSR data was used to construct master curves for each of the aging times. As it can be seen in Figure IV-10, oxidative aging distorted the shape of the neat binder master curve by decreasing the slope and thus decreasing the time-dependency of the material response. Also, the mastics with 4% and 10% of hydrated lime filler showed similar behavior to the neat aged base binder, regardless the filler content.

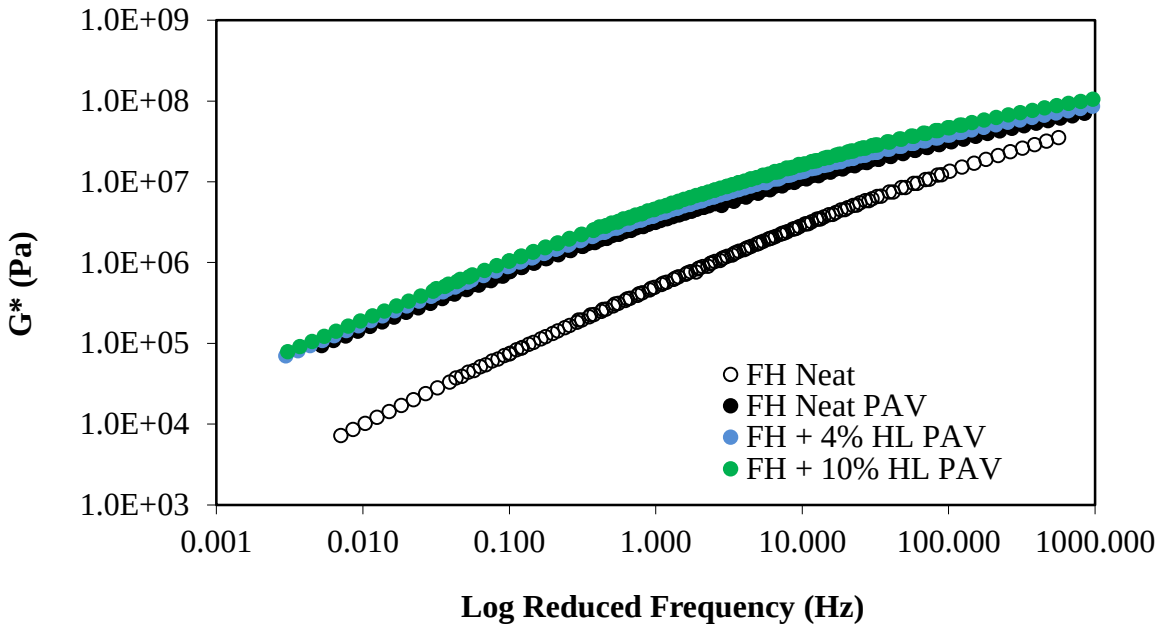

Figure IV-10: Oxidative aging of FH binder and mineral filler for 4% and 10% of hydrated lime.

4.2.2 Mastics Using Valero 64-16 Base Binder

4.2.2.1 DSR Master Curves

DSR data was used to construct master curves for each of the aging times. As it can be seen in Figure IV-11(a), oxidative aging distorted the shape of the VAL neat binder master curve. For this base binder, the aging of the mastic with 40% filler (Figure IV-11(b) through (d)) also resulted

in a rotation of the master curve in the reverse direction of that caused by aging of the binder alone, similar to the behavior observed for the mastics with the FH base binder in the previous section.

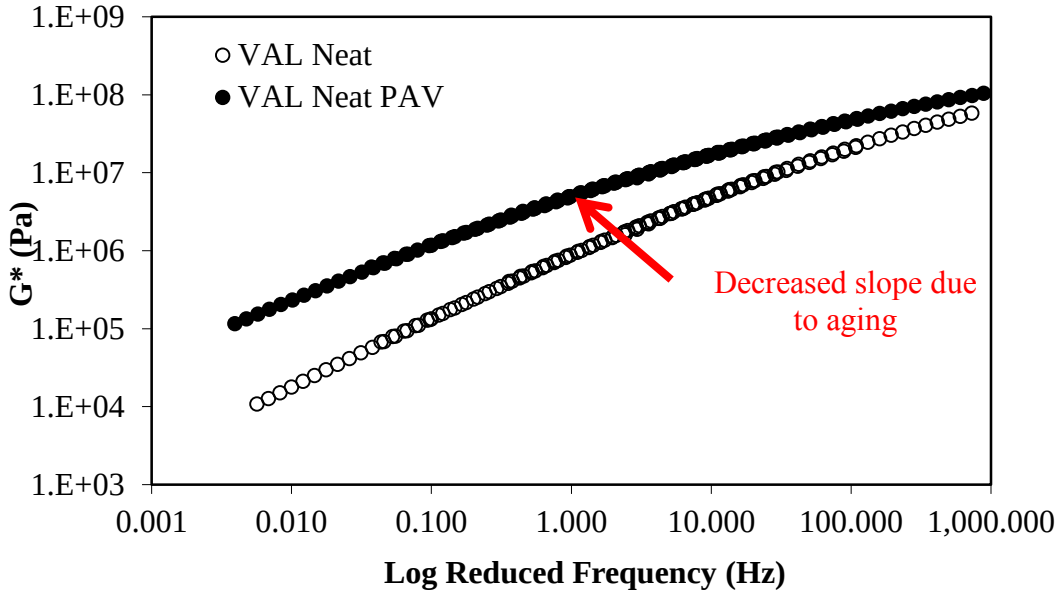

(a)

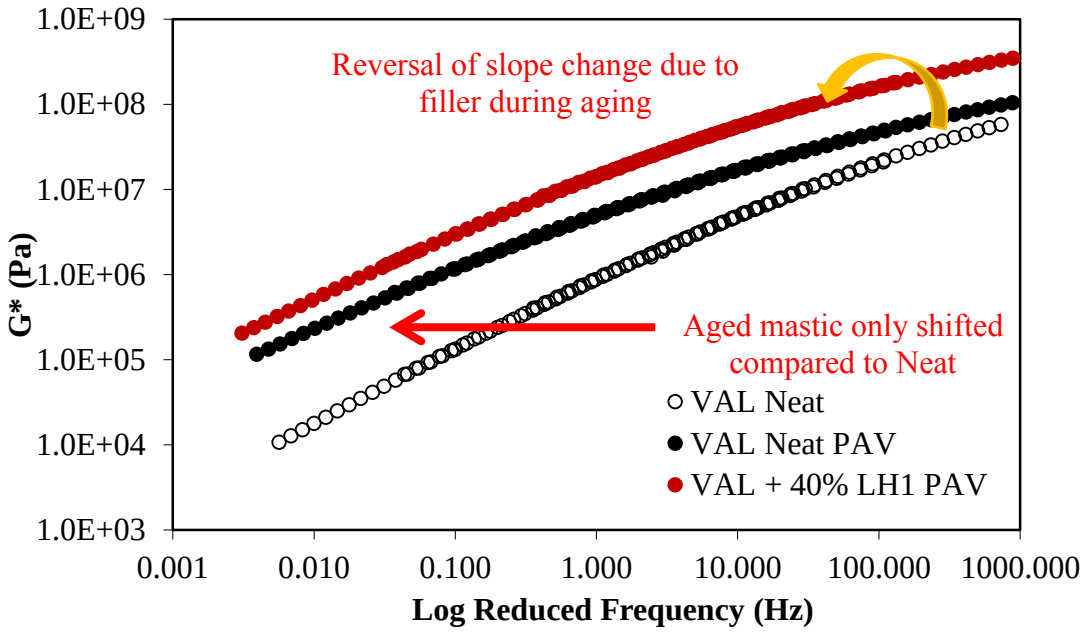

(b)

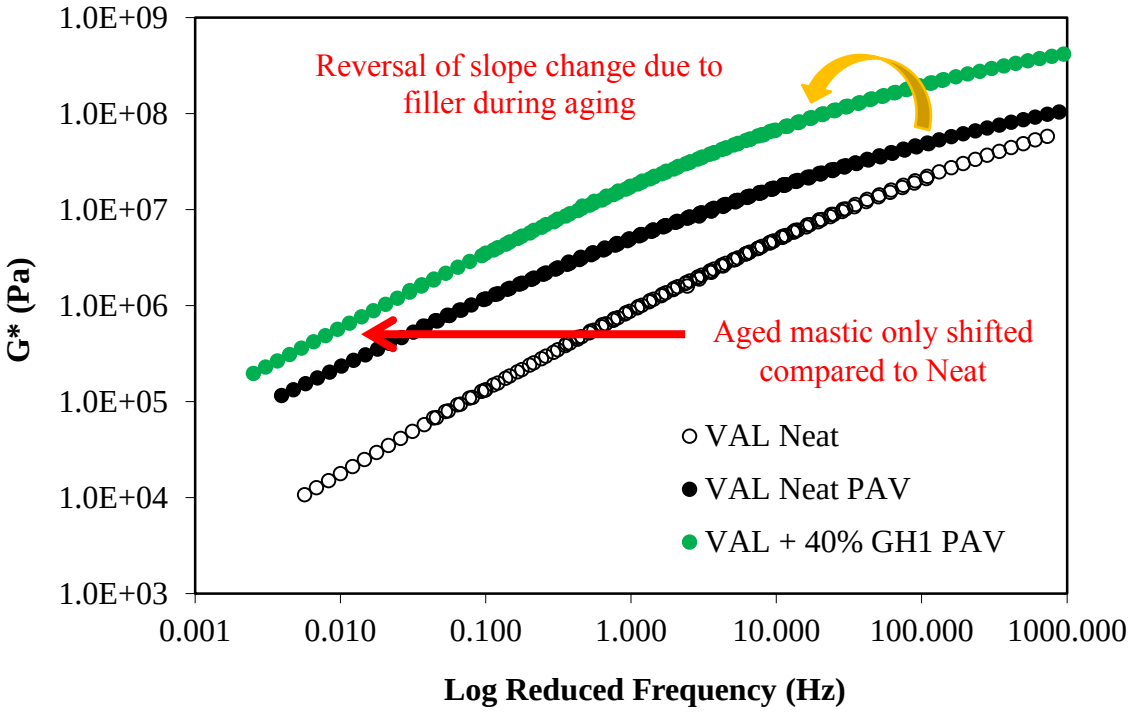

(c)

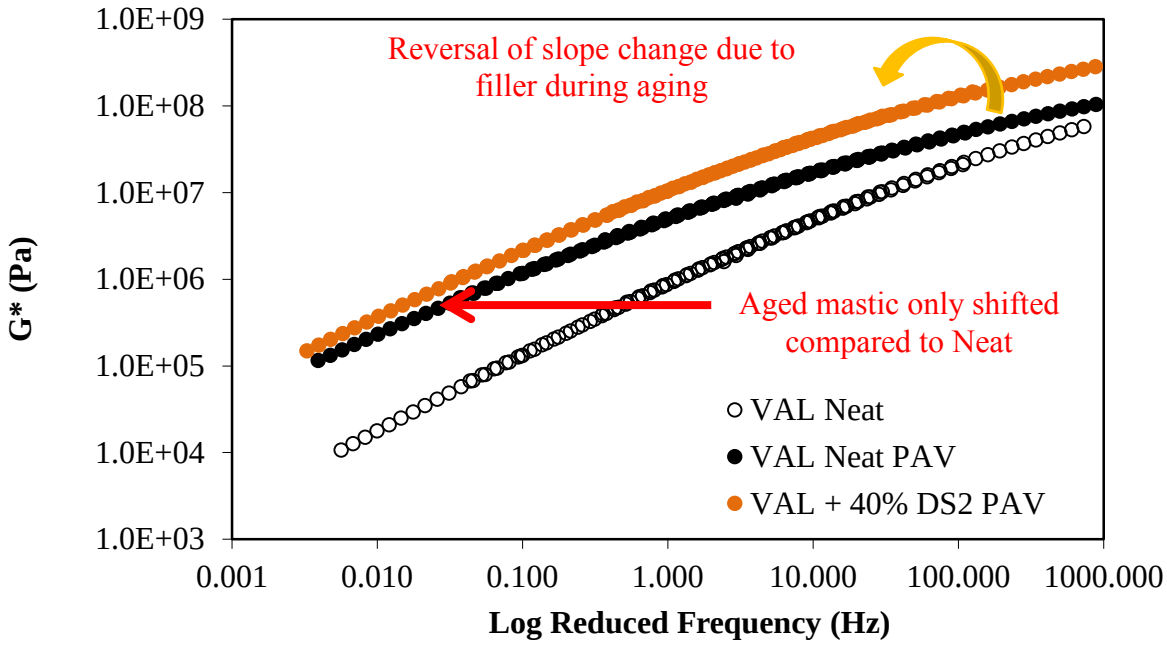

(d)

Figure IV-11: (a) Oxidative aging of VAL binder, (b) oxidative aging and mineral filler for 40% LH_1, (c) 40% GH_1, and (d) 40% DS_2.

4.2.2.2 Aging Index

Figure IV-12 shows the aging index of neat the Valero binder in comparison with the calculated aging index of mastics with 10% of filler. Presence of mineral filler appears to decelerate age hardening of asphalt mastics where filler type (i.e. mineralogy) and surface area characteristics appears to contribute in this process.

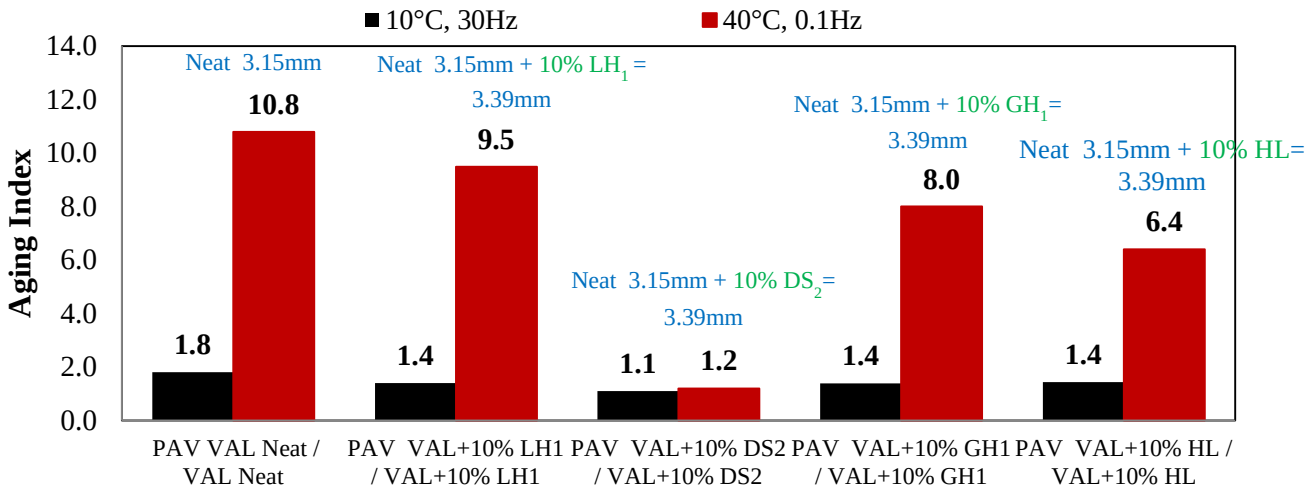

Figure IV-12: Aging index of VAL neat binder (3.15mm) in comparison with the calculated aging indexes of mastics with 10% by volume of limestone (LH_1), dolamite (DS_2) and granite (GH_1) mastics (50g of asphalt was present in each pan).

Figure IV-13 shows the aging index of neat the Valero binder in comparison with the calculated aging index of mastics with 40% of filler. With regards to the complex modulus (|G*|), the presence of mineral filler for this base binder also decreased the aging index of the mastics, indicating that the binder did not harden as much as the neat binder after the aging process. The increase in filler content (now at 40%) also contributed to the deceleration of the age hardening of asphalt mastics.

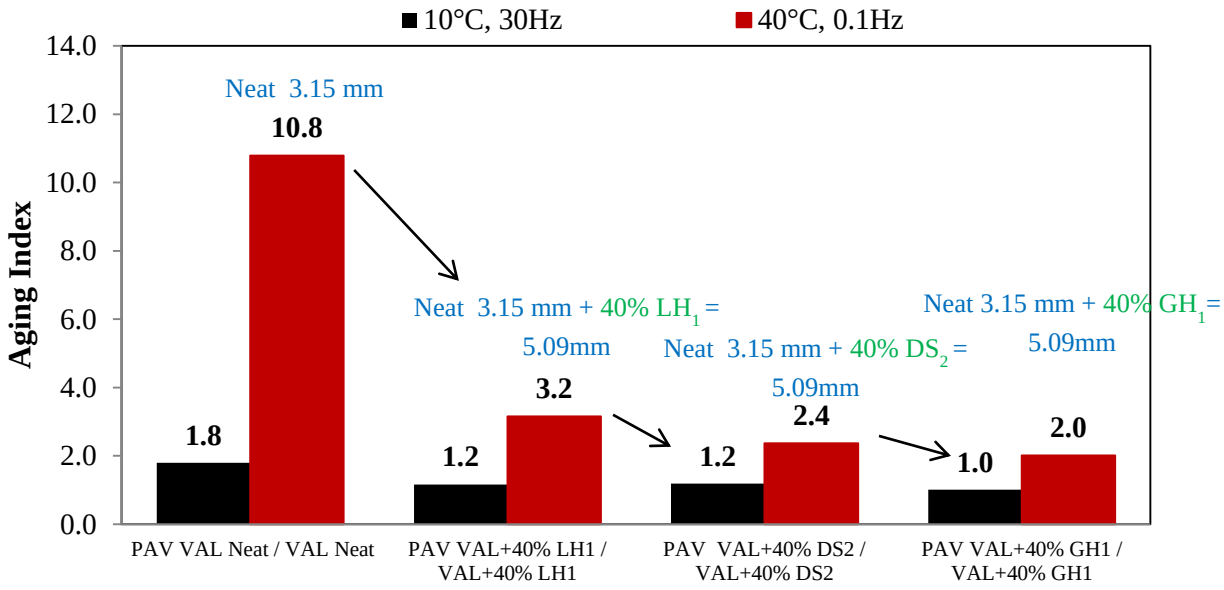

Figure IV-13: Aging index of VAL neat binder (3.15mm) in comparison with the calculated aging indexes of mastics with 40% by volume of limestone (LH_1), dolamite (DS_2) and granite (GH_1) mastics (50g of asphalt was present in each pan).

4.2.2.3 Comparison with Hydrated Lime as Filler

Granite (GH_1) and hydrated lime (HL) mastics were compared with filler content proportional to its surface areas (total filler surface area in 40% GH_1 is equal to 4% HL). As observed for the FH base binder, Figure IV-14 shows that the effect on aging was not equal in both fillers, even though surface area was maintained equal. These results seem to indicate that the surface area is not a contributing factor by itself, as the hydrated lime had close to any effect on aging.

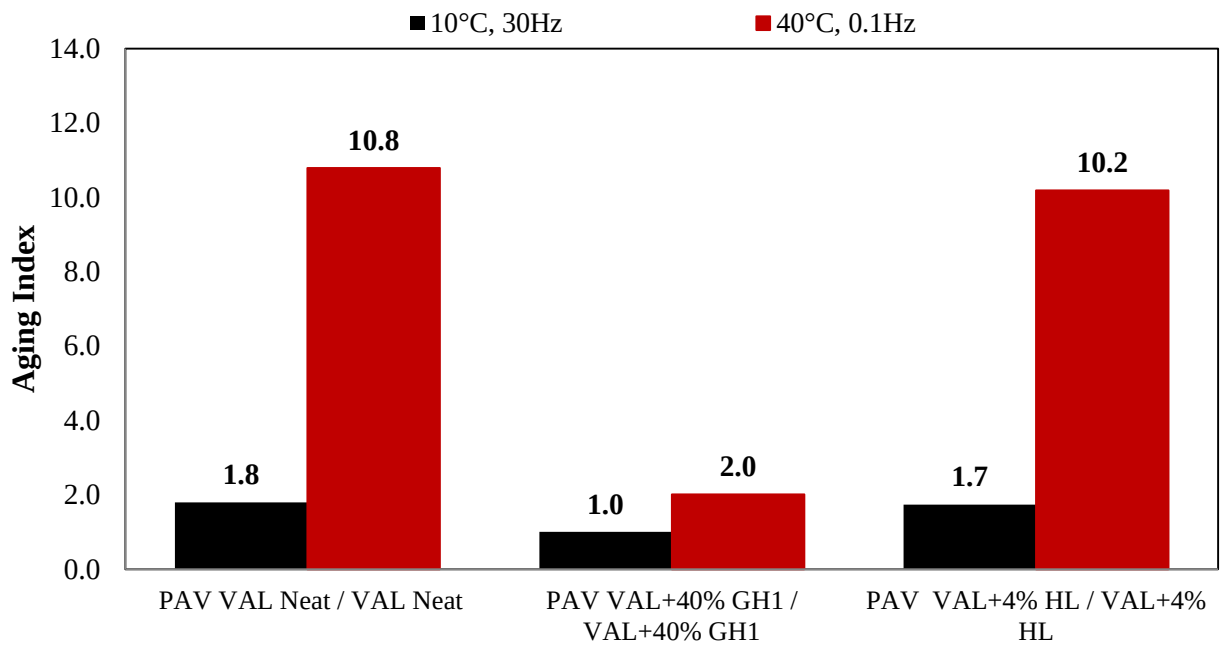

Figure IV-14: Aging indexes of VAL neat binder, granite and hydrated lime mastics. Comparison based on equal total surface area (relative to BET specific area).

DSR data was used to construct master curves for each of the aging times. As it can be seen in Figure IV-15, oxidative aging distorted the shape of the neat binder master curve by decreasing the slope and thus decreasing the time-dependency of the material response. Also, the mastics with 4% and 10% of hydrated lime filler showed similar behavior to the neat aged base binder, regardless the filler content. Same behavior observed for the FH base binder.

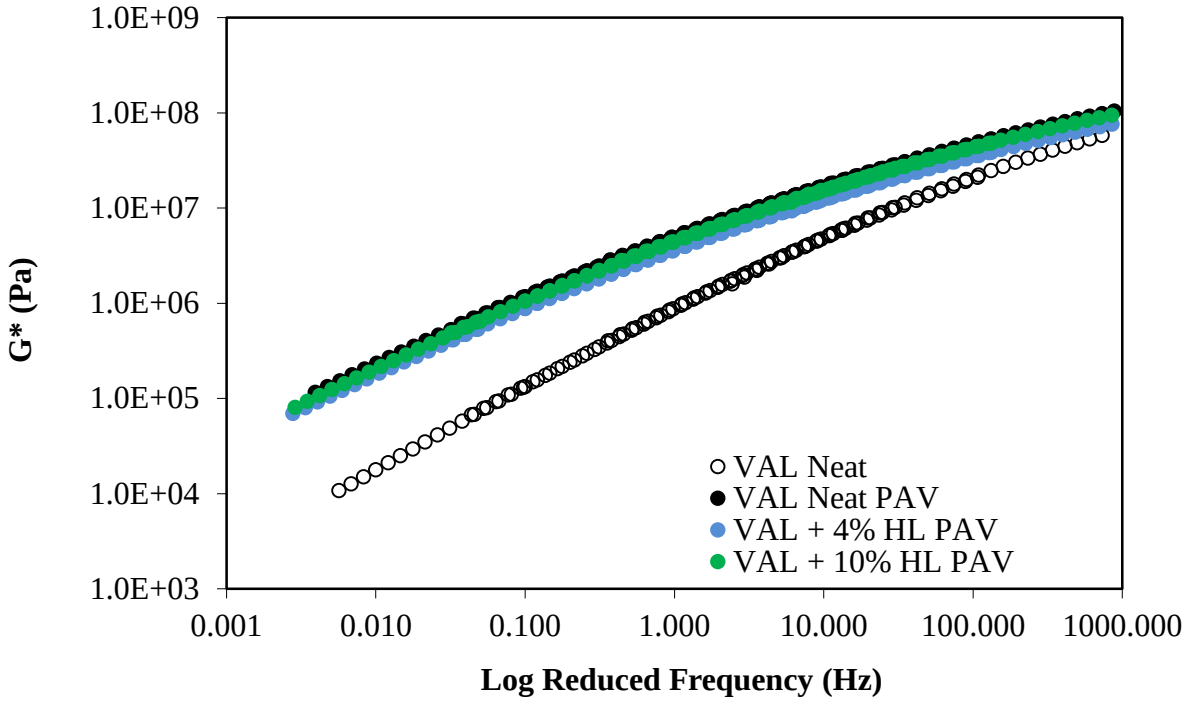

Figure IV-15: Oxidative aging of VAL binder and mineral filler for 4% and 10% of hydrated lime.

4.3 Direct Comparison of Mastics

In order to directly compare binder and mastic aging, a careful consideration of proper normalization of binder volume should be performed in which the most accurate composite theory describing the mechanical response of the studied fillers is used as the basis of normalization. Due to the complication making such corrections, in order to eliminate any confounded effects in comparison of aging, the different mastics are only compared to each other, and not to the individually aged binder in this section.

Figure IV-16 compares the LH_1 and GH_1 mastics at the same volume fraction, sieve size, and aging film thickness.

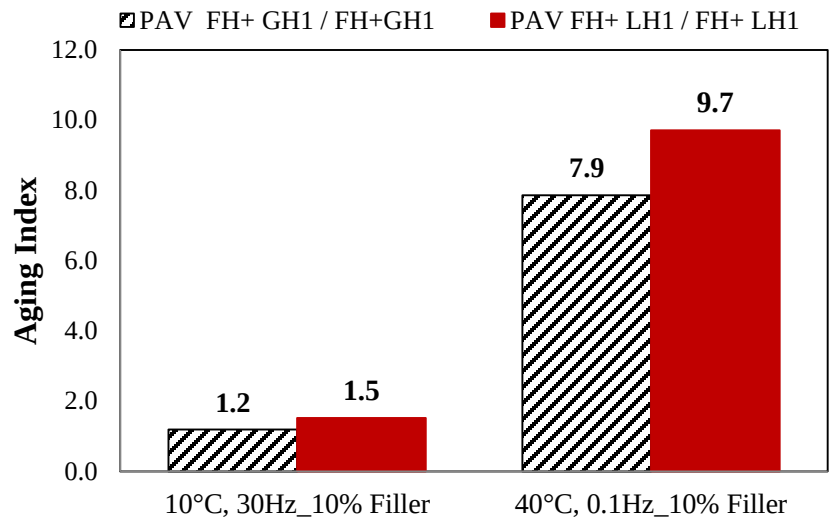

(a)

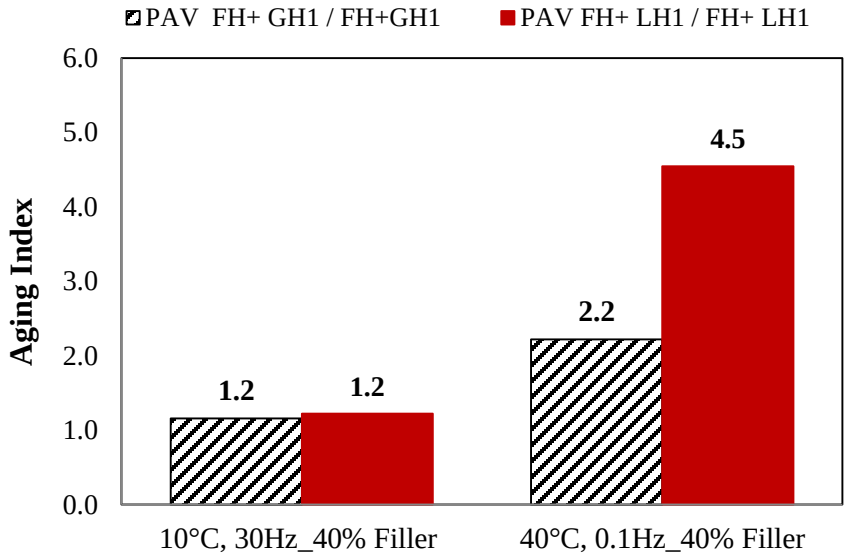

(b)

Figure IV-16: Comparison of the aging indexes without confounding effect of diffusion for (a) 10% filler, and (b) 40% filler in FH binder.

It is clearly seen that the LH_1 results in a higher aging index than that of the GH_1. In the absence of confounded diffusion effects, the difference is attributed to the mineralogy, higher

specific surface area of GH_1 and consequently the higher adsorption. Figure IV-17 confirms that the same trends exist with the Valero base binder.

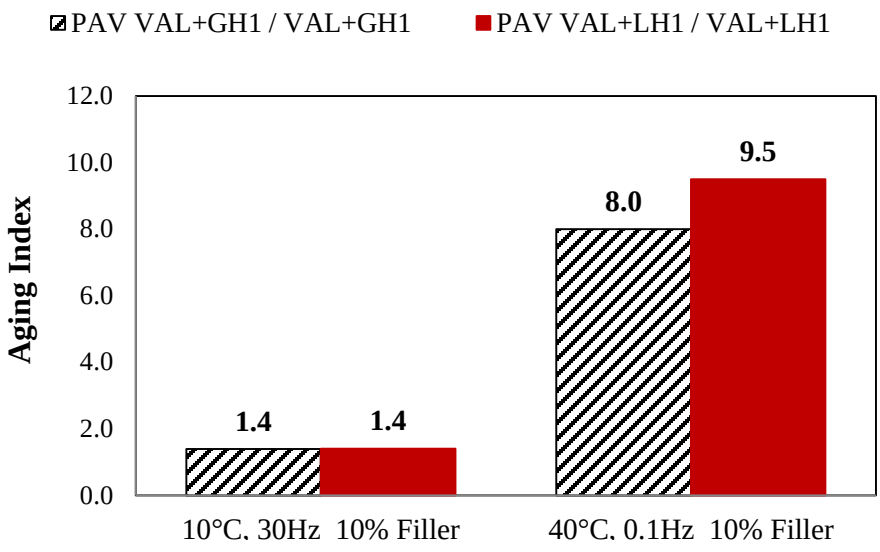

(a)

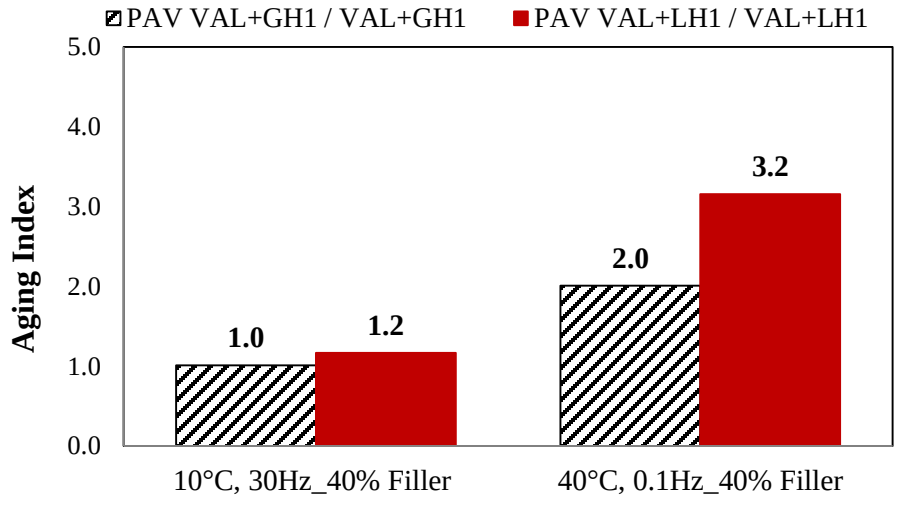

(b)

Figure IV-17: Comparison of the aging indexes without confounding effect of diffusion for (a) 10% filler, and (b) 40% filler in VAL binder.

Figure IV-18 shows a comparison between the aging index of mastic with 40% inert filler (believed to not interact of the oxidation process), and mastic with 40% of granite retained on the #50 sieve (R50). As the filler volume and particle size is similar in both mastics, the effect of the filler on diffusion path length is assumed to be similar, thus the additional decrease in the aging index is believed to indicate the presence of a surface interaction through adsorption mechanisms. This adsorption results in changes in molecular size distributions. These results are believed to confirm the existence of an adsorption effect in addition to any effect on diffusion in the binder.

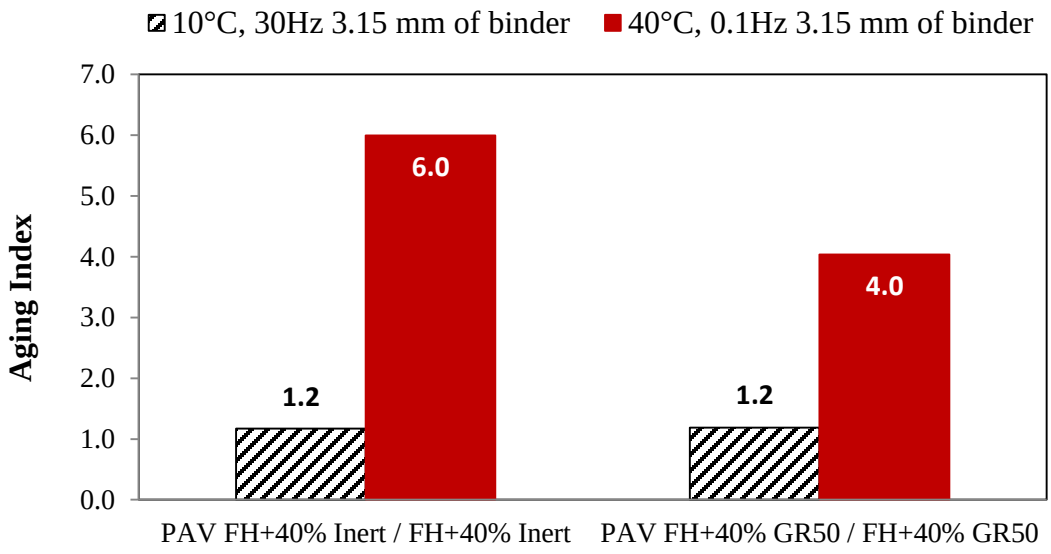

Figure IV-18: Calculated aging indexes of inert and granite R50 mastics.

The irreversible adsorption of polar asphalt components by the mineral filler surface, although not expected to stiffen the binder, will produce compositional changes in the asphalt bulk that may significantly affect asphalt properties and aging characteristics (Petersen, 1984).

4.4 Statistical Analysis of Aging Index of Complex Modulus

A statistical analysis was conducted to verify the effect of binder type and filler type on the aging index of |G*|. The factors selected for the aging study are presented in Table IV-3.

Table IV-3: Factors selected in aging study.

Factor	Levels	Description
Binder Type	2	FH and VAL
Filler Type	2	LH_1 and GH_1

In order to eliminate confounding effects such as temperature history and the diffusion process, the statistical analysis were performed on the |G*| aging index calculated for mastics with 1.0 mm of film thickness during PAV aging.

The results of the statistical analysis are shown in Table IV-4. The analysis showed that filler type is important with +95% confidence interval.

Table IV-4: Statistical analysis.

Aging Index of |G*| at 10°C				
	Df	**F value**	**Pr(>F)**	**Confidence Interval (%)**
Binder Type	1	49.011	0.0009163	99
Filler Type	1	11.211	0.0203685	98
Aging Index of |G*| at 40°C				
	Df	**F value**	**Pr(>F)**	**Confidence Interval (%)**
Binder Type	1	6.7486	0.04838	95.2
Filler Type	1	7.0339	0.04531	95.5

4.5 Analysis of Glass-Transition Temperature Testing Results

The glass-transition temperature is related to the asphalt binder performance at low-temperatures. The transition to glassy behavior is known to increase the brittleness of the binder extensively, reducing the potential for stress relaxation, increasing stiffness, and thus result in higher cracking susceptibility.

The possible effect of aging on the glass-transition temperature and behavior can significantly affect low-temperature behavior and also serve as an indirect assessment on compositional changes occurring in the asphalt (Turner and Branthaver, 1997). This increase in T_g due to an increase in asphaltenes content has been noted in the literature (Wada, 1960). In chemical terms, aging leads first to a decrease in aromatic content and subsequent increase in resin content, together with a higher asphaltene content (Wei et al., 1996).

4.5.1 Glass-Transition Analysis of Neat Asphalt Binder

As it can be seen in Figure IV-19, the glass-transition temperature of the neat asphalt binder decreases from 0 to 6 hours of aging conditioning. After 6 hours of oxidative aging, however, the glass-transition temperature starts to increase.

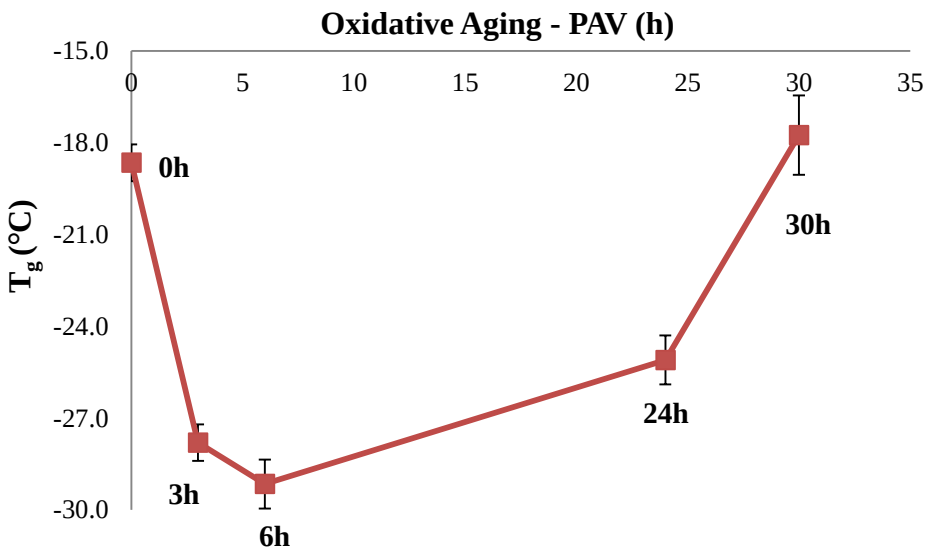

Figure IV-19: Glass-transition temperature of neat asphalt binder after different aging conditioning in PAV.

The behavior presented in Figure IV-19 can be explained as the result of the effect of the aging process on the asphaltenes and resins asphalt fractions. During the beginning of the oxidative aging process, the glass-transition behavior of the neat binder is dominated by the increase in the lower Tg resins fraction which leads to an overall decrease in the glass-transition temperature. After 6 hours of PAV aging, the asphaltenes content starts to increase (as previously shown in Table IV-1) and dominate the aging effect by increasing the Tg.

4.5.2 Glass-Transition Analysis of Asphalt Mastics

Mineral fillers are crystalline solids, thus they do not exhibit a glass-transition temperature as amorphous material such as asphalt do. Therefore, when testing the low-temperature performance of asphalt mastics the changes in the glass-transition can be attributed to the modification of the asphalt matrix.

The glass-transition temperature values were determined with a non-linear phenomenological model used by Nam and Bahia (2004) to fit thermo-volumetric curves, as described in Equation III-1. As it can be seen in Figure IV-20, the glass-transition curve of the mastics showed the same behavior as that of the asphalt binder curve. However, the presence of mineral filler after the initial drop in the Tg due to asphaltenes adsorption on the surface, shifted the curve toward higher temperatures after with aging conditioning. Figure IV-20 (c) schematically describes the observed trend of behavior resulting from aging of the binder in the presence of mineral filler. It can be seen that the shift of the glass-transition behavior curve is influenced by the mineral filler surface area and concentration. Mastics of the filler with higher surface area (Granite) show lower glass-transition temperatures. Furthermore, the mastics with higher filler concentration also show a decrease in the T_g temperature. An explanation for this behavior is the asphaltenes adsorption onto the fillers surface. The asphaltenes adsorption is expected to result in a softening of the bulk binder; this is the reason that T_g is observed to continuously decrease with filler volume concentration and filler surface area (Clopotel, 2012).

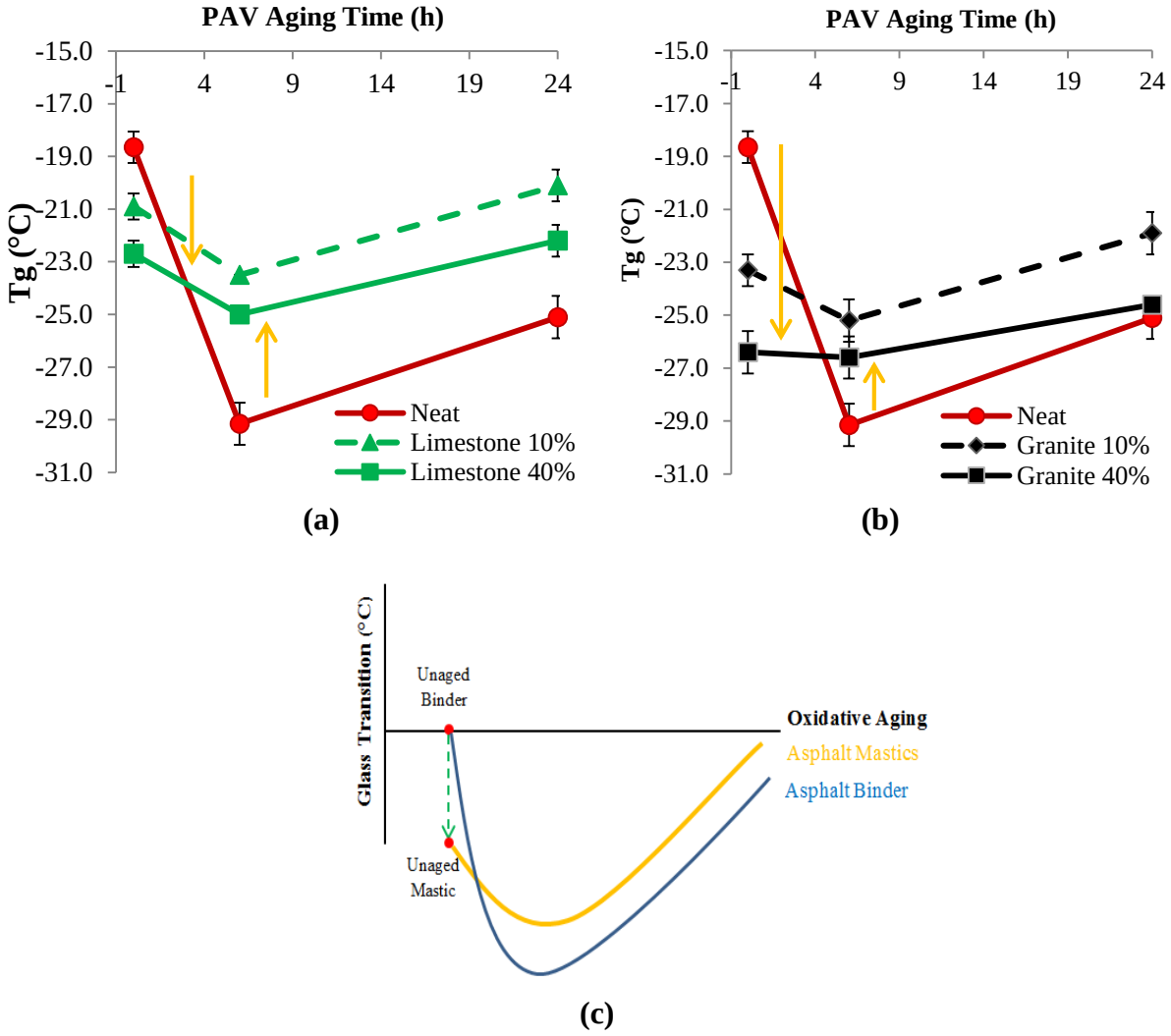

Figure IV-20: T_g temperatures after different aging in PAV for: (a) FH neat and limestone mastics; (b) FH neat and granite mastics; (c) schematic of T_g change for mastics compared to neat binders after different aging conditioning.

4.6 Volumetric Changes Analysis of Asphalt Mastics

In this study, the range of temperature from 25°C to -35°C was selected to calculate the volumetric changes in asphalt binder and mastics (Figures IV-21 and IV-22).

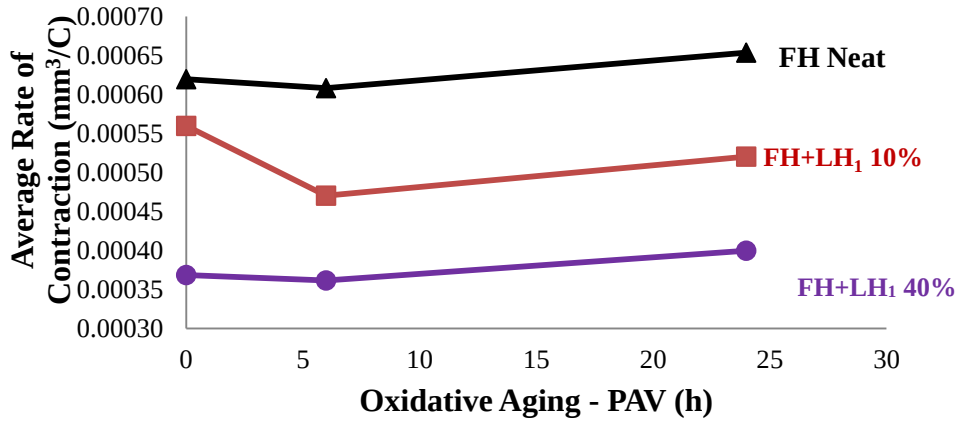

a)

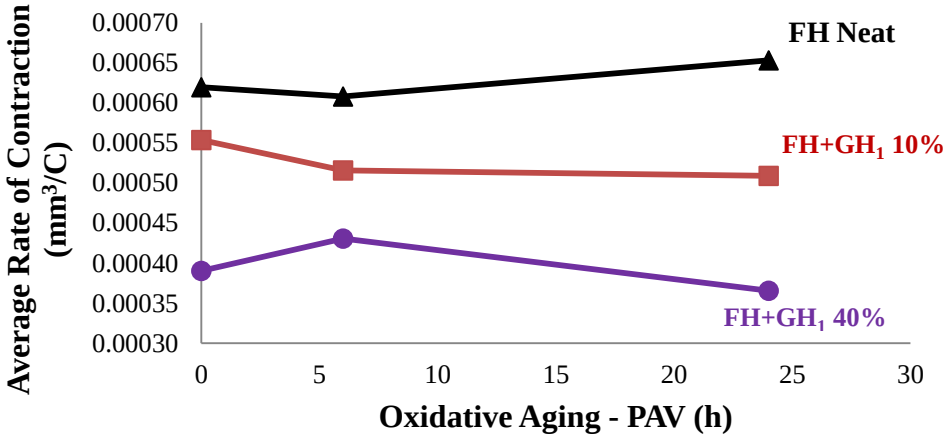

b)

Figure IV-21: Average rate of contraction of asphalt mastics with a) limestone filler, and b) granite filler.

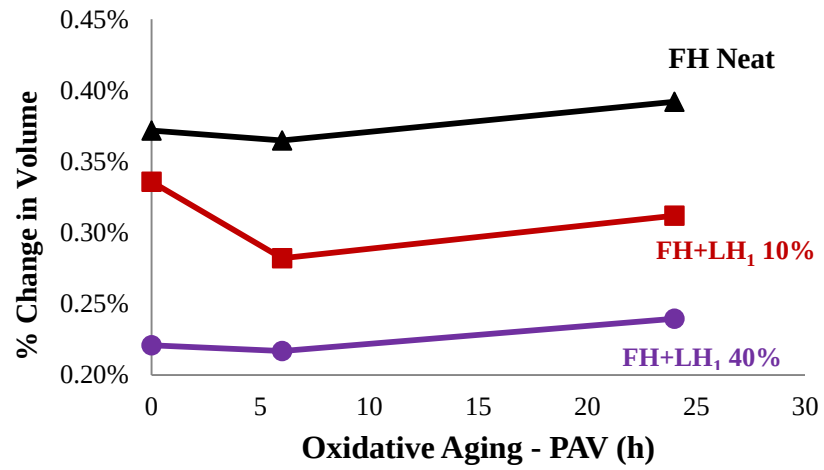

a)

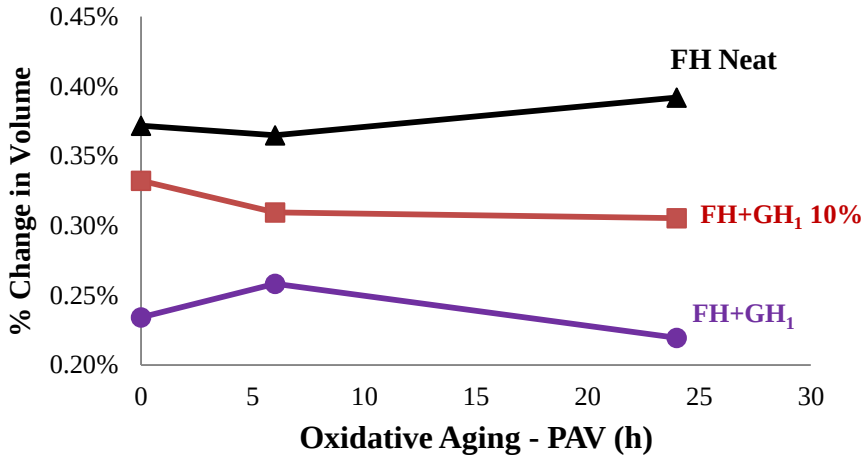

b)

Figure IV-22: % change in volume of asphalt mastics with a) limestone filler, and b) granite filler.

It can be seen that all mastic curves for average rate of contraction and percent change of volume have shifted down with respect to neat asphalt. This can be explained by the inclusion of mineral filler, which has lower rate of contraction than the asphalt binder.

Additionally, there is an inherent difference in behavior of mastic average rate of contraction and percent change in volume with respect to filler type. For limestone, the initial rate

of contraction drops after 6 hours of aging, while after continued aging it begins to increase again. This trend is observable for 10% and 40% filler concentration by volume as well. Such a trend, however, is not observable for granite.

Therefore, by selecting proper filler type, the effect of aging on the filler contraction can be controlled (i.e. avoiding using filler type that leads to large volumetric contraction with aging). Such control may provide better low-temperature performance, leading to fewer pavement thermal cracking distresses.

4.7 Analysis of Bending Beam Rheometer Testing Results

Testing temperatures were selected based on the neat base binder grade. The testing temperatures correspond to the neat binder low-temperature performance grade (LT PG) and the PG temperature plus one grade (LT PG + 6°C) to verify if the addition of filler materials would increase the low-temperature grade. Also, a constant test temperature of -18°C was added for verification of low-temperature performance of both binders.

In order to show the effects of aging on stiffness and m-value of binder and mastics, an aging index was calculated. The aging indexes were calculated according to Equation IV-2.

$$\textbf{Aging Index}\ (\mathbf{S, m-value}) = \frac{(\mathbf{S\ or\ m-value})_{\mathbf{After\ 24h\ PAV}}}{(\mathbf{S\ or\ m-value})_{\mathbf{Unaged}}} \quad \text{(IV-2)}$$

For both FH and VAL base binders, the unaged beams could not be tested at -6°C for comparative purposes due to the excess softness of the material.

As it can be seen in Figure IV-23, the addition of mineral filler appears to decelerate the age hardening (i.e. stiffness, S) of FH asphalt mastics, when compared to the FH base binder. It can also be seen that by lowering the temperature (i.e. -18°C), the effect of different filler types becomes very similar, regardless the filler mineralogy.

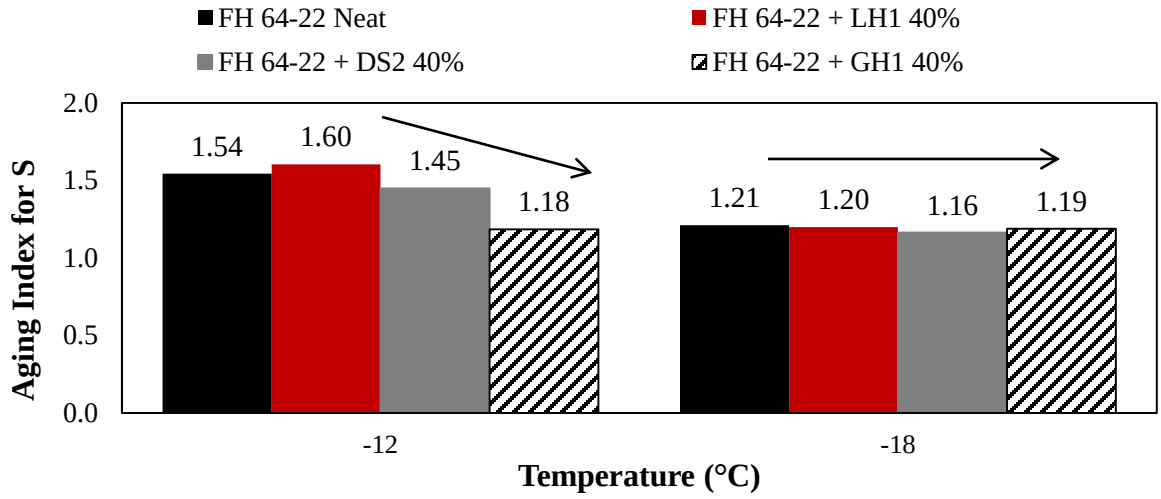

(a)

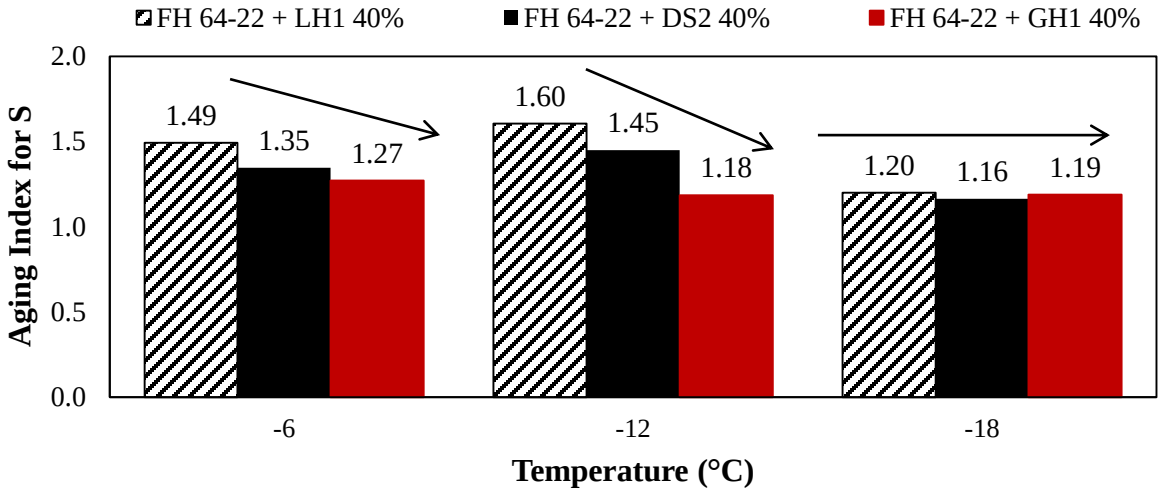

(b)

Figure IV-23: Aging Index for S of (a) FH neat and mastics, and (b) mastics only.

Figure IV-24 shows the effect of mineral filler on m-value (i.e. how the asphalt binder relaxes the load induced stresses) of FH asphalt mastics compared to the FH base binder.

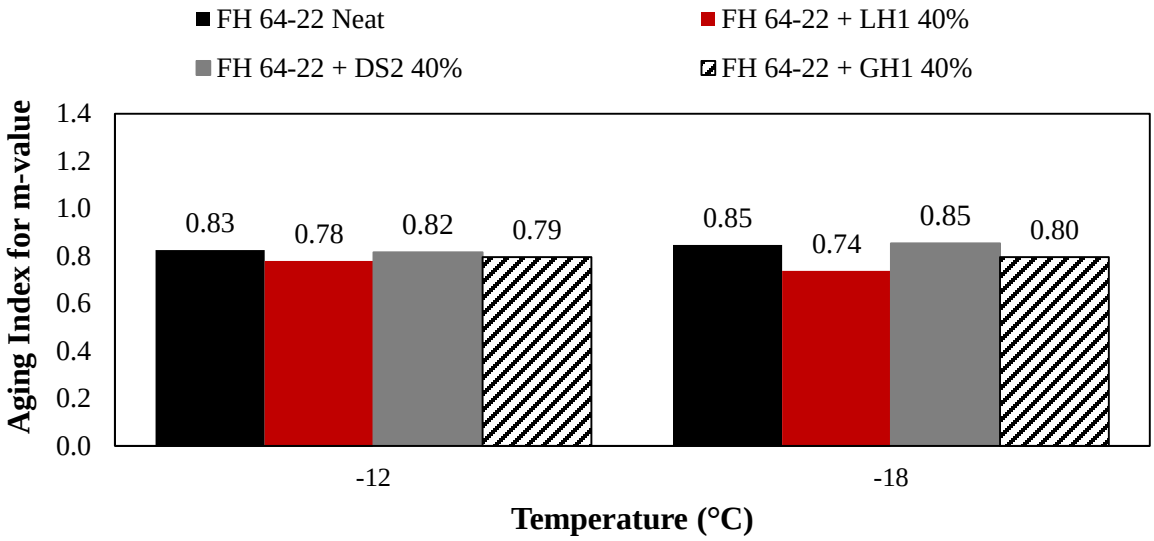

(a)

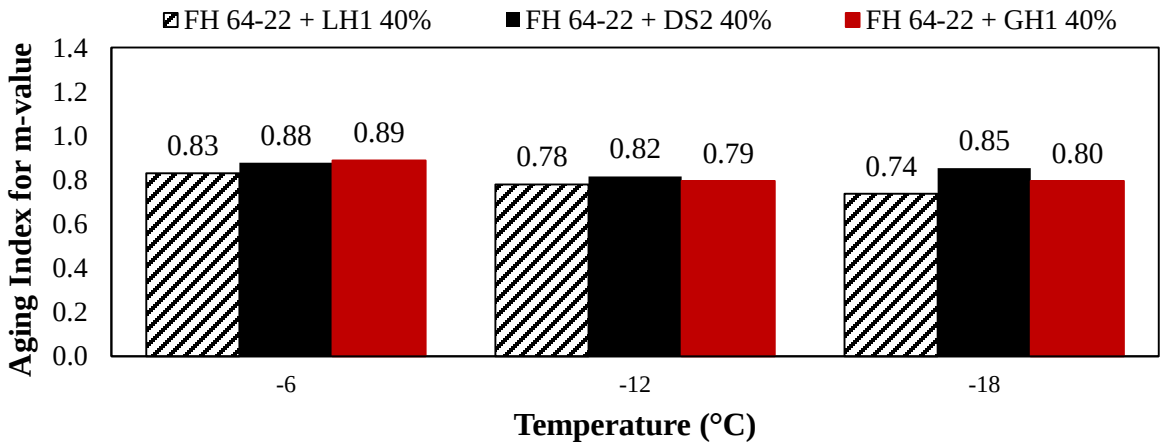

(b)

Figure IV-24: Aging Index for m-value of (a) FH neat and mastics, and (b) mastics only.

According to the results showed in Figure IV-23 and IV-24, filler type (i.e. mineralogy) and filler's surface area appear to contribute to the deceleration of age hardening and positively affect the rate of mastic stress relaxation after aging.

As it can be seen in Figure IV-25, the addition of mineral filler appears to decelerate the age hardening (i.e. stiffness S) of VAL asphalt mastics as measured by the BBR, when compared to the VAL base binder. Figure IV-26 shows the effect of mineral filler on m-value (i.e. how the asphalt binder relaxes the load induced stresses). From both Figures, it is visible that factors other than the fillers' surface area may be contributing to the binder age-hardening. Therefore, to verify the changes in molecular size after addition of mineral filler, Gel Permeation Chromatography (GPC) tests were performed, as will be discussed next in Chapter V.

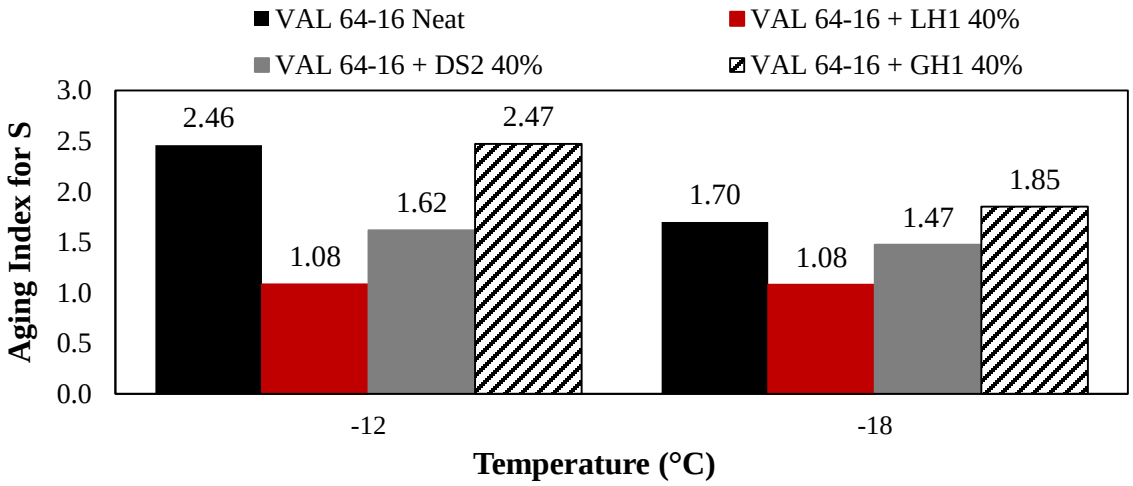

(a)

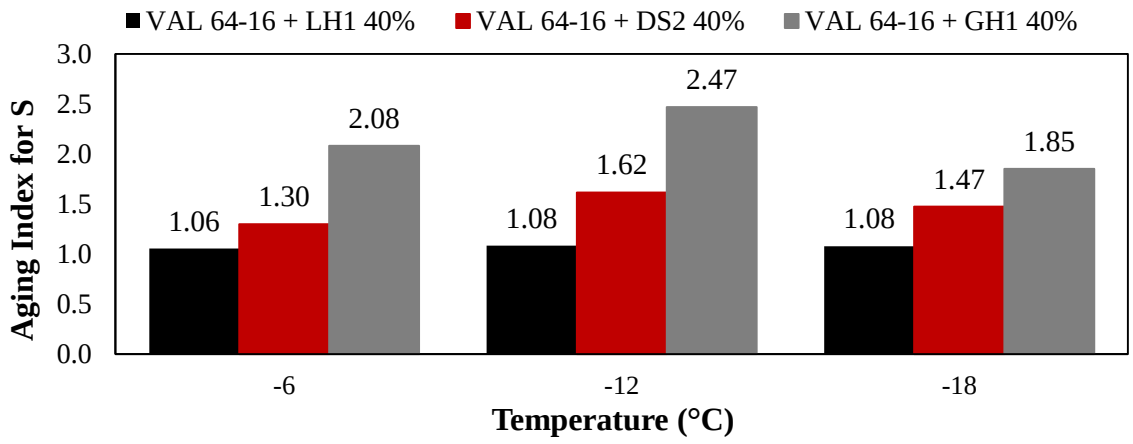

(b)

Figure IV-25: Aging Index for S of (a) VAL neat and mastics, and (b) mastics only.

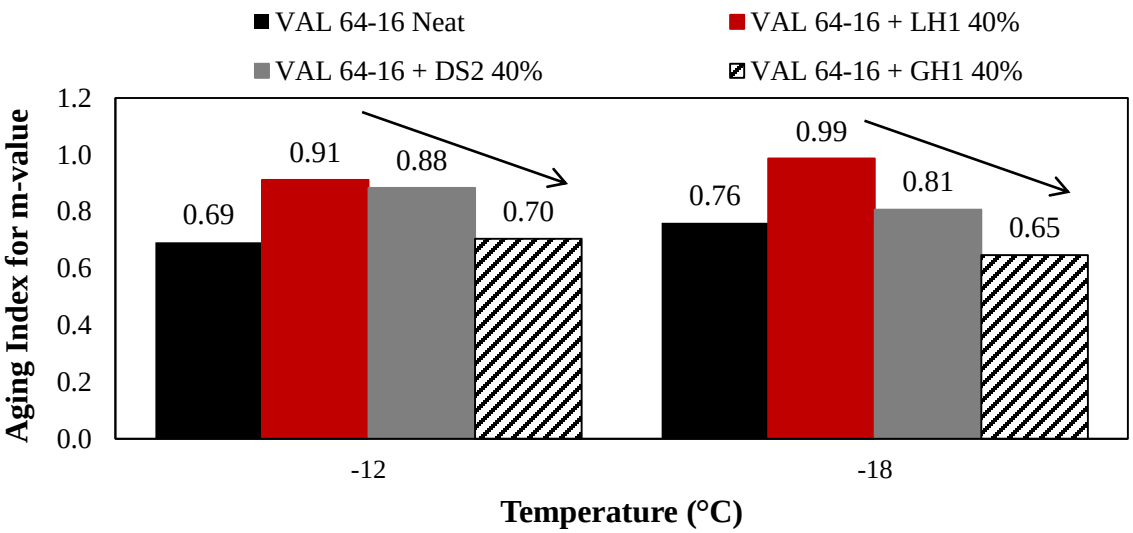

(a)

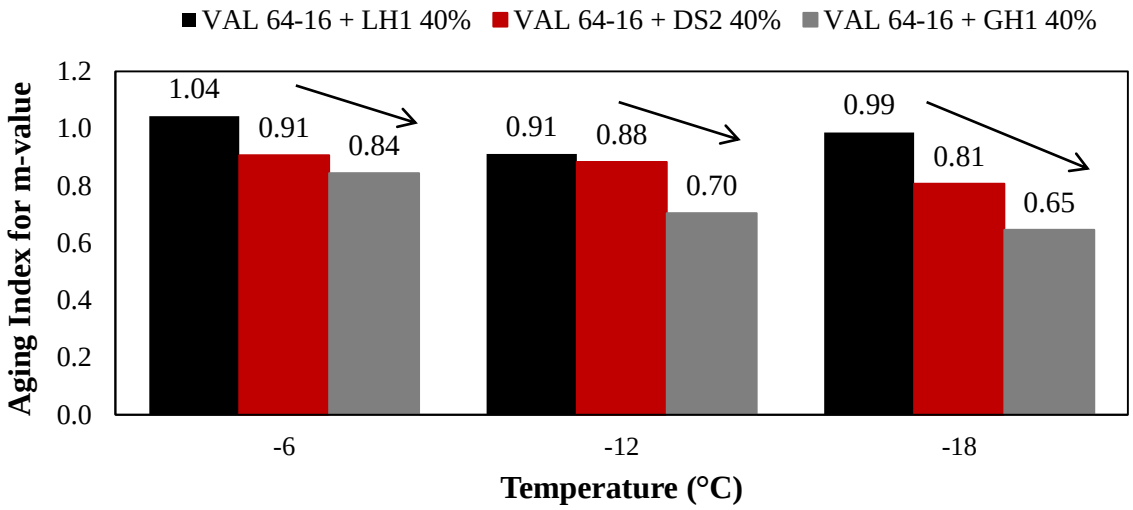

(b)

Figure IV-26: Aging Index for m-value of (a) VAL neat and mastics, and (b) mastics only.

V. Verification of the Effect of Filler on Molecular Size Distribution of Asphalt Binders

In the previous chapter it was shown that the filler surface interactions with the base binder considerably affect the mechanical and rheological properties of the aged material. Much of this effect was attributed to the adsorption mechanism, but additional compositional affects are also believed to be affecting the aging behavior observed in Chapter IV. To further investigate the possible mechanisms, this chapter presents analysis of changes in the molecular size distribution of binders and mastics after oxidative aging. It also includes a correlation between Gel Permeation Chromatograph (GPC) results and rheological data obtained with the Dynamic Shear Rheometer (DSR).

5.1 Analysis of Molecular Size Distribution

By using the Gel Permeation Chromatography (GPC) technique, an evaluation of the effect of filler on aging of asphalt binders was investigated. The GPC spectrum was divided into 13 equal elution time areas as described in Chapter III, section 3.2.4.

The area under the curve represents 100% (or 1.0) of the binder's molecules injected into the GPC system (Kim et al. 2013). Each partition of the chromatogram was divided by the total area under the curve to normalize the comparisons of one chromatogram to another.

5.1.1 Flint Hills 64-22 Base Binder

5.1.1.1 Results After 24 hours of Oxidative Aging

Figure V-1 shows the GPC chromatogram of the FH base binder and mastics before oxidative aging. Figure V-2 shows the GPC chromatogram of the FH base binder and mastics after 24 hours of PAV aging.

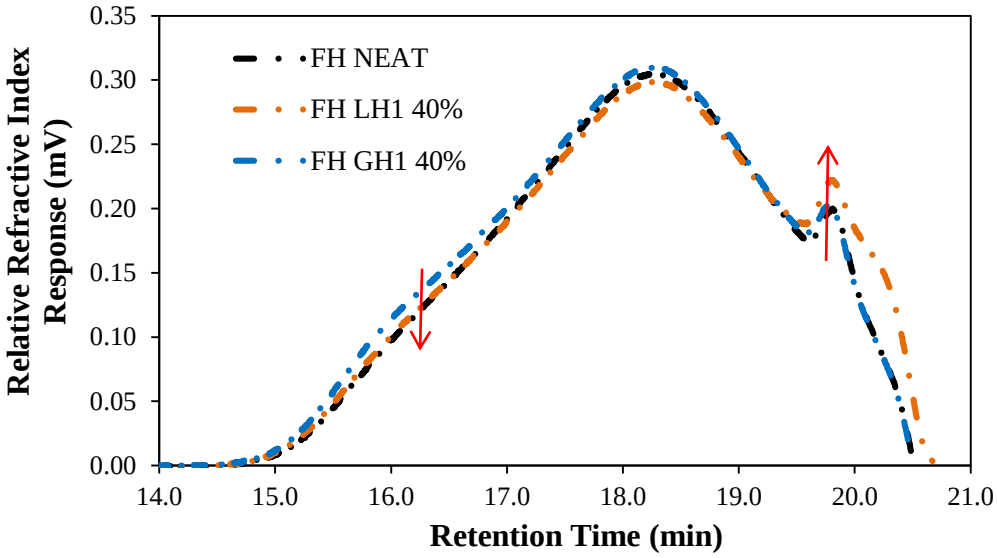

Figure V-1: GPC chromatogram before aging of FH base binder and mastics with 40% by volume of filler.

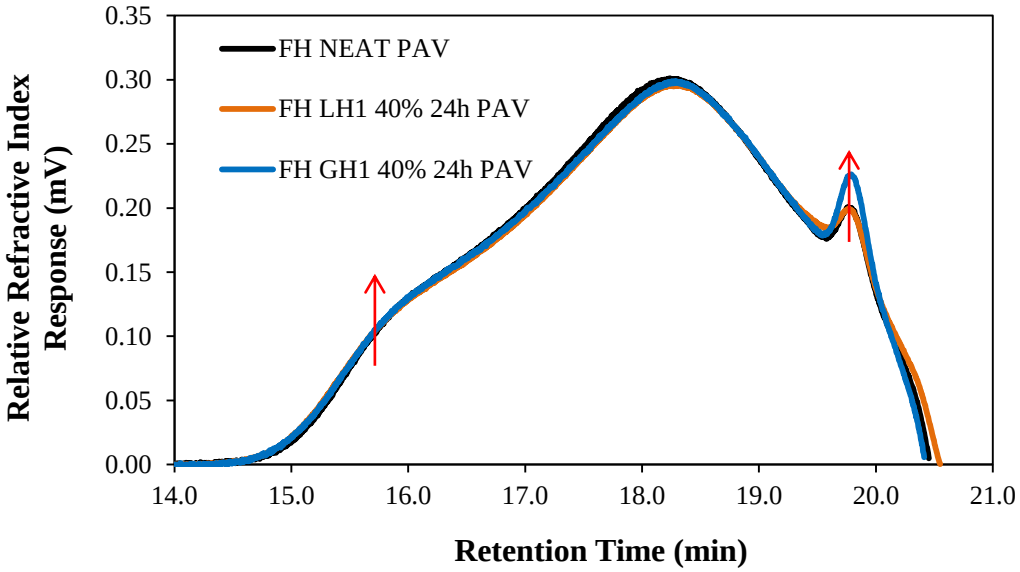

Figure V-2: GPC chromatogram after 24 hours of aging of FH base binder and mastics with 40% by volume of filler.

From both Figures V-1 and V-2 it is visible that there are differences among the GPC curves, especially in the LMS and SMS regions.

In order to better investigate these molecular changes after oxidation, aging indexes based on molecular size obtained by GPC were developed. The aging indexes were calculated according to Equation V-1 through V-3.

$$\text{LMS Aging Index} = \frac{\text{Large Molecular Size Molecules after PAV}}{\text{Large Molecular Size Molecules before PAV}} \quad \text{(V-1)}$$

$$\text{MMS Aging Index} = \frac{\text{Medium Molecular Size Molecules after PAV}}{\text{Medium Molecular Size Molecules before PAV}} \quad \text{(V-2)}$$

$$\text{SMS Aging Index} = \frac{\text{Small Molecular Size Molecules after PAV}}{\text{Small Molecular Size Molecules before PAV}} \quad \text{(V-3)}$$

Figure V-3 shows the calculated aging indexes of molecular size areas for the neat FH binder and mastics with 40% of mineral filler. After 24 hours of PAV aging, the MMS and SMS areas do not change due to aging for any of the tested material (with or without filler) using the FH base. A higher decrease in aging index of LMS was observed for dolamite (DS_2), followed by granite (GH_1). The LMS is the percentage of high molecular weight molecules in a binder, as well described by Jennings (1980). Many studies indicated that the large molecular size of asphalt binder (LMS) presents good correlations with asphalt mixture properties (Jennings et al., 1980; Kim et al., 1993; Al-Abdulwahhab et al., 1999). Furthermore, the incremental increase of LMS due to aging can be correlated to asphalt physical properties (e.g. increased absolute viscosity) (Bynum, 1970, Jennings et al., 1980; Al-Abdulwahhab et al., 1999).

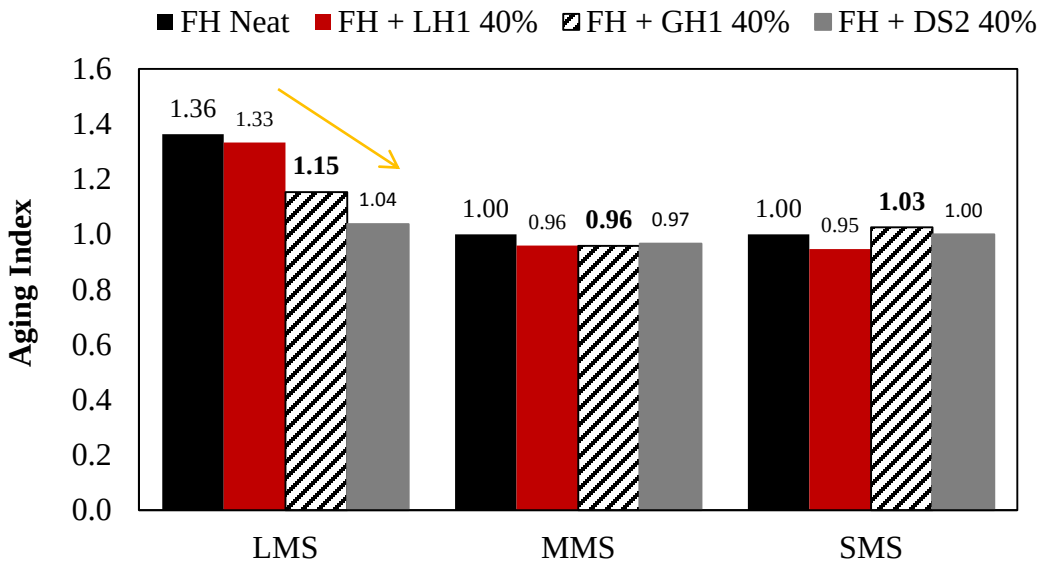

Figure V-3: GPC size area aging indexes of FH base binder and mastics with 40% by volume of filler.

Figure IV-4 shows aging indexes calculated from the quantitative data (i.e. molecular sizes) of the GPC chromatogram. The aging index for each of the molecular size distribution parameters was calculated according to Equation V-4.

$$\text{Aging Index (Mn, Mz, Mw, Mp)} = \frac{\text{(Mn,Mz,Mw,Mp)After 24h PAV}}{\text{(Mn,Mz,Mw,Mp)Unaged}} \quad \text{(V-4)}$$

As it can be seen in Figure V-4, the results of the GPC molecular size aging indexes for the mastics were smaller than that observed for the aged neat binder. The most significant difference between mastic and base binder aging index is observed for the Mz index (z-average molecular size, roughly corresponding to the LMS), where the aging index dropped from 1.54 (neat binder) to 1.13 (granite mastic). These results support the previously mentioned findings in

terms of effect of the fillers on mechanical properties, as well as the visually observed trend in LMS (large molecular size molecules), where the presence of mineral filler appears to decelerate the age hardening of asphalt mastics.

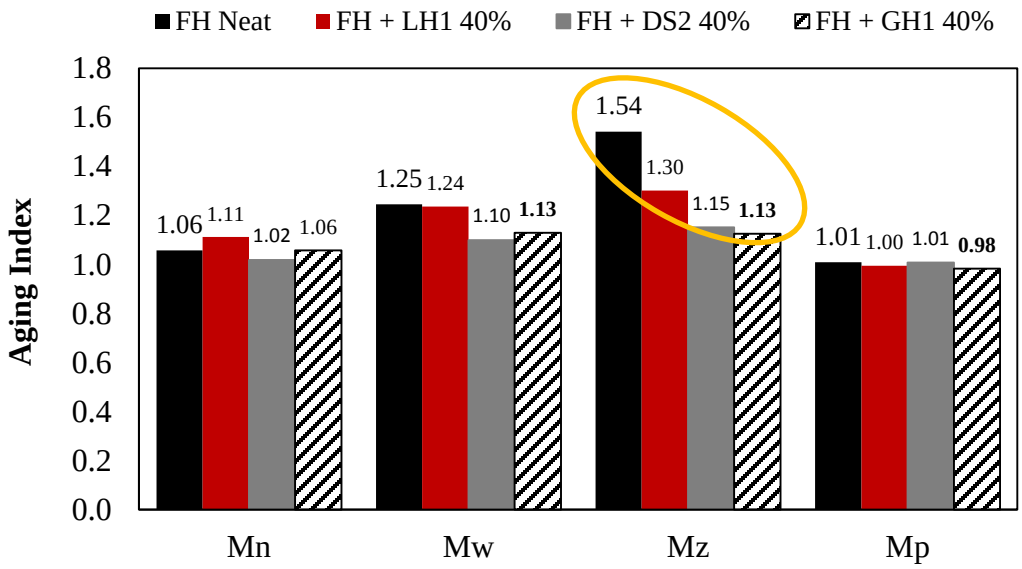

Figure V-4: GPC molecular size aging indexes of molecular weight FH base binder and mastics with 40% by volume of filler.

5.1.1.2 Results After 48 hours of Oxidative Aging

The oxidative aging in the Pressure Aging Vessel (PAV) involves a diffusion mechanism; therefore, film thickness is expected to be an important factor during aging in the PAV. In order to differentiate the diffusion effect from the mineral surface effect, different mastic thicknesses were selected and aged for 48 hours.

Figure V-5 shows the GPC chromatogram of the FH neat and mastics after 48 hours in PAV, where both base binder and mastics presented 3.15 mm of film thickness. Figure V-6 shows

the calculated aging indexes of molecular size areas for the neat FH binder and mastics with 40% of mineral filler also after 48 hours of aging with 3.15 mm of film thickness.

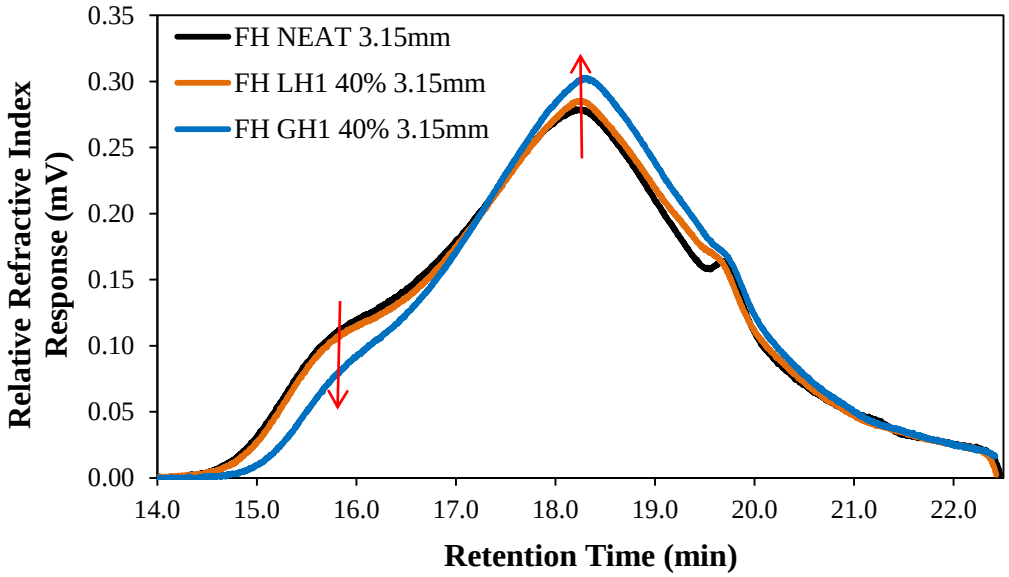

Figure V-5: GPC chromatogram after 48 hours of aging of FH base binder and mastics with 40% by volume of filler (film thickness of 3.15 mm).

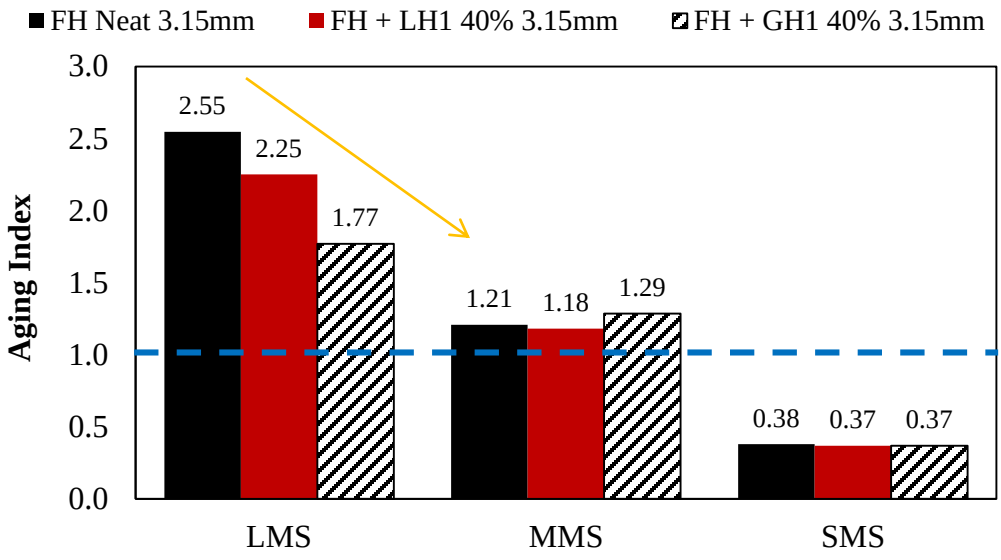

Figure V-6: GPC size area aging indexes of FH base binder and mastics with 40% by volume of filler after 48 hours in PAV (film thickness of 3.15 mm).

As it can be seen in Figure V-5, the addition of filler affects the LMS, MMS, and SMS molecular size areas. A bigger difference in the region of large molecular size molecules was observed for the aged mastic with the granite filler, when comparing to the base binder. Figure V-6 shows that, for all materials (with and without filler), the oxidative aging increases LMS, decreases SMS, but does not change MMS significantly. The effect of filler type is significantly seen in LMS, where the mastic with the granite filler (highest specific surface area) has a lower increase in large molecular size after aging compared to the neat and limestone mastic, possibly due to the increase in surface adsorption of larger molecular size polar components which are consequently unavailable for oxidation during the aging process. Fillers effect on MMS and SMS is minor.

In order to eliminate possible confounded diffusion effects, binder and mastics with film thickness of 1.0 mm were aged for 48 hours in PAV. Figure V-7 shows the GPC chromatogram of the FH neat and mastics after 48 hours in the PAV. Figure V-8 shows the calculated aging indexes of molecular size areas for the neat FH binder and mastics with 40% of mineral filler.

As it can be seen in Figures V-7 and V-8, for the base binder and mastics the effect of filler type is significant for the LMS area. Therefore, even after eliminating diffusion effects, the presence of mineral filler affects the aging process, as observed from the molecular size distribution of the asphalt after the asphalt aging process.

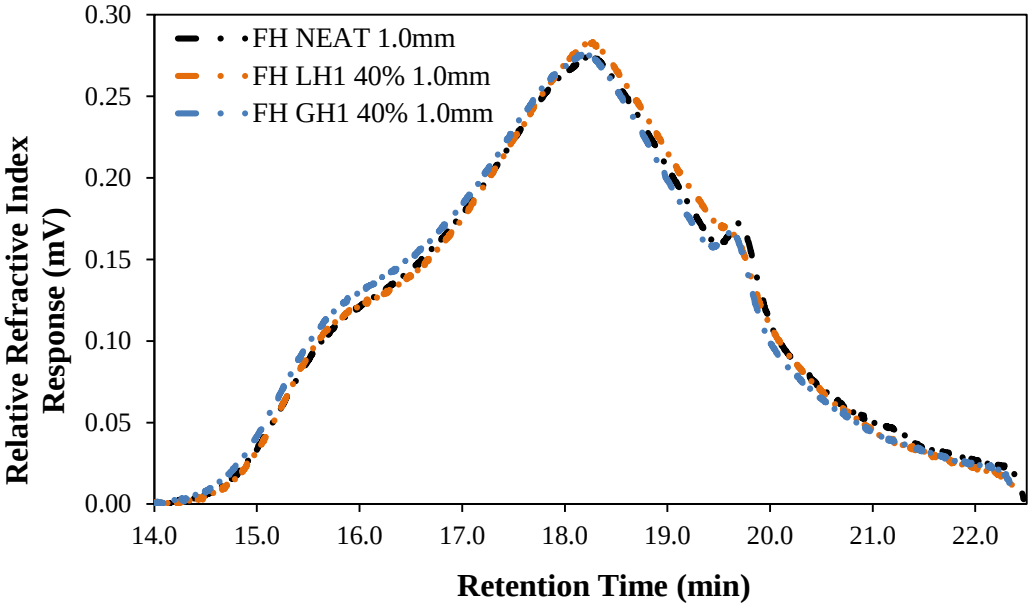

Figure V-7: GPC chromatogram after 48 hours of aging of FH base binder and mastics with 40% by volume of filler (film thickness of 1.0 mm to limit diffusion rate effects).

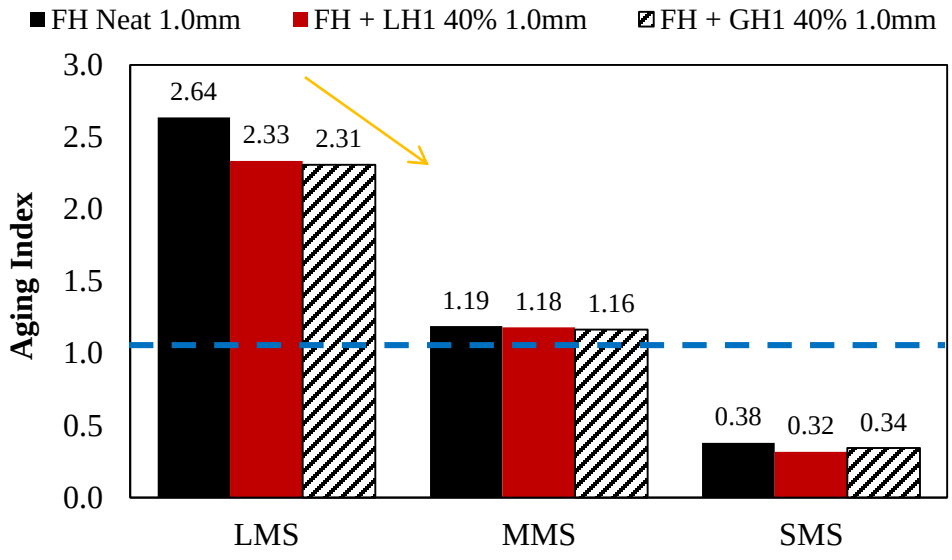

Figure V-8: GPC size area aging indexes of FH base binder and mastics with 40% by volume of filler after 48 hours in PAV (film thickness of 1.0 mm to limit diffusion rate effects).

5.1.2 Valero 64-16 Base Binder

5.1.2.1 Results After 24 hours of Oxidative Aging

Figure V-9 shows the GPC chromatogram of the VAL base binder and mastics before oxidative aging. Figure V-10 shows the GPC chromatogram of the VAL base binder and mastics after 24 hours of PAV aging.

From both Figures V-9 and V-10 it is visible that there are differences among the GPC chromatograms, especially in the LMS and SMS regions. In order to better investigate these molecular changes after oxidation, aging indexes based on molecular size obtained by GPC were calculated (Equation V-1 through V-3).

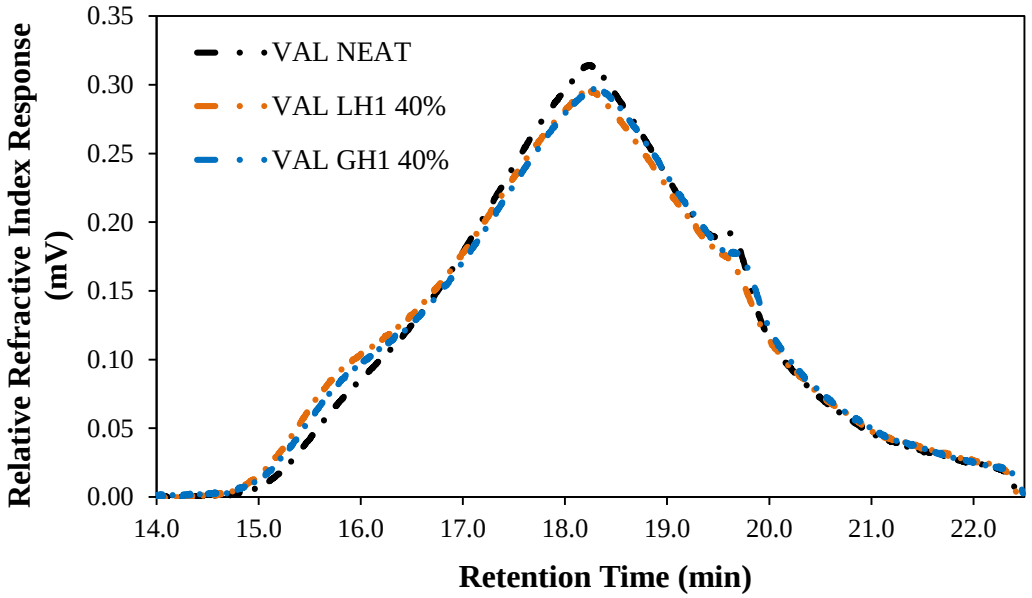

Figure V-9: GPC chromatogram before aging of VAL base binder and mastics with 40% by volume of filler.

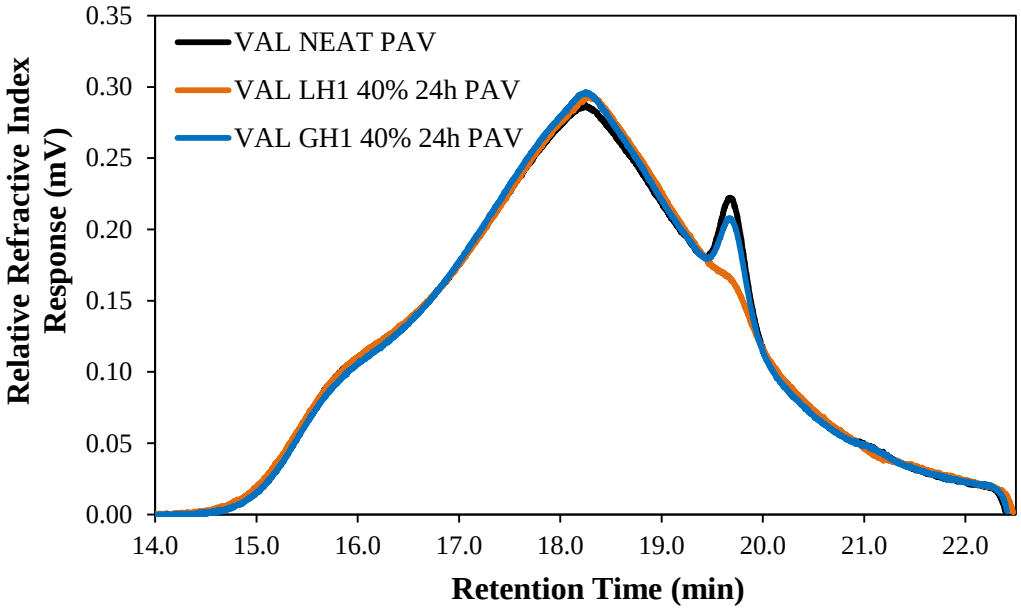

Figure V-10: GPC chromatogram after 24 hours of aging of VAL base binder and mastics with 40% by volume of filler.

Figure V-11 shows the calculated aging indexes of molecular size distribution areas for the neat VAL binder and mastics with 40% of mineral filler. After 24 hours of PAV aging, equal behavior is observed in the aging index of LMS for limestone (LH_1) and granite (GH_1) fillers. A higher decrease in the aging index of small molecular size is observed for limestone. Figure IV-12 shows aging indexes (Equation V-4) calculated from the quantitative data (i.e. molecular size distribution) of the GPC chromatogram.

As it can be seen, the results of the GPC LMS aging indexes for the mastics were smaller than that of the neat binder, but this difference was less pronounced than that of the FH base binders and mastics. The higher decrease is observed for the Mz index (roughly corresponding to the LMS), where the aging index dropped from 1.39 (neat binder) to 1.12 (granite mastic). Same observed behavior for the FH base binder.

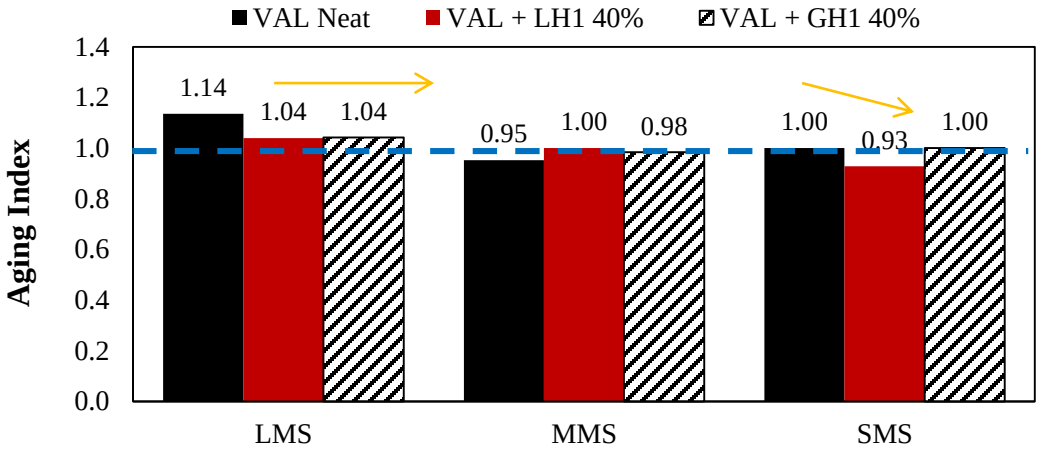

Figure V-11: GPC size area aging indexes of VAL base binder and mastics with 40% by volume of filler.

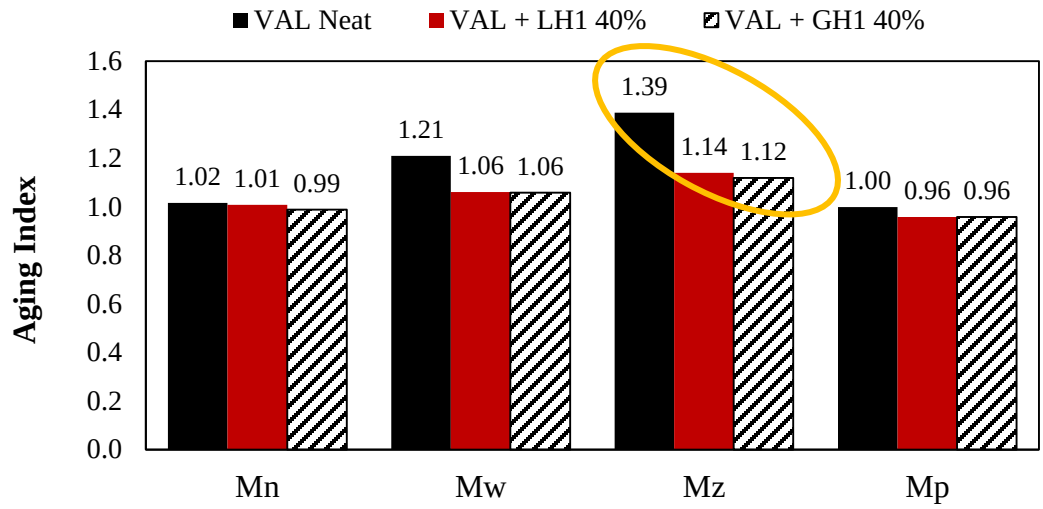

Figure V-12: GPC molecular weight aging indexes of molecular weight VAL base binder and mastics with 40% by volume of filler.

5.1.2.2 Results After 48 hours of Oxidative Aging

Figure V-13 shows the GPC chromatogram of the VAL neat binder and mastics after 48 hours in PAV, where both base binder and mastics presented 3.15 mm of film thickness. Figure V-14 shows the calculated aging indexes of molecular size distribution areas for the neat VAL

binder and mastics with 40% of mineral filler also after 48 hours of aging with 3.15 mm of film thickness.

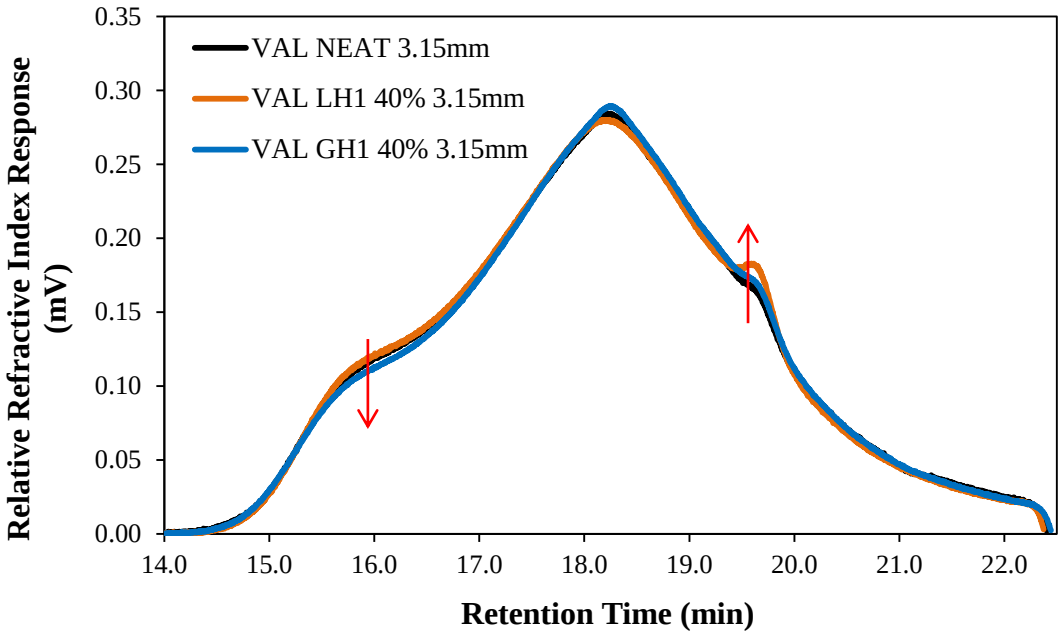

Figure V-13: GPC chromatogram after 48 hours of aging of VAL base binder and mastics with 40% by volume of filler (film thickness of 3.15 mm).

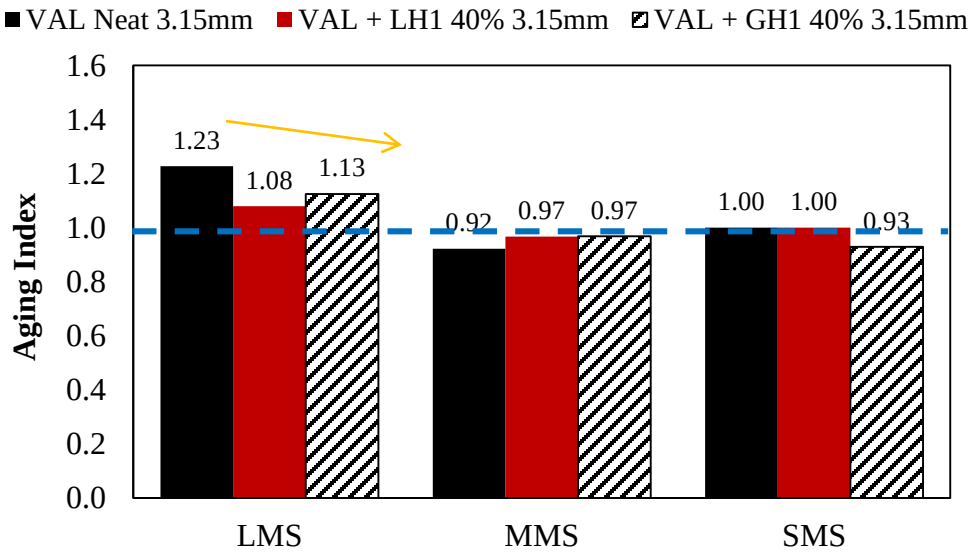

Figure V-14: GPC size area aging indexes of VAL base binder and mastics with 40% by volume of filler after 48 hours in PAV (film thickness of 3.15 mm).

From Figure V-13 it is observed that the addition of filler affects the molecular size distribution of the binder. Figure V-14 show a higher decrease in aging index of LMS with addition of filler, when comparing with the neat binder. Presence of filler has not affected the aging effect on the molecular size distribution of the medium molecular size and small molecular size molecules.

Binder and mastics with film thickness of 1.0 mm were aged for 48 hours in PAV to eliminate the confounded diffusion effects. Figure V-15 shows the GPC chromatogram of the VAL neat and mastics after 48 hours in PAV. Figure V-16 shows the calculated aging indexes of molecular size areas for the neat VAL binder and mastics with 40% of mineral filler. Results show a higher decrease in aging index of LMS when comparing with neat binder. However, similar behavior is observed for both limestone and granite fillers.

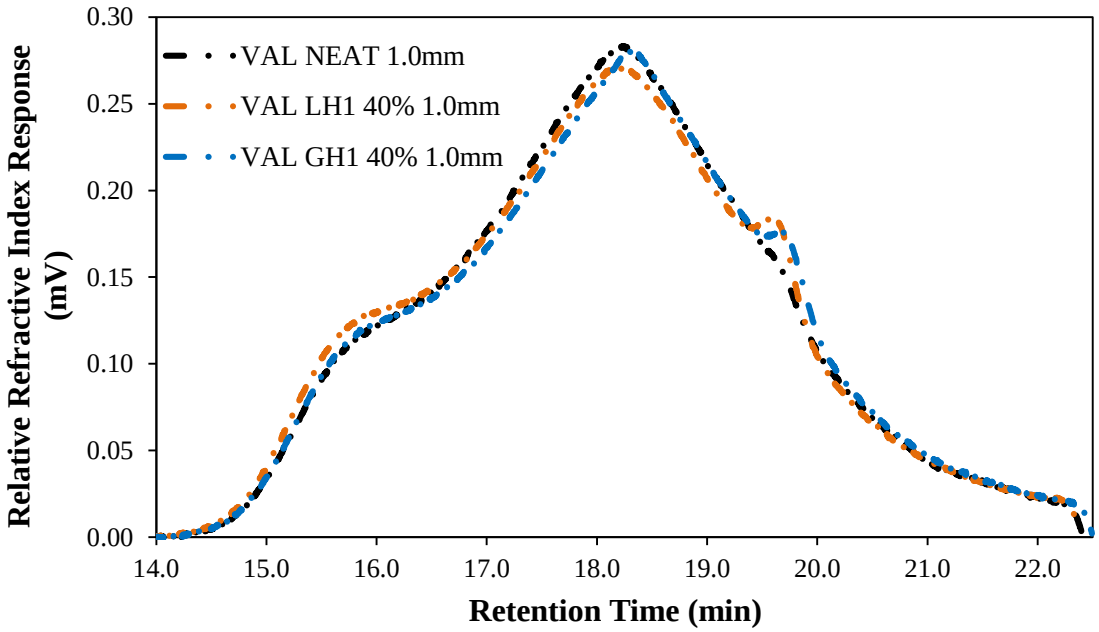

Figure V-15: GPC chromatogram after 48 hours of aging of VAL base binder and mastics with 40% by volume of filler (film thickness of 1.0 mm to eliminate diffusion rate effect).

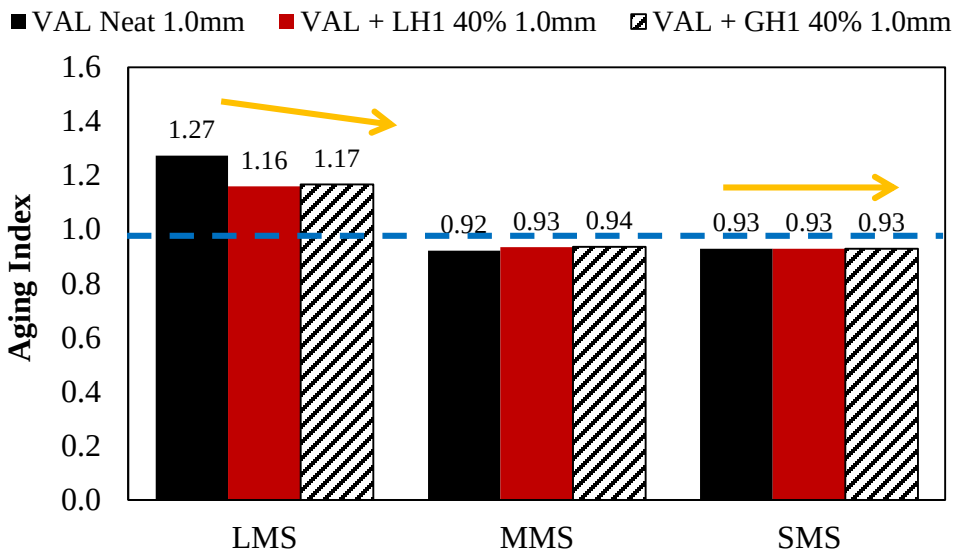

Figure V-16: GPC size area aging indexes of VAL base binder and mastics with 40% by volume of filler after 48 hours in PAV (film thickness of 1.0 mm to eliminate diffusion rate effect).

5.2 Relating Effect of Aging on GPC Results to Rheology

5.2.1 Relating Effect of Aging on GPC Results to the Master Curve

A master curve slope parameter was calculated for both high and low-temperature, as described in Equation V-5. The determination of the region of slope calculation at low-temperature (i.e., high frequencies), and high temperature (i.e., low frequencies) is demonstrated in Figure V-17.

$$Slope\ (HT,\ LT) = \frac{\frac{logG_1^* - logG_2^*}{logf_1 - logf_2}}{} \quad \text{(V-5)}$$

where,

Slope (HT) = Slope at high-temperature

Slope (LT) = Slope at low-temperature

Log G_1* = log of complex modulus, 1

Log G_2* = log of complex modulus, 2

Log f_1 = log of frequency, 1

Log f_2 = log of frequency, 2

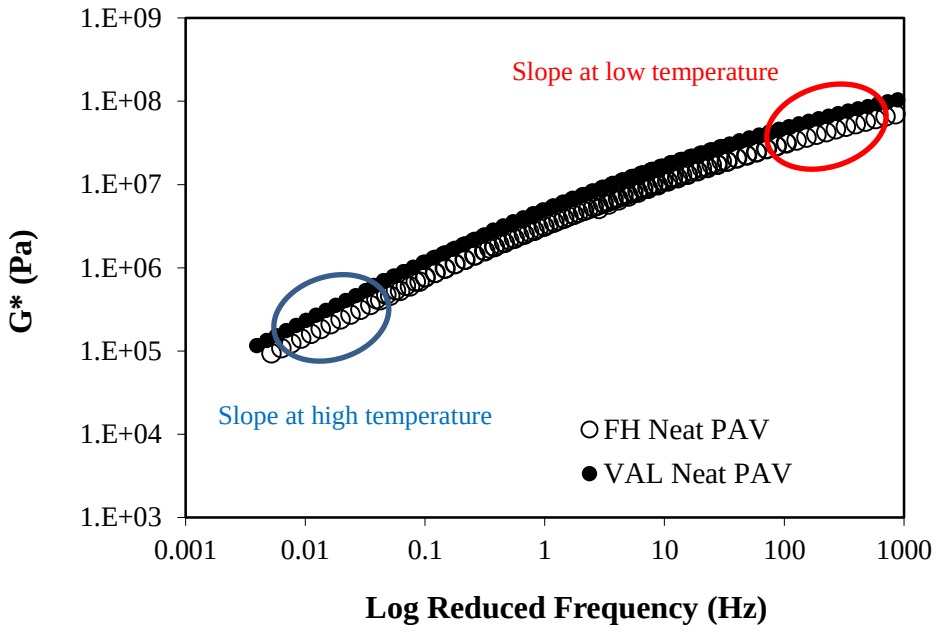

Figure V-17: Slope of master curve calculation.

In order to investigate correlation between the molecular changes after oxidation and rheological response, a new ratio based on molecular size obtained by GPC was developed. The ratios were calculated according to Equation V-6 and V-7.

$$\text{Ratio of LMS} = \frac{\text{Large Molecular Size Molecules after PAV}}{\text{Large Molecular Size Molecules before PAV}} \quad \text{(V-6)}$$

$$\text{Ratio of SMS} = \frac{\text{Small Molecular Size Molecules after PAV}}{\text{Small Molecular Size Molecules before PAV}} \quad \text{(V-7)}$$

Figure V-18 shows the correlations between the master curve slopes and the ratio of molecular size of FH mastics.

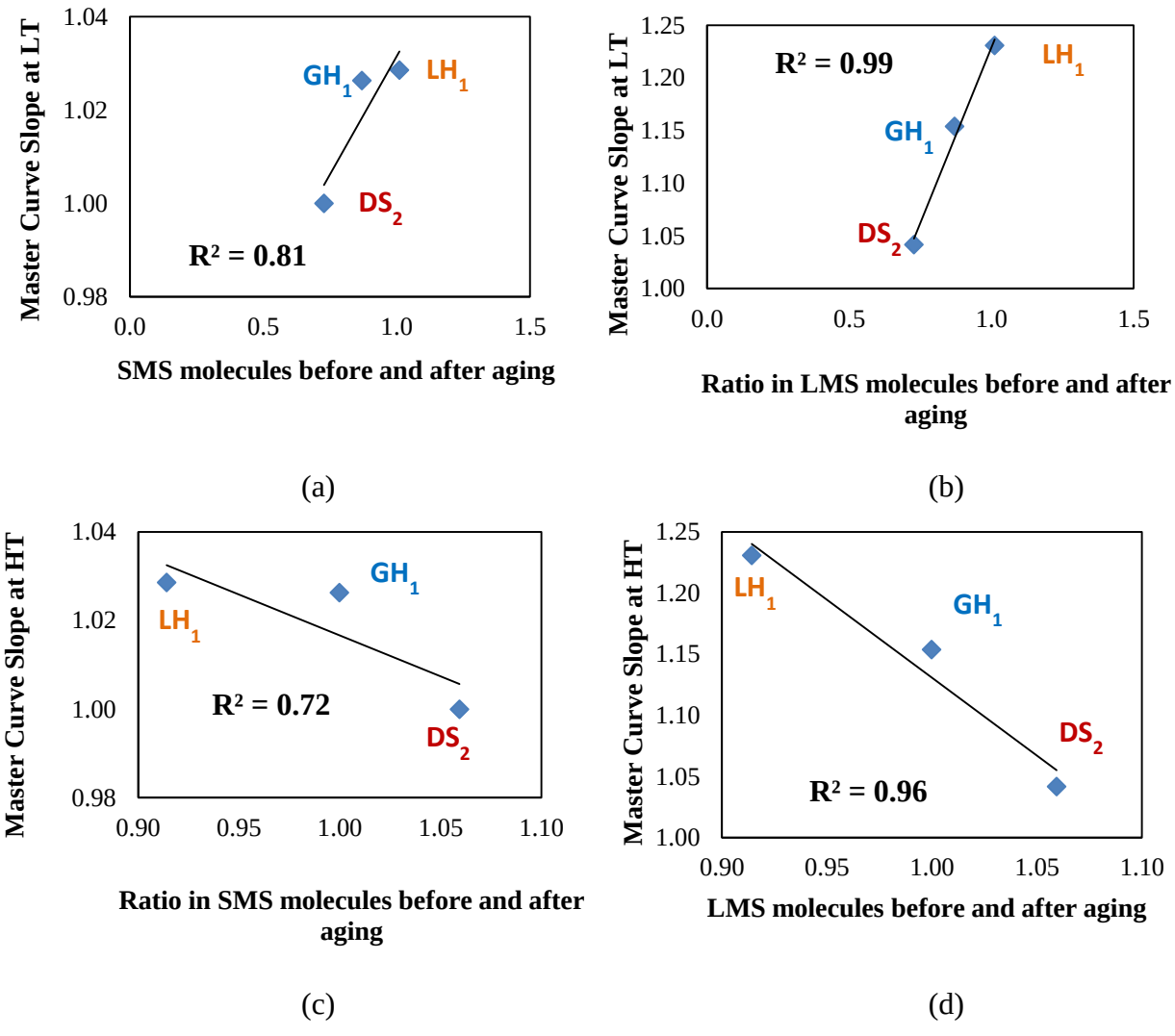

Figure V-18: Correlation between FH mastics master curve slope: (a) at low-temperature and ratio of SMS, (b) at low-temperature and ratio of LMS, (c) at high-temperature and ratio of SMS, and (d) at high-temperature and ratio of LMS.

As it can be seen in Figure V-18, results show that mastics that led to a higher increase in SMS after aging (higher Ratio of SMS) showed a higher increase in low-temperature master curve slope (higher LT temperature susceptibility after aging). On the other hand, mastics that caused greater increase in LMS after aging (higher ratio of LMS) led to lower high-temperature master curve slope (lower HT temperature susceptibility.)

As performed for the FH base binder, correlations between the master curve slopes (Equation V-5) and the ratio of molecular size (Equation V-6 and V-7) where performed for VAL mastics.

Figure V-19 shows that a higher loss of small molecular size molecules (smaller SMS ratio) results in a higher decrease in master curve slope at low-temperatures (i.e., more loss of temperature susceptibility due to aging). It is also observed that a higher gain in large molecular size molecules (larger LMS ratio) results in an increase in the master curve slope at high temperatures (i.e., more HT temperature susceptibility due to aging).

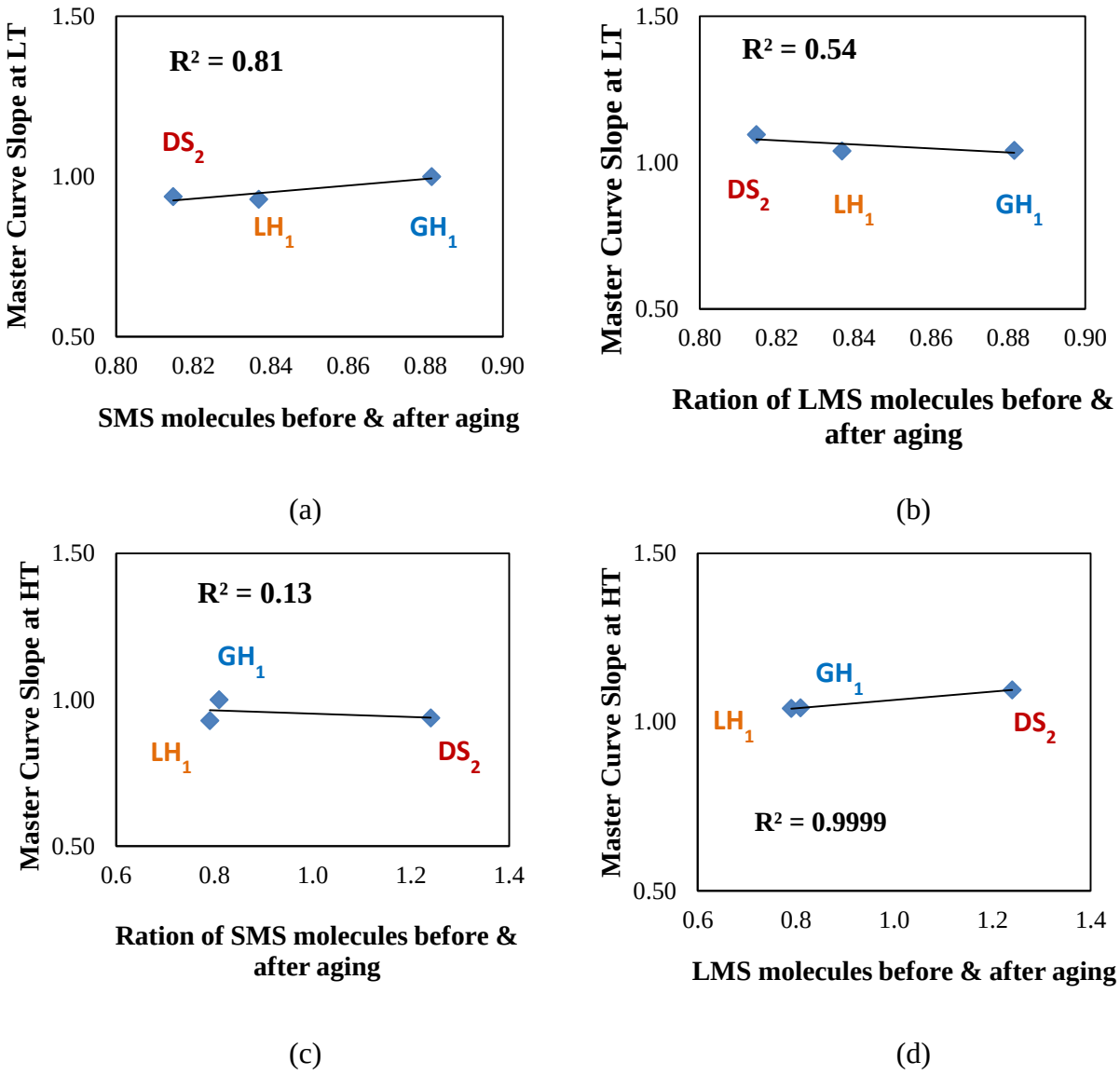

Figure V-19: Correlation between VAL mastics master curve slope: (a) at low-temperature and ratio of SMS, (b) at low-temperature and ratio of LMS, (c) at high-temperature and ratio of SMS, and (d) at high-temperature and ratio of LMS.

5.2.2 Relating Effect of Aging on GPC Results to Aging Index

In order to verify the effect of filler after the oxidative aging of mastics, GPC chromatograms after PAV aging were subtracted from GPC chromatograms before aging, for both neat binder and mastics.

Figure V-20 shows the subtraction analysis of the FH base binder and mastics. A comparison between the area under each peak presented on the large molecular size molecules area (i.e. from 14.5 and 17.0 minutes of elution time) was performed. Another comparison was established between the area under each peak of the small molecular size molecules (i.e. from 19.5 and 20.5 minutes of elution time). The results of the area under each of the observed peaks are shown in Table V-1.

Table V-1: Values of peaks areas for FH base binder and mastics.

Subtraction	LMS Peak Area	SMS Peak Area
FH Neat PAV from FH Neat Unaged	4.17E-02	-5.50E-03
FH + LH_1 PAV from FH + LH_1 Unaged	4.48E-02	-3.84E-02
FH + GH_1 PAV from FH + GH_1 Unaged	2.52E-02	3.48E-03
FH + DS_2 PAV from FH + DS_2 Unaged	1.31E-02	4.39E-03

As it can be seen from Figure V-20 and from the results presented in Table V-1, all fillers showed a smaller increase in LMS after aging when compared with their corresponding base binder. Relatively less increase in LMS after aging when DS_2 was added is observed. Regarding the SMS area, the LH_1 filler showed a smaller increase in SMS after aging when compared with the base binder.

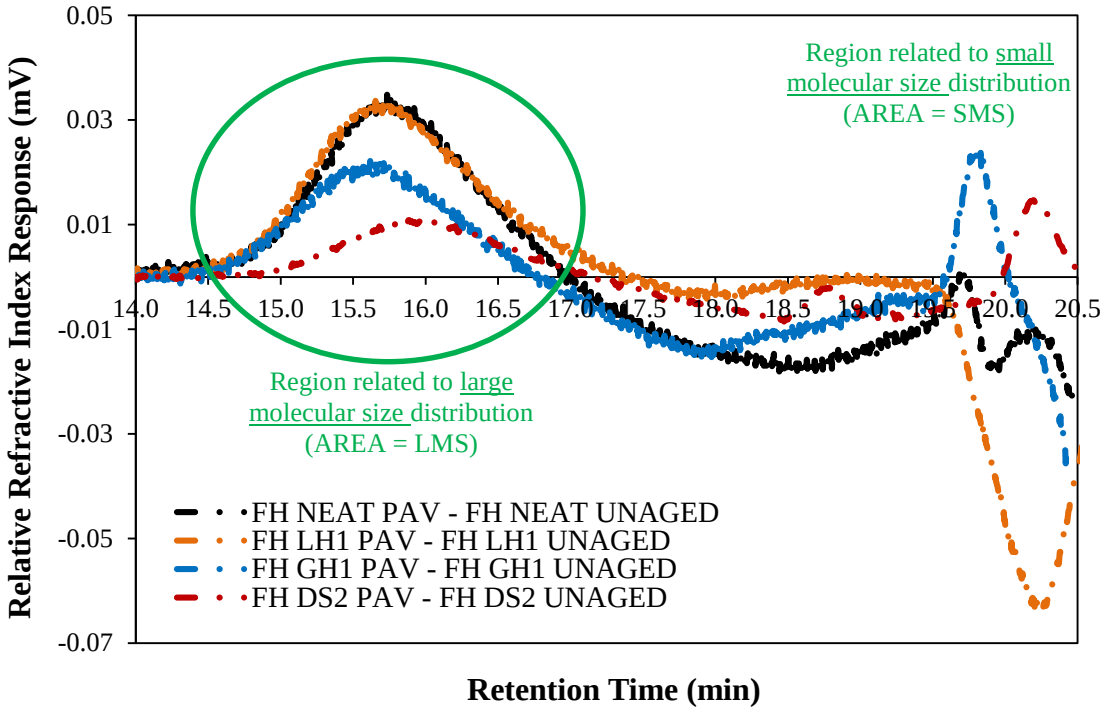

(a)

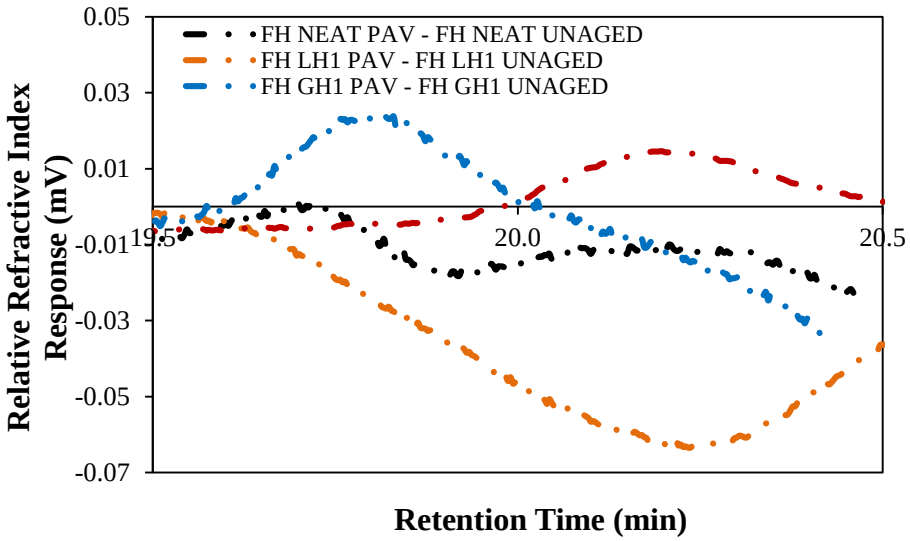

(b)

Figure V-20: (a) GPC subtraction analysis of FH base binder and mastics with 40% by volume of filler after 24 hours in PAV, and (b) zoomed of the region related to small molecular size molecules (SMS).

Another asphalt base binder (VAL 64-22) was selected for the changes in molecular size after filler addition study. Figure V-21 shows the subtraction analysis of the VAL base binder and mastics. A comparison between the area under each peak presented on the large molecular size molecules area (i.e. from 14.5 and 17.0 minutes of elution time) was performed. Another comparison was established between the area under each peak of the small molecular size molecules (i.e. from 19.5 and 20.0 minutes of elution time). The results of the area under each of the observed peaks are shown in Table V-2.

Table V-2: Values of peaks areas for VAL base binder and mastics.

Subtraction	LMS Peak Area	SMS Peak Area
VAL Neat PAV from VAL Neat Unaged	3.49E-02	9.56E-03
VAL + LH_1 PAV from VAL + LH_1 Unaged	1.02E-02	1.14E-03
VAL + GH_1 PAV from VAL + GH_1 Unaged	1.86E-02	5.62E-03
VAL + DS_2 PAV from VAL + DS_2 Unaged	1.72E-02	-2.89E-03

As it can be seen from Figure V-21 and from the results presented in Table V-2, all fillers showed a smaller increase in LMS after aging when compared with base binder. Less increase in LMS after aging is observed when LH_1 was added. Regarding the SMS area, the LH_1 and GH_1 fillers showed a smaller increase in SMS after aging when compared with base binder. A decrease in SMS after aging is observed when DS_2 mineral filler is added.

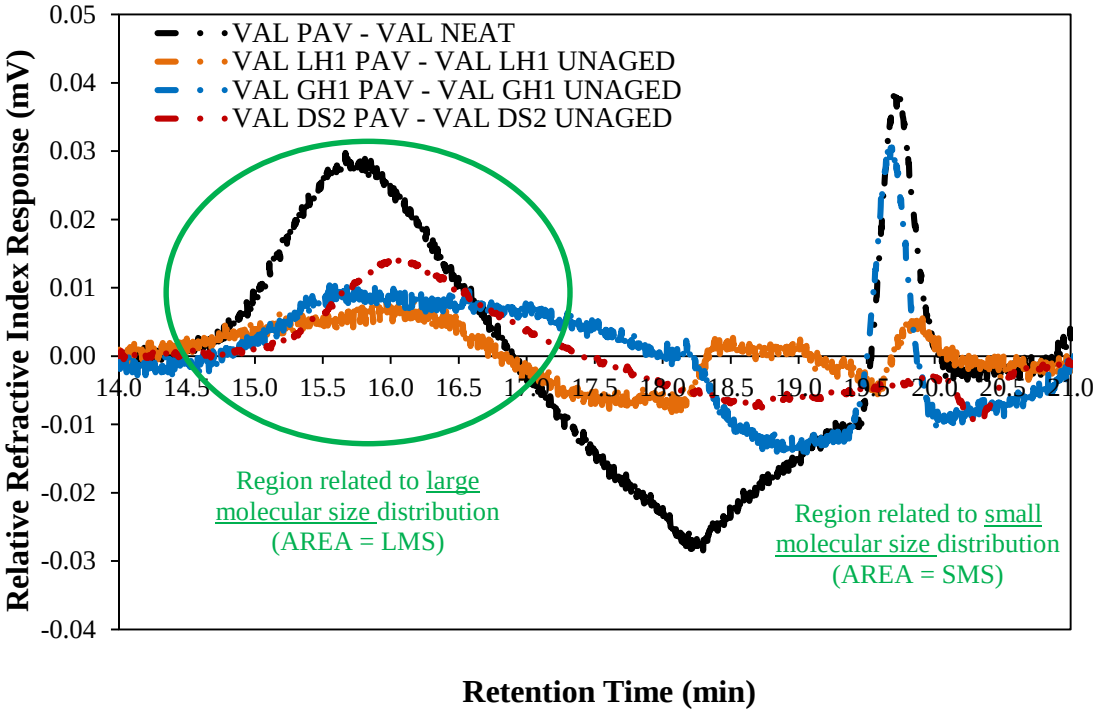

(a)

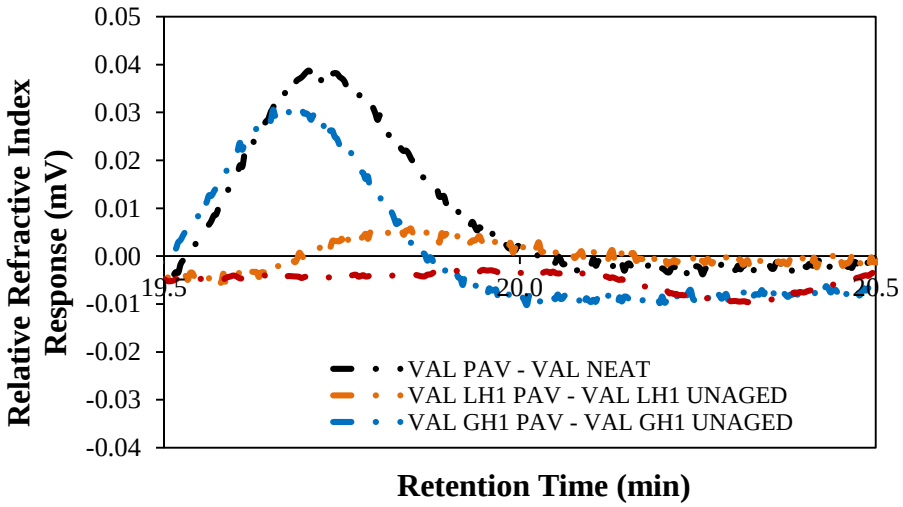

(b)

Figure V-21: (a) GPC subtraction analysis of VAL base binder and mastics with 40% by volume of filler after 24 hours in PAV, and (b) zoomed of the region related to small molecular size molecules (SMS).

A correlation between aging index of |G*| (at 40°C and 10°C) and observed GPC difference in areas of molecular size distribution of mastics was performed (Figure V-22). The aging index of |G*| is described in Equation IV-1. The GPC difference in areas of molecular size distribution of mastics is calculated as described in Equation V-8.

$$\text{Difference in GPC areas (LMS, SMS)} = \text{After 24h PAV} - \text{Unaged} \quad \text{(V-8)}$$

As it can be seen in Figure V-22, FH base binder mastics showed very poor correlation for both SMS and LMS areas. VAL base binder, however, showed a good correlation between aging index of |G*| (at 40°C and 10°C) and observed GPC difference in areas of molecular size. Correctness of the peak area parameter, especially for FH base, will need to be further investigated.

Figure V-22(b) shows that for the small molecular size molecules the observed trend between peaks at ~19.5 and 20 min (SMS area) and rheology is opposite. A higher increase in small molecular size area is leading to a smaller stiffness increase at high-temperature after aging. Figure V-22(d) shows that the observed trend between the area under the peak between ~15 and 17.5 min (LMS area) and rheology data is also opposite. A higher increase in large molecular size area is corresponding to a smaller stiffness increase at high-temperature after aging. Although this observation is unusual, it may be explained by the observed trend in SMS area.

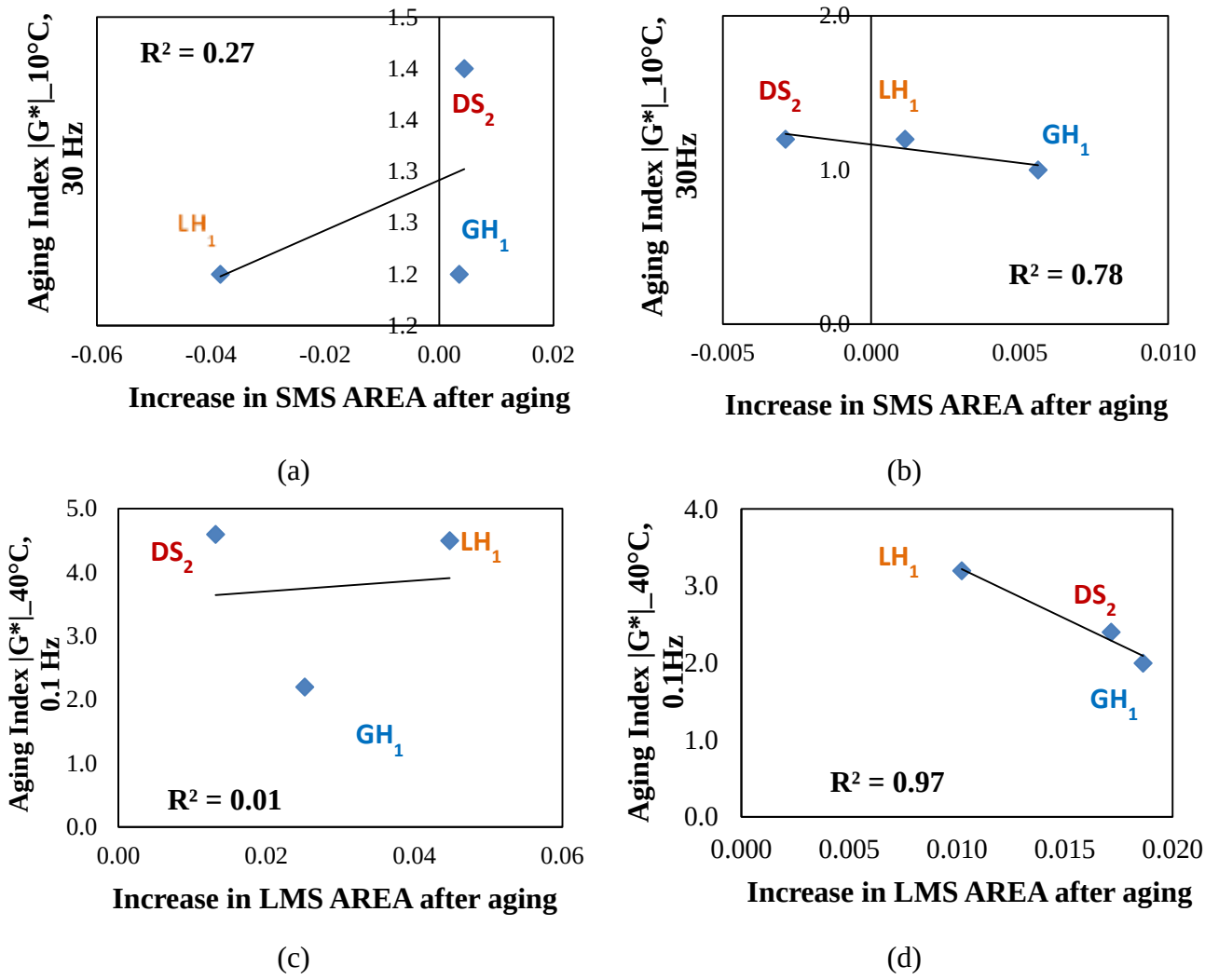

Figure V-22: Correlation between observed GPC difference in areas of molecular size distribution and aging index of |G*| (a) FH mastics at 10°C, (b) VAL mastics at 10°C, (c) FH mastics at 40°C, and (d) VAL mastics at 40°C.

In order to further investigate the relation between the filler effects and changes in molecular size distribution, another correlation was established. This time between aging index of |G*| (at 40°C and 10°C) and the ratio of Mz (average molecular weight) GPC parameter. The ratio of Mz is described in Equation V-9.

Ratio of Mz (average molecular weight) = After 24h PAV / Unaged (V-9)

As it can be seen in Figure V-23, the correlation between stiffness and molecular weight shows that a higher increase in Mz (average molecular weight) leads to a higher stiffness at both low and high-temperatures. Also, it is observed that the presence of fillers decreased the decreases the change in average molecular weight of mastics after aging. Same behavior was observed for both Flint Hills and Valero base binders.

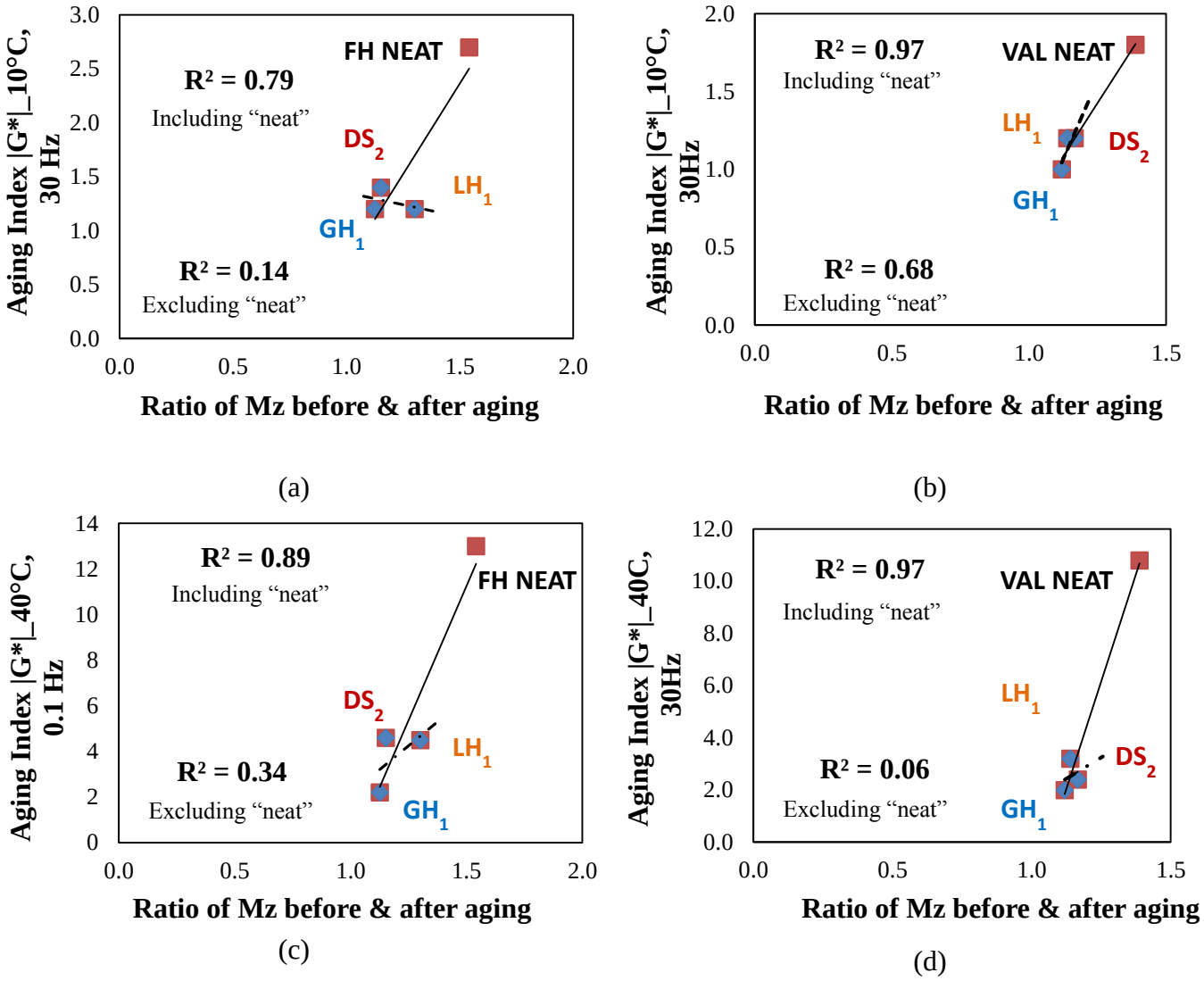

Figure V-23: Correlation between the ratio of Mz (average molecular weight) and aging index of |G*| (a) FH mastics at 10°C, (b) VAL mastics at 10°C, (c) FH mastics at 40°C, and (d) VAL mastics at 40°C.

5.2.3 Relating Effect of Aging on GPC Results to Rheology for Hydrated Lime as Filler

Since preparing a 40% mastic of hydrated lime (HL) was not physically possible, a separate comparison of GPC results between different HL concentrations and the FH neat binder was

performed. GPC chromatograms after PAV aging were subtracted from GPC chromatograms before aging, for both neat binder and hydrated lime mastics, as described in Section 5.2.2. Figure V-24 shows the subtraction analysis of the FH base binder and hydrated lime mastics.

A comparison between the area under each peak presented on the large molecular size molecules area (i.e. from 14.5 and 17.4 minutes of elution time) was performed. Another comparison was established between the area under each peak of the small molecular size molecules (i.e. from 20.1 and 20.5 minutes of elution time). The results of the area under each of the observed peaks are shown in Table V-3.

Table V-3: Values of peaks areas for FH base binder and hydrated lime mastics.

Subtraction	LMS Peak Area	SMS Peak Area
FH Neat PAV from FH Neat Unaged	1.50E-02	-6.34E-03
FH + 4% HL PAV from FH + 4% HL Unaged	2.30E-02	-4.10E-03
FH + 10% HL PAV from FH + 10% HL Unaged	8.36E-03	7.90E-04

As it can be seen from Figure V-24 and from the results presented in Table V-2, a smaller increase in large molecular size molecules area is observed after aging when 10% of hydrated lime was added. The reduction in LMS molecules indicates a decrease of highly polar functional groups. Regarding the smaller molecular size molecules, a smaller increase in the SMS peak area is observed for the FH neat binder.

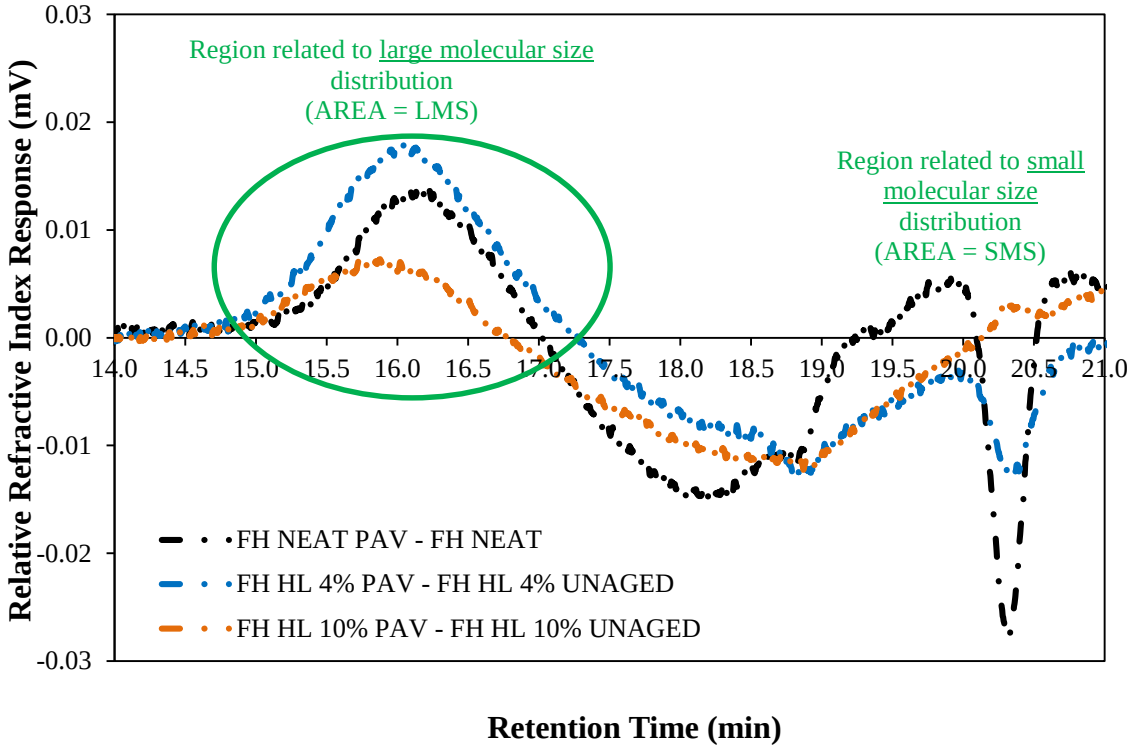

(a)

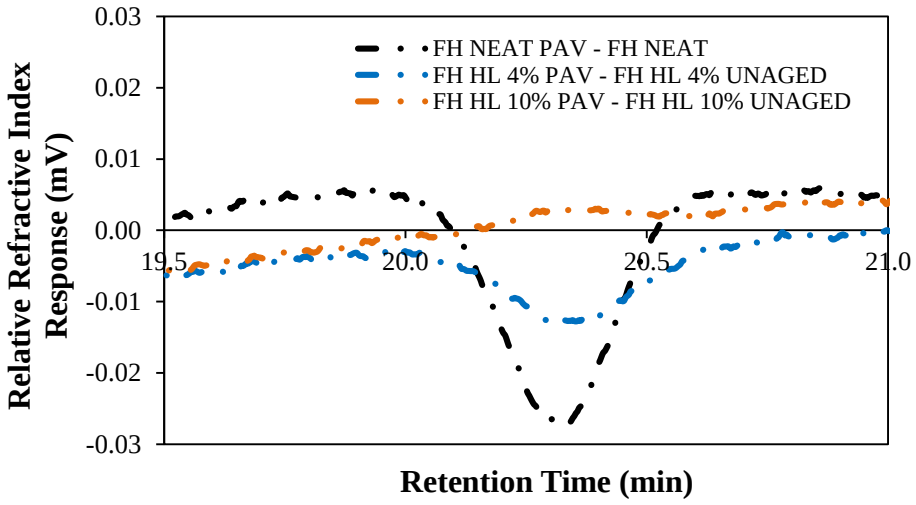

(b)

Figure V-24: (a) GPC subtraction analysis of FH base binder and hydrated lime mastics with 4% and 10% by volume of filler after 24 hours in PAV, and (b) zoomed of the region related to small molecular size molecules (SMS).

Another asphalt base binder (VAL 64-22) was selected for the changes in molecular size after hydrated lime addition study. Figure V-25 shows the subtraction analysis of the VAL base binder and mastics.

A comparison between the area under each peak presented on the large molecular size molecules area (i.e. from 15.0 and 17.5 minutes of elution time) was performed. Another comparison was established between the area under each peak of the small molecular size molecules (i.e. from 20.0 and 20.5 minutes of elution time). The results of the area under each of the observed peaks are shown in Table V-4.

Table V-4: Values of peaks areas for VAL base binder and hydrated lime mastics.

Subtraction	LMS Peak Area	SMS Peak Area
VAL Neat PAV from VAL Neat Unaged	1.81E-02	-3.10E-03
VAL + 4% HL PAV from VAL + 4% HL Unaged	2.81E-02	-2.85E-03
VAL + 10% HL PAV from VAL + 10% HL Unaged	2.94E-02	1.70E-04

According with the results showed in Figure V-25, a smaller increase in LMS after aging is observed for VAL neat binder. Unlike other fillers, addition of hydrated lime, at 4% or 10% by volume, did not decrease the LMS peak area difference after aging. Earlier observation on rheology also shows limited improvement in terms of hydrated lime preventing aging effects.

Regarding the region of small molecular size molecules, a smaller increase of the SMS area after aging is observed for the neat binder. Same observed behavior for the FH base binder.

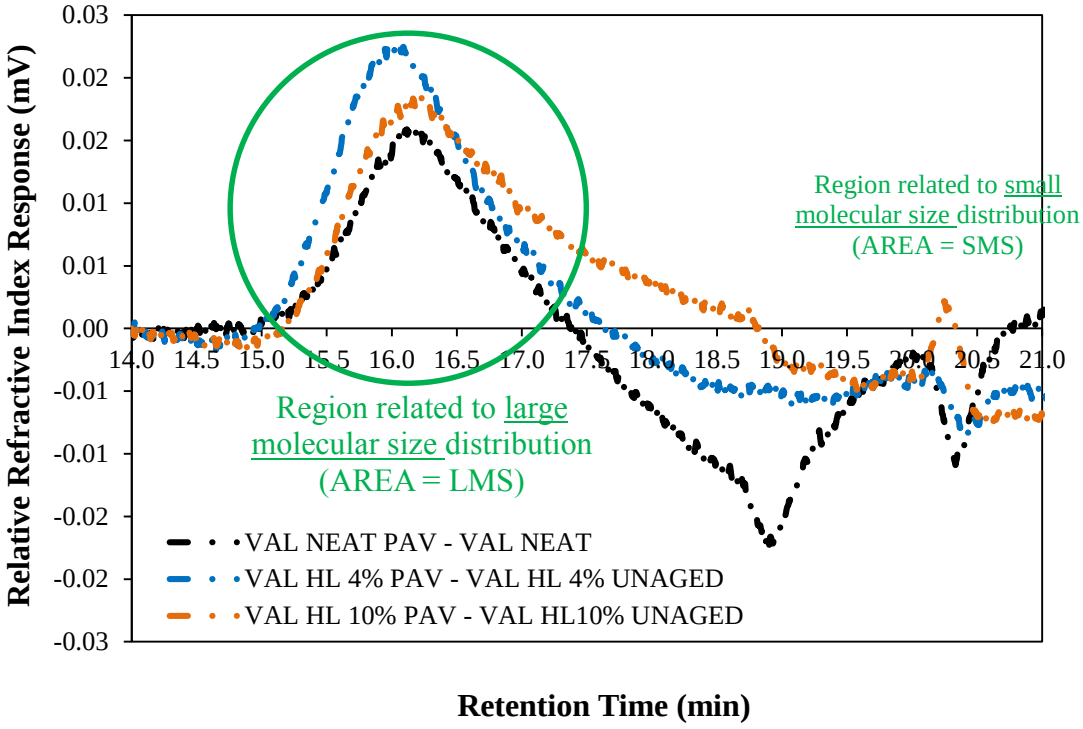

(a)

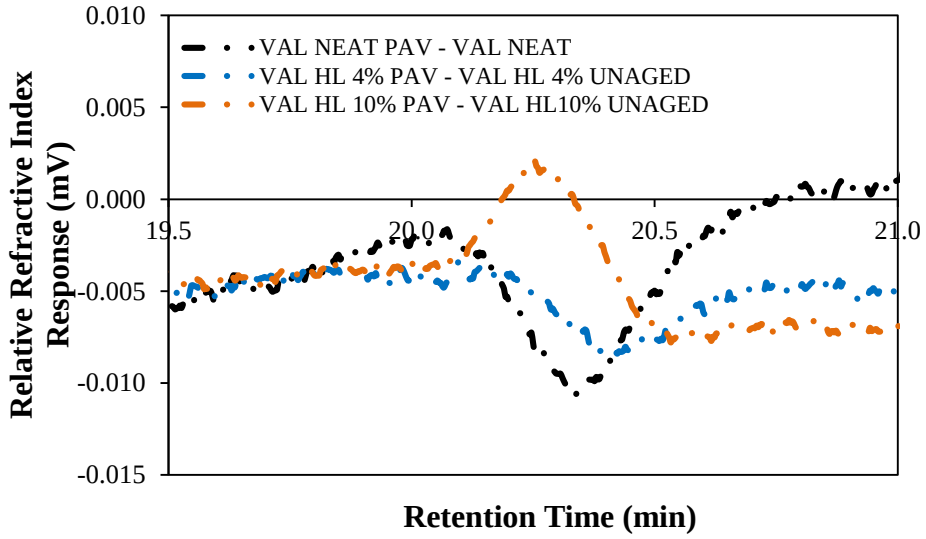

(b)

Figure V-25: (a) GPC subtraction analysis of VAL base binder and hydrated lime mastics with 4% and 10% by volume of filler after 24 hours in PAV, and (b) zoomed of the region related to small molecular size molecules (SMS).

A correlation between aging index of |G*| (at 40°C and 10°C) and observed GPC difference in areas of molecular size distribution of mastics was performed for the mastics with hydrated lime (Figure V-26). The aging index of |G*| is described in Equation IV-1. The GPC difference in areas of molecular size distribution of mastics is described in Equation V-8.

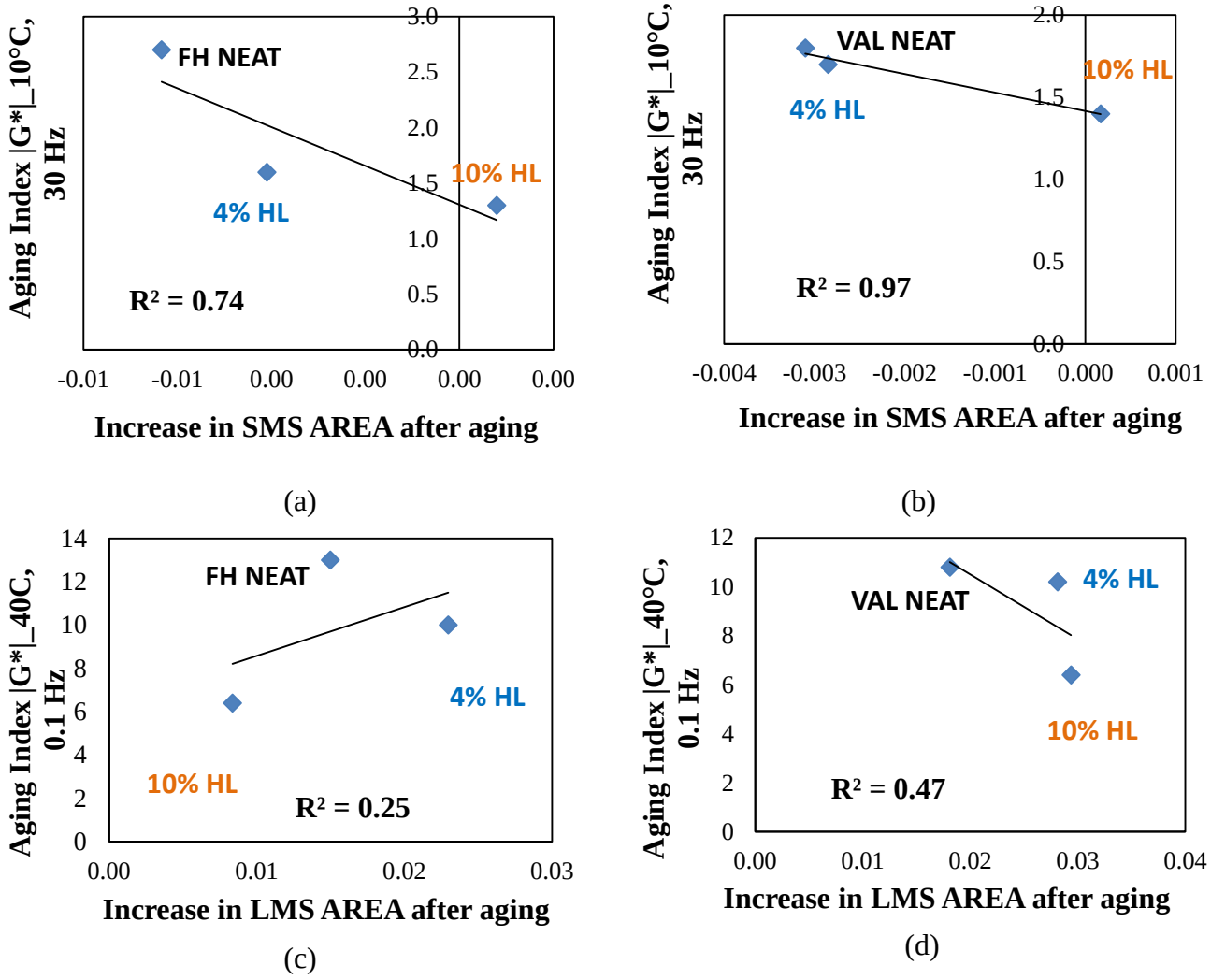

Figure V-26: Correlation between observed GPC difference in areas of molecular size distribution and aging index of |G*| (a) FH mastics at 10°C, (b) VAL mastics at 10°C, (c) FH mastics at 40°C, and (d) VAL mastics at 40°C. Hydrated lime as mineral filler.

As it can be seen in Figure V-26(a) and (c), FH + HL mastics showed very poor correlation for both LMS and SMS areas. This poor correlation between aging index of |G*| and GPC difference in areas of molecular size distribution of mastics is also observed for FH with granite, limestone, and dolomite fillers.

For the VAL base binder and mastics the correlation was better, when compared to the results of FH base binder. The trend between area under peak between ~15 and 17.5 min (LMS area) and rheology is opposite, with higher increase in large molecular size area leading to a smaller stiffness at high-temperature. For the SMS area (peak between ~20 and 20.5 min), higher increase in small molecular size is also leading to a smaller stiffness at high-temperature.

VI. Conclusions and Recommendations

6.1 Conclusions

In this study, a comprehensive experimental test matrix was completed in order to develop a fundamental understanding of asphalt mastic aging and its possible mechanisms (e.g., interaction between binder and filler surface area). The results were used to identify the filler characteristics responsible for the changes in mechanical and thermo-volumetric properties of mastics as a result of asphalt binder aging in the presence of mineral filler particles. The Gel Permeation Chromatography (GPC) technique was used to monitor the changes in the molecular size distribution due to aging, since these changes can significantly influence the asphalt binder consistency and consequently its mechanical and physical properties. The following points summarize the major findings of this study:

- The properties of the asphalt binder in the presence of mineral filler can be different from the bulk properties of the binder, depending on the interaction intensity between these two phases.
- The low temperature behavior of aged asphalt mastic can be modified, and potentially improved, by controlling filler concentration and type.
    - It is observed that fillers act as an agent adsorbing heavy fractions of asphalt binder, therefore, reducing the stiffness and shifting the glass transition temperature to lower values before any aging is induced.

  - The asphaltenes adsorption is the reason why T_g is observed to continuously decrease with filler volume concentration and filler surface area. This was evident from asphaltenes separation in this study and confirmed in earlier studies.

- Regarding the |G*| master curves, it is observed that aging of the mastic resulted in a reversal of the master curve slope, resulting in a softer mastic at lower temperatures. This finding is very significant, as it can potentially indicate that the mechanical properties attributed to aging of binders alone, which is generally believed to be increase in stiffness, are not important if the mastic phase is considered rather than binder itself.
- During oxidative aging of asphalt binders and mastics, both diffusion and adsorption mechanisms play a role in the rate of aging of the asphalt material. An analysis of the increase in diffusion path length increase in mastics was used to show that the increase in diffusion path cannot explain the magnitude of effect observed by addition of fillers to the binder.
  - The adsorption of the asphaltic polar fraction (i.e., asphaltenes) on filler surface is the main cause of the softening of the mastics after the aging process. Two fillers characteristics appear to contribute: filler type (i.e., mineralogy), and surface area.
- A new GPC sample preparation procedure was selected for preparation of both binder and mastic samples, where the solution of sample + tetrahydrofuran was filtered through a 0.20 µm phobic PTFE syringe filter prior to GPC testing;
  - The refined GPC sample preparation procedure seems to be a repeatable method of analysis. Overall, the GPC test was a relatively effective technique to quantify the fillers' effect on binders after aging as MSD will change.

- GPC can be used to characterize asphalt binders and determine changes at the molecular level before and after oxidative aging.
    - Changes caused by oxidative aging in the colloidal structure of the asphalt due to changes in the degree of association of the different asphalt fractions (i.e., asphaltenes and maltenes) is clearly reflected in the molecular size distribution as obtained by GPC.
    - The addition of mineral filler to the asphalt phase affects the molecular size distribution of the binder, and consequently its response to aging.
- The large molecular size (LMS) molecules are very sensitive to aging, with asphalts showing an increase in their LMS contents upon aging. Therefore, the GPC technique can be used to monitor the aging process of asphalt binders with regards to the production of high molecular weight molecules, and can clearly show the influence of fillers in mastics on the rate of aging of binders.
    - Mineral filler appears to decelerate the rate of production of larger molecular size oxidation products in the binder phase of mastics, reducing the aging effects on mechanical properties.
- The change in molecular size distribution after the interaction of mineral filler with the asphalt binder, as showed by GPC results, is showed as the main cause of the decrease in stiffness due to aging, when compared to the base binder.
    - The adsorption of the asphaltic polar fraction is the main cause of the softening of the mastics after the aging process.
    - The implication of this finding is that the molecular size of asphalts can be engineered by the addition of mineral filler.

- A method to characterize the behavior of mastics with aging was found to be through monitoring its complex modulus aging index.
- By selecting a proper type and amount of filler, the aging of the pavement and consequently the performance (especially crack resistance) can be controlled.

6.2 Recommendations for Future Work

The results of this study provide a significant contribution to the understanding and characterization of aged asphalt mastics. However, there are areas that merit further investigation. The following provides recommendation for future research based on the results of this study:

- Establish a relationship between total mixture aging with different aggregate mineralogy and the corresponding mastic aging results. These relationships should ultimately be related to the field aging behavior if possible.
- It is highly recommended to perform elemental analysis (SARA classification) of asphalt binders and mastics samples for a comprehensive qualitative and quantitative chemical investigation of the filler effect after the samples were subjected to oxidative aging.
- Evaluate the effect of mastic's aging on fracture properties as measured by the Single-Edge Notched Bending (SENB) fracture tests.
- Estimate the reinforcement effect of particles using simple composite theory models for the proper estimation of aging index from DSR testing.

VII. References

AASHTO T 313. *Standard Method of Test for Determining the Flexural Creep Stiffness of Asphalt Binder Using the Bending Beam Rheometer (BBR).* American Association of State Highway and Transportation Officials (AASHTO), 2005.

Al-Abdul Wahhab, H. I., I. M. Asi, F. M. Ali, and I. A. AL-Dubabi. Prediction of Asphalt Rheological Properties Using HP-GPC. In *Journal of Materials in Civil Engineering*, Vol. 11, 1999, pp. 6-14.

Altgelt, K. H. Gel Permeation Chromatography of Asphalts and Asphaltenes. In *Die Makromolekulare Chemie*, Vol. 88, 1965, pp. 75-89.

Anderson, D. A., and M. O. Marasteanu. Physical Hardening of Asphalt Binders Relative to their Glass-Transition Temperatures. In *Transportation Research Record: Journal of the Transportation Research Board*, No. 1661, Transportation Research Board of the National Academies, Washington, D.C., 1999, pp. 27-34.

Anderson, D. A., D. W. Christensen, H. U. Bahia, R. Dongre, M. G. Sharma, and C. E. Antle. Binder Characterization and Evaluation: Volume 3 Physical Characterization. Strategic Highway Research Program: Report No. SHRP-A-369, National Research Council, Washington DC, 1994.

Anderson, D. A., L. Lapalu, M. O. Marasteanu, Y. M. Le Hir, J-P. Planche, and D. Martin. Low-Temperature Thermal Cracking of Asphalt Binders as Ranked by Strength and Fracture Properties. In *Transportation Research Record: Journal of the Transportation Research Board*, No. 1766, Transportation Research Board of the National Academies, Washington, D.C., 2001, pp. 1-6.

Anderson, D. A., H. U. Bahia, and R. Dongre. Rheological Properties of Mineral Filler-Asphalt Mastics and Their Relationship to Pavement Performance. Effects of Aggregates and Mineral Fillers on Asphalt Mixture Performance: ASTM STP 1147. Richard C. Meininger, editor, American Society for Testing Materials, Philadelphia, 1992.

Anderson, D. A., R. Bonaquist. Investigation of Short-Term Laboratory Aging of Neat and Modified Asphalt Binders. NCHRP Report 709, National Cooperative Highway Research Program, Transportation Research Board, Washington, D.C., 2012.

ASTM D 4124. *Standard Test Method for Separation of Asphalt Into Four Fractions*. American Society for Testing and Materials, West Conshohocken, Pennsylvania, 2009.

ASTM D 6560. *Standard Test Method for Determination of Asphaltenes (Heptane Insolubles) in Crude Petroleum and Petroleum Products*. American Society for Testing and Materials, West Conshohocken, Pennsylvania, 2012.

Bahia, H. U. *Low-Temperature Isothermal Physical Hardening of Asphalt Cements*. Ph.D. Thesis. Pennsylvania State University, University Park, Pennsylvania, 1991.

Bahia, H. U., and D. A. Anderson. Glass Transition Behavior and Physical Hardening of Asphalt Binders. In *Journal of the Association of Asphalt Paving Technologists*, Vol. 62, 1993, pp. 93-129.

Bahia, H. U., D. I. Zeng, H., Khatri, M. A. Zhai, and R. M Anderson. *Characterization of Modified Asphalt Binders in Superpave Mix Design, NCHRP Report 459.* Washington D.C.: National Cooperative Highway Research Program, 2001.

Bahia, H. U., and D. A. Anderson. The Pressure Aging Vessel (PAV): A Test to Simulate Rheological Changes Due to Field Aging. ASTM Special Technical Publication 1241, Hardin, J.C., ed. American Society for Testing and Materials. West Conshohocken, PA., 1995.

Barbour, F. A., R. V. Barbour, and J. C. Petersen. A Study of Asphalt-Aggregate Interactions Using Inverse Gas-Liquid Chromatography. In *Journal of Applied Chemistry and Biotechnology*, Vol. 24, 1974, pp. 645-654.

Braunauer, S., P. H. Emmett, and E. Teller. Adsorption of Gases in Multimolecular Layers. In *Journal of the American Chemical Society*, Vol. 60, No. 2, 1938, pp. 309-319.

Becker, Y., A. J. Muller, and Y. Rodrıguez. Use of Rheological Compatibility Criteria to Study SBS Modified Asphalts. In *Journal of Applied Polymer Science*, Vol. 90, 2003, pp. 1772-1782.

Bell, C. A., A. J. Wieder, and M. J. Fellin. Laboratory Aging of Asphalt-Aggregate Mixtures: Field Validation. Strategic Highway Research Program: Report No. SHRP-A-390, National Research Council, Washington, DC, 1994.

Bowers, B. F. *Investigation of Asphalt Pavement Mixture Blending Utilizing Analytical Chemistry Techniques*. PhD Thesis, University of Tennessee-Knoxville, Tennessee, 2013.

Bynum, D., and R. N. Traxler. Gel Permeation Chromatography Data on Asphalt before and After Service in Pavement. In *Association of Asphalt Paving Technologists Procedures*, Vol. 39, 1970, pp. 683-702.

Churchill, E. V., S. N. Amirkhanian, J. L. Burati Jr. HP-GPC Characterization of Asphalt Aging and Selected Properties. In *Journal of Materials in Civil Engineering*, Vol. 7, 1995, pp. 41-49.

Clopotel, C. S. *Filler Reinforcement Mechanisms in Asphalt Mastic*. PhD Thesis, University of Wisconsin-Madison, Madison, Wisconsin, 2012.

Corbett, L. W. Composition of Asphalt Based on Generic Fractionation Using Solvent Deasphalteneing, Elution-Adsorption Chromatography and Densiometric Characterization. In *Analytical Chemistry*, Vol. 41, 1969, pp. 576-579.

Curtis, C. W., K. Ensley, and J. Epps. Fundamental Properties of Asphalt-Aggregate Interactions Including Adhesion and Absorption. Strategic Highway Research Program: Report No. SHRP-A-341, National Research Council, Washington, DC, 1993.

Davis, T. C., J. C. Petersen, and W. E. Haines. Inverse Gas-Liquid Chromatography A New Approach for Studying Petroleum Asphalts. In *Analytical Chemistry*, Vol. 38, 1966, pp. 241-243.

Dawkins, J. V. Theory of Gel Permeation Chromatography. Mechanism of Separation and the Influence of Polymer-Sorbent Interaction. In *Pure and Applied Chemistry*, Vol. 51, 1979, pp. 1473-1481.

Dehouche, N., M. Kaci, and K. A. Mokhtar. Influence of Thermo-Oxidative Aging on Chemical Composition and Physical Properties of Polymer Modified Bitumens. In *Construction and Building Materials*, Vol. 26, 2012, pp. 350-356.

Doh, Y. S., S. N. Amirkhanian, K. W. Kim. Analysis of Unbalanced Binder Oxidation Level in Recycled Asphalt Mixture Using GPC. In *Construction and Building Materials*, Vol. 22, 2008, pp. 1253-1260.

Domke, C. H., R. R. Davison, and C. J. Glover. Effect of Oxygen Pressure on Asphalt Oxidation Kinetics. In *Industrial & Engineering Chemistry Research*, Vol. 39, 2000, pp. 592-598.

Dong, X., Q. Lei, W. Fang, and Q. Yu. Thermogravimetric Analysis of Petroleum Asphaltenes Along with Estimation of Average Chemical Structure by Nuclear Magnetic Resonance Spectroscopy. In *Thermochimica Acta*, Vol. 427, 2005, pp. 149-153.

Droste, D.H., A. T. Dibenedetto. The Glass Transition Temperature of Filled Polymers and Its Effect on Their Physical Properties. In *Journal of Applied Polymer Science*, Vol. 13, 1969, pp. 2149-2168.

Enustum, B. V., S. S. Kim, D. Y. Lee. Correlation of Locally-Based Performance of Asphalts with Their Physicochemical Parameters. Iowa DOT Project HR-298, Engineering Research Institute Project 1942, 1990.

Faheem, A., H. U. Bahia, C. Hintz, I. Al-Qadi, G. Reinke, E. Dukatz. Test Methods and Specification Criteria for Mineral Filler Used in HMA. Final Report 9-45 Prepared for National Cooperative Highway Research Program, Transportation Research Board, National Research Council, 2010.

Ferry, J. D. *Viscoelastic Properties of Polymers*. New York, NY: John Wiley & Sons, Inc., 1980.

Fesko, D. G., and N. W. Tschoegl. Time-Temperature Superposition in Thermorheologically Complex Materials. In *Journal of Polymer Science: Part C*, No. 35, 1971, pp. 51-69.

Garrick, N. W. Use of Gel Permeation Chromatography in Predicting Properties of Asphalt. In *Journal of Materials in Civil Engineering*, Vol. 6, 1994, pp. 376-389.

Gehrke, C. W., and C. D. Ruyle. Gas-Liquid Chromatographic Analysis of Nucleic Acid Components. In *Journal of Chromatography*, Vol. 38, 1968, pp. 473-491.

Gilmore, D. W., M. R. Weisman, R. S. Dalter and T. G. Kugele. Determination of the Presence of Anti-stripping Agents in Asphalt Cement by High-performance Liquid Chromatography. In Properties of Flexible Pavement Materials, American Society for Testing and Materials Special Technical Publication 807, J. J. Emery, Ed., 1983, pp. 46-54.

Glover, C. J., R. R. Davison, J. A. Bullin, J. W. Button, and G. R. Donaldson. Chemical Characterization of Asphalt Cement and Performance Related Properties. In *Transportation Research Record: Journal of the Transportation Research Board*, No. 1171, Transportation Research Board of the National Academies, Washington, D.C., 1988, pp. 71-81.

Graham, R. T., and L. N. Lynch. Gel Permeation Chromatograph Analysis of Asphalt-Based Joints Sealants. Technical Report GL-93-13, July, 1993.

Hagos, E. T. *The Effect of Aging on Binder Properties of Porous Asphalt Concrete*. PhD Thesis, Delft University of Technology, Delft, Netherlands, 2008.

Haley, G. A. Molecular and Unit Sheet Weights of Asphalt Fractions Separated by Gel Permeation Chromatography. In Analytical Chemistry, Vol. 43, 1971, 371-375.

Iqbal, M. H., I. A. Hussein, H. I. Al-Abdul Wahhab, and H. B. Amin. Rheological Investigation of the Influence of Acrylate Polymers on the Modification of Asphalt. In *Journal of Applied Polymer Science*, Vol. 102, 2006, pp. 3446-3456.

Jacobson, M., J. F. O'Brien, and C. Hedgcoth. Determination of Nucleoside Composition of Ribonucleic Acid By Gas-Liquid Chromatography. In *Analytical Biochemistry*, Vol. 25, 1968, pp. 363-369.

Jennings, P. W., P. W. Pribanic, M. F. Raub, J. A. Smith, T. M. Mendes. Advanced High Performance Gel Permeation Chromatography Methodology. Strategic Highway Research Program: Report No. SHRP-A-630, National Research Council, Washington, DC, 1993.

Jennings, P. W., P. W. Pribanic, W. Campbell, K. Dawson, S. Shane, and R. Taylor. *High Pressure Liquid Chromatography as a Method of Measuring Asphalt Composition*. *FHWA-MT-79-30 Final Report*, Bozeman, Montana, 1980.

Jimenez-Mateos, J. M., L. C. Quintero, and C. Rial. Characterization of Petroleum Bitumens and their Fractions by Thermogravimetric Analysis and Differential Scanning Calorimetry. In *Fuel*, Vol. 75, 1996, pp. 1691-1700.

Jung, S. H. *The Effects of Asphalt Binder Oxidation on Hot Mix Asphalt Concrete Mixture Rheology and Fatigue Performance*. PhD Thesis, Texas A&M University, College Station, Texas, 2006.

Jung, S. H., and T. S. Vison. Low-Temperature Cracking: Test Selection. Strategic Highway Research Program: Report No. SHRP-A-400, National Research Council, Washington, DC, 1994.

Kennedy, T. W., and R. J. Cominsky. Hypotheses and Models Employed in the SHRP Asphalt Research Program. Strategic Highway Research Program: Report No. SHRP-A/WP-90-008, National Research Council, Washington, DC, 1990.

Kim, H., Lee, S-J., Amirkhanian, S. N., and Jeong, K-D. Quantification of Oxidative Aging of Polymer-Modified Asphalt Mixes Made with Warm Mix Technologies. In *Journal of Materials in Civil Engineering*, Vol. 25, 2013, pp. 1-8.

Kim, K. W., and J. L. Burati. Use of GPC Chromatograms to Characterize Aged Asphalt Cements. In *Journal of Materials in Civil Engineering*, Vol. 5, 1993, pp. 41-52.

Kim, K. W., K. Kim, Y. S. Doh, and S. N. Amirkhanian. Estimation of RAP's Binder Viscosity Using GPC without Binder Recovery. In *Journal of Materials in Civil Engineering*, Vol. 18, 2006, pp. 561-567.

Kim, S. S. Direct Measurement of Asphalt Binder Thermal Cracking. In *Journal of Materials in Civil Engineering*, Vol. 17, No. 6, 2005, pp. 632-639.

Klompen, E. T. J. *Deformation Behaviour of Glassy Polymers; Consequences of Thermorheological Complex Behaviour*. In WFW Report 96.140, Eindhoven University of Technology, 1996.

Knorr, D. B., R. R. Davison, and C. J. Glover. Effect of Various Aging Techniques on Asphalt Low-Temperature Properties. In *Transportation Research Record: Journal of the Transportation Research Board*, No. 1810, Transportation Research Board of the National Academies, Washington, D.C., 2002, pp. 9-16.

Kriz, P., J. Stastna, L. Zanzotto. Glass Transition and Phase Stability in Asphalt Binders. In *Road Materials and Pavement Design*, Vol. 9/SI, 2008, pp. 37-65.

Lee, S. A., S. N. Amirkhanianb, and K. W. Kim. Laboratory Evaluation of the Effects of Short-Term Oven Aging on Asphalt Binders in Asphalt Mixtures Using HP-GPC. In *Construction and Building Materials*, Vol. 23, 2009, pp. 3087-3093.

Lesueur, D. The Colloidal Structure of Bitumen: Consequences on the Rheology and on the Mechanisms of Bitumen Modification. In *Advances in Colloid and Interface Science*, 145(1–2), 2009, pp. 42-82.

Liu, M. M., M. S. Lin, J. M. Chaffin, R. R. Davison, and C. J. Glover. Oxidation Kinetics of Asphalt Corbett Fractions and Compositional Dependence of Asphalt Oxidation. In *Petroleum Science and Technology*, Vol. 16, 1998, pp. 827-850.

Lu, X., and U. Isacsson. Artificial Aging of Polymer Modified Bitumens. In *Journal of Applied Polymer Science*, Vol. 76, 2000, pp. 1811-24.

Lu, X., and U. Isacsson. Effect of Ageing on Bitumen Chemistry and Rheology. In *Construction and Building Materials*, Vol. 16, 2002, pp. 15-22.

Marasteanu, M., A. Zofka, M. Turos, X. Li, R. Velasquez, X. Li, W. Buttlar, G. Paulino, A. Braham, E. Dave, J. Ojo, H. Bahia, C. Williams, J. Bausano, A. Gallistel, and J. McGraw. Investigation of Low Temperature Cracking in Asphalt. Pavements National pooled Fund Study 776: Report N. MN/RC 2007-43, Minnesota Department of Transportation, St. Paul, MN, 2007.

McCann, M., J. F. Rovani, K. P. Thomas. Detection of Polymers in Asphalt Binders. Transportation and Development Institute Congress, 2011, pp. 514-527.

Murgich, J., J. M. Rodrigues, and Y. Aray. Molecular Recognition and Molecular Mechanics of Micelles of Some Model Asphaltenes and Resins. In *Energy & Fuels*, Vol. 10, 1996, pp. 68-76.

Musser, B. J., and P. K. Kilpatrick. Molecular Characterization of Wax Isolated from a Variety of Crude Oils. In *Energy & Fuels*, Vol. 12, 1998, pp. 715-725.

Nam, K., and H. U. Bahia. Effect of Modification on Fracture Failure and Thermal-Volumetric Properties of Asphalt Binders. In *Journal Materials in Civil Engineering*, Vol. 21, 2009, pp. 198-209.

Noureldin, A. S., and L. E. Wood. Variation in Molecular Size Distribution of Virgin and Recycled Asphalt Binders Associated with Aging. *Transportation Research Record: Journal of the Transportation Research Board,* No. 1228, Transportation Research Board of the National Academies, Washington, D.C., 1989, pp. 191-197.

Ortega-Rodrıguez, A., S. A. Cruz, A. Gil-Villegas, F. Guevara-Rodrıguez, and C. Lira-Galeana. Molecular View of the Asphaltene Aggregation Behavior in Asphaltene-Resin Mixtures. In *Energy & Fuels*, Vol. 17, 2003, pp. 1100-1108.

O'Sullivan, K. A. Rejuvenation of Reclaimed Asphalt Pavement (RAP) in Hot Mix Asphalt Recycling with High RAP Content. MSc Thesis, Worcester Polytechnic Institute, Massachusetts, 2011.

Petersen, J. C, F. A. Barbour, and S. M. Dorrence. Catalysis of Asphalt Oxidation by Mineral Aggregate Surfaces and Asphalt Components. In *Asphalt Paving Technology*, Vol. 43, 1974, pp. 162-177.

Petersen, J. C. A Review of the Fundamentals of Asphalt Oxidation - Chemical, Physicochemical, Physical Property, and Durability Relationships. Transportation Research Circular E-C140, Transportation Research Board, 2009.

Petersen, J. C. Chemical Composition of Asphalt Related to Asphalt Durability: State of the Art. In *Transportation Research Record: Journal of the Transportation Research Board*, No. 999, Transportation Research Board of the National Academies, Washington, D.C., 1984, pp. 13-30.

Petersen, J. C., J. F. Branthaver, R. E. Robertson, P. M. Harnsberger, J. J. Duvall, and E .K. Ensley. Effects of Physicochemical Factors on Asphalt Oxidation Kinetics. In *Transportation Research Record: Journal of the Transportation Research Board*, No. 1391, Transportation Research Board of the National Academies, Washington, D.C., 1993, pp. 1-10.

Petersen, J. C., P. M. Harnsberger, and R. E. Robertson. Factors Affecting the Kinetics and Mechanisms of Asphalt Oxidation and the Relative Effects of Oxidation Products on Age Hardening. In *American Chemical Society Division of Fuel Chemistry Preprints*, Vol. 41, No. 4, 1996, pp. 1232-1244.

Petersen, J. C., and P. M. Harnsberger. Asphalt Aging: Dual Oxidation Mechanism and Its Interrelationships with Asphalt Composition and Oxidative Age Hardening. In *Transportation Research Record: Journal of the Transportation Research Board*, No. 1638, Transportation Research Board of the National Academies, Washington, D.C., 1998, pp. 47-55.

Petersen, J. C., R. V. Barbour, S. M. Dorrence, F. A. Barbour, and R. V. Helm. Molecular Interactions of Asphalt - Tentative Identification of 2-Quinolones in Asphalt and Their Interaction with Carboxylic Acids Present. In *Analytical Chemistry*, Vol. 43, 1971, pp. 1491-1496.

Plancher, H., E. L. Green, and J. C. Petersen. Reduction of Oxidative Hardening of Asphalts by Treatment with Hydrated Lime: A Mechanistic Study. In *Association of Asphalt Paving Technologist*, Vol. 45, 1976, pp. 1-24.

Plancher, H., and J. C. Petersen. Reduction of Oxidative Hardening in Asphalts by Treatment with Hydrated Lime: A Mechanistic Study. In *Association of Paving Technologists*, Vol. 45, 1976, pp. 1-24.

Plummer, M. A., and C. C. Zimmerman. Asphalt Quality and Yield Predictions from Crude Oil Analyses. In *Association of Asphalt Paving Technologists*, Vol. 53, 1984, pp. 138-159.

Puello, J, N. Afanasjeva, and M. Alvarezc. Thermal Properties and Chemical Composition of Bituminous Materials Exposed to Accelerated Ageing. In *Road Materials and Pavement Design*, Vol.14, Issue 2, 2013, pp. 278-288.

Read, J., and D. Whiteoak. *The Shell Bitumen Handbook*, Fifth Edition, 2003.

Roberts, F. L., P. S. Kandhal, E. R. Brown, D. Y. Lee, and T. W. Kennedy. Hot Mix Asphalt Materials, Mixture Design, and Construction. National Asphalt Pavement Association Education Foundation, Lanham, MD. 1996.

Robertson, R. E. Chemical Properties of Asphalts and their Relationship to Pavement Performance. Strategic Highway Research Program: Report No. SHRP-A/UWP-91-510, National Research Council, Washington, DC, 1991.

Rostler, F. S., and R. M. White. Composition and Changes in Composition of Highway Asphalts, 85-100 Penetration Grade. In *Association of Asphalt Paving Technologists*, Vol. 31, 1962, pp. 35-89.

Sajjad, M., B. Feichtenschlager, S. Pabisch, J. Svehla, T. Koch, S. Seidler, H. Peterlikc, and G. Kickelbickd. Study of the Effect of the Concentration, Size and Surface Chemistry of Zirconia and Silica Nanoparticle Fillers within an Epoxy Resin on the Bulk Properties of the Resulting Nanocomposites. In *Polymer International*, Vol. 61, 2012, pp. 274-285.

Shen, J., S. Amirkhanian, and F. Xiao. High-Pressure Gel Permeation Chromatography of Aging of Recycled Crumb Rubber-Modified Binders with Rejuvenating Agents. In *Transportation Research Record: Journal of the Transportation Research Board*, No. 1962, Transportation Research Board of the National Academies, Washington, D.C., 2006, pp. 21-27.

Shen, J., S. N. Amirkhanian, and S-J. Lee. HP-GPC Characterization of Rejuvenated Aged CRM Binders. In *Journal of Materials in Civil Engineering*, Vol. 19, 2007, pp. 515-522.

Sheu, E. Y. Petroleum Asphaltenes - Properties, Characterization and Issues. In *Energy & Fuels*, Vol. 16, 2002, pp. 74-82.

Sheu, E. Y., and O. C. Mullins. *Asphaltenes: Fundamentals and Applications*. Plenum Press, New York, 1995.

Siddiqui, M. N., and M. F. Ali. Investigation of Chemical Transformations by NMR and GPC During the Laboratory Aging of Arabian Asphalt. In Fuel, Vol. 78, 1999, pp. 1407-1416.

Snyder, L. R. Determination of Asphalt Molecular Weight Distributions by Gel Permeation Chromatography. In *Analytical Chemistry*, Vol. 41, 1969, pp. 1223-1227.

Swiertz, D. R. *Development of a Test Method to Quantify the Effect of RAP and RAS on Blended Binder Properties without Binder Extraction*. Master Thesis, University of Wisconsin-Madison, Madison, Wisconsin, 2012.

Togunde, O. P., and S. A. M. Hesp. Physical Hardening in Asphalt Mixtures. In *International Journal of Pavement Research and Technology*, Vol. 5, 1997, pp. 46-53.

Tabatabaee, H. A., R. Velasquez, and H. U. Bahia. Modeling Thermal Stress in Asphalt Mixtures Undergoing Glass Transition and Physical Hardening. In *Transportation Research Record: Journal of the Transportation Research Board*, Vol. 2296, 2012a, pp. 106-114.

Tabatabaee, H. A., R. Velasquez, and H. U. Bahia. Predicting Low Temperature Physical Hardening in Asphalt Binders. In *Construction and Building Materials*, Vol. 34, 2012b, pp. 162-169.

Tarefder, R. A., and I. Arisa. Molecular Dynamic Simulations for Determining Change in Thermodynamic Properties of Asphaltene and Resin Because of Aging. In *Energy & Fuels*, Vol. 25, 2011, pp. 2211-2222.

Turner, T. F., and J. F. Branthaver. DSC Studies of Asphalts and Asphalt Components. In *Asphalt Science & Technology*, Arthur Usmani: Editor, New York, Marcel Dekker, 1997.

Velasquez, R., H. A. Tabatabaee, H. U. Bahia. Low Temperature Cracking Characterization of Asphalt Binders by Means of the Single-Edge Notch Bending (SENB) Test. In *Journal of the Association of Asphalt Paving Technologists*, Vol. 80, 2011, pp. 583-614.

Yapp, M. T., A. Z. Durrani, F. N. Finn. HP-GPC and Asphalt Characterization Literature Review. Strategic Highway Research Program: Report No. SHRP- A/UIR-91-503, National Research Council, Washington, DC, 1991.

Yau, W. W., and C. P. Malone. An Approach to Diffusion Theory of Gel Permeation Chromatographic Separation. In *Journal of Polymer Science Part B: Polymer Letters*, Vol. 5, 1967, pp. 663-669.

Ying, G., G. Fan, Z. YongLi. Thermal Oxidative Aging Characterization of SBS Modified Asphalt. In *Journal of Wuhan University of Technology*, Vol. 28, 2013, pp. 88-91.

Wada, Y., and H. Hirose. Glass Transition Phenomenon and Rheological Properties of Petroleum Asphalt. In *Journal of the Physical Society of Japan*, Vol. 15, No.10, 1960, pp. 1885-1894.

Wei, J., J. C. Shull, J. Barak, and M. C. Hawley. Characterization of Asphalt Binders Based on Chemical and Physical Properties. In *International Journal of Polymer Analysis and Characterization*, Vol. 3, 1996, pp. 33-58.

Wu. J. *The Influence of Mineral Aggregates and Binder Volumetrics on Bitumen Ageing*. PhD Thesis, University of Nottingham, England, UK, 2009.

Xiao, F., S. N. Amirkhanian, and J. Shen. Effects Of Various Long-Term Aging Procedures on the Rheological Properties of Laboratory Prepared Rubberized Asphalt Binders. In *ASTM Journal of testing and Evaluation*, Vol. 37, 2009, pp. 129-138.

Zenewitz, J. A., and K. T. Tran. A Further Statistical Treatment of the Expanded Montana Asphalt Quality Study. In *Public Roads*, Vol. 57, 1987, pp. 72-81.

Zhao, S., B. Bowers, B. Huang, and X. Shu. Characterizing Rheological Characterizing Rheological Properties of Binder and Blending Efficiency of Asphalt Paving Mixtures Containing RAS through GPC. In *Journal of Materials in Civil Engineering*, 10.1061/(ASCE)MT.1943-5533.0000896, 2013.